Simona Regenspurg

Characterisation of Schwertmannite - Geochemical Interactions with Arsenate and Chromate and Significance in Sediments of Lignite Opencast Lakes

Charakterisierung von Schwertmannit –
Geochemische Wechselwirkungen mit Arsenat und Chromat
und Bedeutung in Sedimenten von Restseen des Braunkohletagebaus

Simona Regenspurg

Characterisation of Schwertmannite - Geochemical Interactions with Arsenate and Chromate and Significance in Sediments of Lignite Opencast Lakes

Dissertation aus dem
Lehrstuhl für Hydrologie
der Fakultät für Chemie, Biologie und Geowissenschaften,
der Universität Bayreuth

Promotionsgesuch eingereicht am 10.04.2002

Vollständiger Abdruck der von der Fakultät für Biologie, Chemie und Geowissenschaften der Universität Bayreuth zur Erlangung des akademischen Grades eines Doktors des Naturwissenschaften eingereichte Dissertation.

Wissenschaftliches Kolloquium am 31.10.2002

1. Gutachter Professor Dr. S. Peiffer
2. Gutachter Professor Dr. F. Seifert

TABLE OF CONTENTS

III. FORMATION AND TRANSFORMATION OF SCHWERTMANNITE IN SEDIMENTS OF ACID LIGNITE OPENCAST LAKES

LIST OF TABLES

LIST OF FIGURES

LIST OF ABBREVIATIONS AND DEFINITIONS

AAS	atom-absorption spectroscopy
adsorbent	on the surface of this (solid) material adsorption takes place
adsorbate	material, which adsorbs (in this study: anions)
AMD	acid mine drainage
AML	acidic mining lake
BET	method to determine the surface area (Brunauer-Emmett-Teller)
dl	detection limit
d-value (nm)	net plane distance of a crystal
EXAFS	extended X-ray absorption fine structure
FTIR	Fourier-Transform infrared
IAP	Ionic-activity product
IC	ionic chromatography
ICP	inductive-coupled plasma
incorporation	in this study (non-specific) expression for the molecule „uptake“ of a mineral
hkl	Miller indices: the smallest, whole-numbered multiple of the reciprocal axis-segments of a crystal net plane
metastable	thermodynamic unstable
minerals	Fh ferrihydrite Gt goethite Jt jarosite Kt kaolinite Qz quartz Sh schwertmannite
ML	mining lake
n.d.	not determinable
n.m.	not measured
ppb	parts per billion
ppm	parts per million
pH_{iep}	point of zero charge, determined by electrophoresis
pH_{pzc}	point of zero charge, determined by acid-base titration
SEM	scanning electron microscopy
SI	saturation index
wt.-%	weight-%
XRD	X-ray diffraction
ζ-Potential	electric potential in the diffuse layer of a surface
θ (°)	diffraction angle (X-ray diffractometry)
λ (nm)	Wavelength
≡	surface group
{≡X}	surface concentration (X is any ion)

ABSTRACT

Fe(III) oxyhydroxysulfate schwertmannite [idealised formula: $Fe_8O_8(OH)_6SO_4$], frequently precipitates as a product of sulphide weathering in acidic, sulfate-rich waters. In order to investigate the environmental importance of schwertmannite, geochemical and mineralogical methods were applied in field- and laboratory-experiments. Thereby this thesis focussed on two consequential questions: The first (1) was if schwertmannite could enrich toxic compounds and therefore act as a sink in natural systems. By means of the anions arsenate and chromate, the uptake capacity by adsorption or substitution and consequential changes in crystal structure were characterised. Additionally, a possible re-mobilisation of these compounds was investigated because the metastable schwertmannite easily dissolves or transforms into other minerals. Predominantly, experiments with synthetically produced schwertmannite took place. The other main focus (2) comprised examinations of schwertmannite formation in the chemical environment of acidic lignite mining opencast lakes. Thereby its importance as pH-buffer, its formation probability and its variation by ageing were to be characterised.

(1) Schwertmannite, as contained in precipitates of former ore mines, featured extraordinary high amounts of arsenic (up to 6700 ppm) and chromium (up to 800 ppm). Since there was hardly any detection of these elements in the corresponding drainage waters, the hypothesis arose that schwertmannite acts as a scavenger for these compounds. Assuming that in the redox environment of schwertmannite formation, arsenic and chromium are mostly present in their highest oxidation-level (as arsenate and chromate) these oxyanions were used for coprecipitation-, adsorption- and stability-investigations with synthetic schwertmannite, to characterise its geochemical interactions. Synthesis (or coprecipitation) experiments proved that schwertmannite, normally containing 12 to 14 wt.-% sulfate (both, structurally and adsorptively bound), incorporates up to 10.4 wt.- % arsenate and up to 15.4 wt.-% chromate. While the complete substitution of sulfate by chromate was possible without substantial variation of the crystal structure, the incorporation of arsenate only took place in presence of sulfate or chromate. Oxyanion uptake resulted in an advanced stability of schwertmannite as confirmed in long-term experiments at constant pH. This means that the transformation (due to ageing) to the mineral goethite, as well as mineral dissolution as a consequence of acid addition, was decelerated and toxic compounds were released in lower concentrations compared to sulfate.

Activity of Fe(III)-reducing bacteria also results in the dissolution of schwertmannite. A combination of microbiological and geochemical methods was used to quantify the influence of oxyanion incorporation on Fe(III) reduction in schwertmannite and the associated mobilisation of oxyanions. Microbiological experiments were performed in co-operation with the Department of Ecological Microbiology (BITÖK). Peine et al. (1998) have already described that acidophilic bacteria reduce the well available Fe(III) of schwertmannite. (This reduction is a requirement for the immobilisation of iron as Fe(II) sulfide and therefore an important step to neutralise acidic waters). The bacteria *Acidiphilium cryptum* JF-5 (acidophile, facultative anaerobic, non-fermentative Fe(III) reducer) were added to a medium of synthetic schwertmannite, partly consisting of arsenate and chromate. It was shown that Fe(III) reduction of schwertmannite was twice as high as in arsenated schwertmannite and that the mobilisation of arsenate was very low, compared to that of sulfate. Chromate was proven to be toxic for these micro-organisms. As a side effect of this research it was observed that autoclavation of schwertmannite (heating up to 121 °C for 20 min), a common method for micro-biological experiments, results in transformation to goethite. The presence of arsenate and chromate prevents this effect, indicating once more the stabilising effect of these oxyanions compared to sulfate.

Adsorption experiments confirmed that schwertmannite, even after its synthesis, is able to take up high amounts of arsenate and chromate. FTIR spectroscopy was used to differentiate bonding structures (adsorptive or structural) of anions in schwertmannite. Thereby it was shown that oxyanions predominantly bind to the iron hydroxide by specific bidentate sorption (complexes of Fe-O-X(O_2)-O-Fe where X is either S, Cr or As). This method did not yet differentiate between structural and adsorptive binding.

Synthesis and adsorption experiments showed that both, arsenate and arsenite, can be enriched in similar concentrations in schwertmannite. FTIR analysis demonstrated, that during the As(III) incorporation the redox state of arsenite did not change.

Due to the crucial importance of the schwertmannite surface which influences its solubility as well as its adsorption capacity, the mineral surface was characterised in various experiments. Results suggest an extraordinary high surface of the crypto-crystalline mineral (< 300 $m^2 \cdot g^{-1}$) which is always positively charged within the pH range of its formation (= metastability range: pH 2.3 to 4.5) and contains high amounts of adsorbed sulfate (at least 35 wt.-% of the total mineral sulfate). The electrophoretic determined pH point-of–zero-charge was 6.6. Adsorption experiments of arsenate and chromate to schwertmannite as a function of pH

demonstrated a relatively pH-independent adsorption. As opposed to adsorption, the simultaneously occurring desorption of sulfate strongly depends on the pH-value and increases with increasing pH.

(2) The chemical environment in opencast lakes of lignite mining frequently shows perfect optimal requirements for schwertmannite formation. Hydrochemistry of surface waters, as well as the sediment composition and partly the colloids were examined in 18 acidic mining lakes (AML) located in Lusatia, Middle-Germany and Upper-Palatinate. In order to predict the formation of solid phases in the lakes, chemical processes in surface waters were modelled by chemical equilibrium calculations. Surface-water composition (measured data) served as input for calculations of chemical reactions by the computer program “PhreeqC”. The results showed that nearly all investigated lignite mining lakes are saturated with schwertmannite. Moreover, this mineral is the Fe(III)-controlling solid-phase and it is in a redox equilibrium with most surface waters. These theoretical results were confirmed by mineralogical and chemical analysis of sediment samples which proved that schwertmannite is the primary crystalline phase forming in the acidic lakes.

It was supposed that a steady supply of ferrous iron (caused by groundwater inflow from pyrite containing lignite-dumps) into the oxygen-rich lake water provokes schwertmannite precipitation as consequence of Fe(II) oxidation. The associated release of protons debases the pH of lake water to a value of ~ 3. Due to the high solubility of schwertmannite, further acidification results in mineral dissolution, a reaction which is associated with a release of hydroxide or an increasing pH-value, respectively. Therefore, the cycle of precipitation and mineral dissolution adjusts the pH in the surface waters of these lignite mining lakes to a constant value and in this way schwertmannite acts as pH-buffer.

The orange-coloured layer of several centimetres frequently found at the sediment-water interface of AML, mostly consists of schwertmannite and goethite. It was shown that with increasing sediment-depth the proportion of schwertmannite to goethite decreases in this layer. According to equilibrium calculations, schwertmannite is thermodynamically unstable with respect to goethite, signifying a mineral transformation by time. Sediment analysis confirmed the model assumption that goethite forms with increasing age (or sediment-depth) as a stable transformation product. Enhanced ageing can be achieved by increasing pH found in further depth due to microbial sulfate-reduction. Experimental confirmation of these field observations was obtained by a long-term stability experiment (1 year) with synthetic schwertmannite in dependence on pH. Even at low pH (3-4) transformation to goethite occurred which was accelerated at high pH (5-7).

KURZFASSUNG

Das Eisenoxyhydroxysulfat Schwertmannit [$Fe_8O_8(OH)_6SO_4$] bildet sich in sauren und sulfatreichen Gewässern, die meist in Folge von Sulfidverwitterung entstehen. Im Rahmen dieser Arbeit wurde Schwertmannit mit geochemischen und mineralogischen Methoden charakterisiert. Ziel war es, seine umweltrelevanten Funktionen zu bestimmen. Die Untersuchungen basierten auf Beobachtungen im Gelände und auf Laborexperimenten. Zwei Fragestellungen standen dabei im Vordergrund. Zum einen (1) sollte untersucht werden, ob das Mineral Schwertmannit toxische Stoffe in sich anreichern kann und somit als Giftstoffsenke in natürlichen Systemen fungiert. Anhand der Anionen Arsenat und Chromat wurde die Aufnahmekapazität und der Aufnahmeprozess durch oberflächliche Adsorption oder strukturellen Einbau untersucht. Ferner sind mögliche kristalline Veränderungen von synthetischem Schwertmannit analysiert worden. Auch eine potentielle Remobilisierung dieser Stoffe im Zuge einer Auflösung oder Umwandlung des metastabilen Minerals wurde untersucht. Der andere Schwerpunkt (2) umfasst die Bildung von Schwertmannit im chemischen Milieu saurer Braunkohle-Tagebau-Restlochseen. Dabei sollte seine Bedeutung als pH-Wert Puffer, seine Bildungswahrscheinlichkeit und seine Zeit-abhängigen Veränderungen erklärt werden.

(1) Schwertmannit-Präzipitate, die in ehemaligen Erzbergwerken entnommen wurden, wiesen außergewöhnlich hohe Gehalte an Arsen (bis zu 6700 ppm) und Chrom (bis zu 800 ppm) auf. Da diese Elemente in den dazugehörigen Drainage-Wässern kaum nachgewiesen werden konnten, wurde die Hypothese aufgestellt, daß Schwertmannit sie „herausfiltert“. Unter der Annahme, daß Arsen und Chrom im Redoxmilieu des Schwertmannits vorwiegend in ihrer höchsten Oxidationsstufe als Arsenat und Chromat vorliegen, wurden Kopräzipitations-, Adsorptions- und Stabilitäts-Untersuchungen dieser Anionen mit synthetischem Schwertmannit durchgeführt, Damit sollen stattfindende Wechselwirkungen charakterisiert werden. In den Synthese-, (=Kopräzipitations-) Experimenten zeigte sich, daß Schwertmannit, der normalerweise etwa 12 bis 14 Gew.-% Sulfat enthält (strukturell und adsorptiv gebunden), bis zu 10.4 Gew.-% Arsenat und bis zu 15.4 Gew.-% Chromat inkorporieren konnte. Während eine komplette Substitution des Sulfats durch Chromat ohne wesentliche Veränderung seiner Kristallstruktur möglich war, konnte die Inkorporation von Arsenat nur in Anwesenheit von Sulfat oder Chromat erfolgen. Die Aufnahme der Oxoanionen führte zu einer erhöhten Stabilität des Schwertmannits. Das wurde in Langzeitversuchen unter konstanten pH-Bedingungen nachgewiesen. Sowohl die alterungsbedingte Transformation von Schwertmannit in Goethit, als auch die Auflösung in Folge von Säure-Addition verlangsamte

sich mit dieser wachsenden Stabilität und die toxischen Substanzen wurden in geringeren Konzentrationen (verglichen mit Sulfat) freigesetzt.

Die Aktivität Fe(III)-reduzierender Bakterien führt ebenfalls zur Auflösung von Schwertmannit. Eine Kombination mikrobiologisch und geochemischer Methoden sollte den Einfluss der Oxoanionen-Inkorporation auf die Fe(III)-Reduzierung von Schwertmannit und die damit verbundene Mobilisierung der Oxoanionen quantifizieren. Peine et al. (1998), beschrieben die bakterielle Reduktion des gut verfügbaren Fe(III) des Schwertmannits in Sedimenten und die anschließende Festlegung des Eisens als Fe(II)-Sulfid. Für die hier vorliegende Studie erfolgten die mikrobiologischen Versuche in Zusammenarbeit mit dem Bayreuther Institut für Terrestrische Ökosystemforschung (BITÖK). Die Bakterien *Acidiphilium cryptum* JF-5 (azidophile, fakultativ anaerobe, nicht-fermentative Fe(III) Reduzierer) wurden in ein Medium, das synthetischen, z.T. Arsenat- oder Chromat-haltigen Schwertmannit enthielt, gegeben. Es zeigte sich, daß die Fe(III)-Reduktion des Schwertmannits doppelt so hoch war, wie die des arsenatisiertem Schwertmannits. Eine Mobilisierung von Arsen war kaum nachzuweisen. Chromat erwies sich als toxisch für die Mikroorganismen. Als Nebeneffekt dieser Untersuchungen wurde festgestellt, daß die zur Erforschung mikrobiologischer Prozesse übliche Methode des Autoklavierens, also das Erhitzen auf 121 C (20 min) bei Schwertmannit zu einer Umwandlung zum Goethit führt und diese in Anwesenheit von Chromat oder Arsenat verhindert wird. Diese Ergebnisse bestätigten den stabilisierenden Einfluss von Arsenat und Chromat verglichen mit Sulfat.

Adsorptionsuntersuchungen zeigen, daß Schwertmannit auch nach seiner Synthese hohe Konzentrationen Arsenat und Chromat aufnehmen kann. Zur Unterscheidung der Bindungsart der Anionen in Schwertmannit (adsorptiv oder strukturell) wurden FTIR-spektroskopischen Messungen durchgeführt. Dabei ergab sich, daß sich die Oxoanionen vorwiegend über spezifische bidentate Sorption d.h. als Fe-O-X(O_2)-O-Fe-Komplex (X = S, Cr, As) an das Fe-Hydroxid binden. Mit dieser Methode konnte jedoch nicht zwischen struktureller und adsorptiver Bindung differenziert werden.

Synthese und Adsorptionsexperimente weisen nach, daß Arsen nicht nur in seiner 5-wertigen Oxidationsstufe als Arsenat, sondern auch als 3-wertiges Arsenit von Schwertmannit in vergleichbaren Konzentrationen aufgenommen wird. FTIR-Analysen bestätigten eine Bindung von Arsenit an Schwertmannit.

Aufgrund der großen Bedeutung der Schwertmannit-Oberfläche, die sowohl die Löslichkeit als auch die Adsorptionskapazität des Minerals beeinflusst, wurde die Oberfläche in

unterschiedlichen Experimenten charakterisiert. Es zeigte sich, daß der kryptokristalline Schwertmannit eine sehr hohe Oberfläche besitzt (< 300 $m^2 \cdot g^{-1}$), die innerhalb seines Stabilitätsbereiches (pH 2.5 bis 4.5) stets positiv geladen ist und mit hohen Konzentrationen adsorbierten Sulfats angereichert ist (mind. 35 Gew.-% des Gesamtsulfats). Eine elektrophoretische Bestimmung des Ladungsnullpunktes ergab einen Wert von 6.6. Adsorptionsisothermen von Arsenat und Chromat, eine relativ pH-Wert unabhängige Adsorptionsreaktion. Demgegenüber ist die gleichzeitig erfolgende Desorption von Oberflächensulfat stark pH-Wert abhängig.

(2) Restlochseen des Braunkohletagebaus besitzen häufig das optimale chemische Milieu, das die Vorraussetzung für die Bildung von Schwertmannit ist. Daher wurden im Rahmen dieser Arbeit insgesamt 18 Seen (in der Lausitz, Mitteldeutschland und der Oberpfalz) hinsichtlich der Hydrochemie ihrer Oberflächenwässer sowie der eisenmineralischen Zusammensetzung ihrer Sedimente und teilweise der Kolloide im Seewasser untersucht. Durch eine Modellierung der chemischen Prozesse im Seewasser sollten letztlich Aussagen getroffen werden, welche eisenmineralische Phase sich am wahrscheinlichsten bildet, bzw. welche Festphasen im Gleichgewicht mit der Wasserchemie im See vorliegen. Die hydrochemische Analyse der Oberflächenwässer lieferte dabei die Eingabe-Daten für die chemischen Reaktionen die in den einzelnen Seen stattfinden. Sie werden mit dem geochemischen Modellierungsprogramm „PhreeqC“ berechnet. In nahezu allen untersuchten Restlochseen liegt Sättigung von Schwertmannit vor. Er stellt die Fe(III)-kontrollierende Festphase dar befindet sich im Redox-Geichgewicht mit den Gewässern. Eine Bestätigung dieses Modells durch die Festphasenanalytik konnte für einen Großteil der untersuchten Sediment-Proben erbracht werden. D.h. Schwertmannit stellt die primäre kristalline Phase dar, die sich im Wasser der Restseen bildet und daher für den Eisen-Schwefel-Kreislauf eine tragende Rolle spielt. D.h. bei steter Zulieferung von Fe(II) (durch Grundwasserzuflüsse aus den Pyrit-haltigen Abraum der Braunkohle) in das O_2-reiche Seewasser fällt Schwertmannit bei der Oxidation des Eisens aus. Durch die gleichzeitige Freisetzung von Protonen sinkt der pH-Wert des Seewassers auf ungefähr 3. Aufgrund der hohen Löslichkeit von Schwertmannit, bewirkt eine pH-Wert Erniedrigung unter 2.5 seine mit der Freisetzung von OH^- -Ionen verbundene Auflösung. Somit bewirkt der Kreislauf von Schwertmannit-Fällung und -Auflösung eine Pufferung des pH-Wertes in den Seen.

An der Sediment-Wasser-Grenze bildet Schwertmannit eine meist mehrere Zentimeter dicke, orangerote Schicht, die proportional mit der Tiefe einen zunehmenden Anteil Goethit enthält. Wie Gleichgewichtsberechnungen zeigten, ist Schwertmannit gegenüber den Eisenmineralen

Jarosit und Goethit thermodynamisch instabil. Das bedeutet, daß in älteren Sedimenten und in Abhängigkeit des chemischen Milieus diese Minerale zu erwarten sind. Beobachtungen im Sediment bestätigten die Modellvorstellung, daß mit zunehmendem Alter Goethit als stabiles Produkt der Transformation entsteht. Eine Beschleunigung dieses Alterungsprozesses von Schwertmannit kann durch ansteigende pH-Werte in der Tiefe, aufgrund Sulfat-reduzierender Prozesse, erreicht werden. Eine experimentelle Bestätigung erfolgte durch einen 1 Jahr dauernden Laborversuch, bei dem die Umwandlung bzw. Auflösung des Minerals in Abhängigkeit des pH-Wertes quantifiziert wurde. Es zeigte sich, daß auch bei niedrigen pH-Werten (3 bis 4) Transformation zum Goethit stattfindet. Bei hohen pH-Werten (5-7) wird dieser Prozess beschleunigt.

I. INTRODUCTION

1. STATE OF THE ART

Occurrence

In the surroundings of former mines an orange coloured deposit consisting of an iron(III) and sulfate containing material can be frequently found which precipitates from waters influenced by acid mine drainage (AMD). Until a few years ago these precipitates were scarcely noticed and considered to be amorphous. Though Glockner described the new "Eisensinter" discovered in a mine as early as 1853, its mineral characteristic was only recognised, and an appropriate crystal structure characterised, in 1990 (Bigham et al., 1990). A few years later the compound with the idealised chemical formula $Fe_8O_8(OH)_6SO_4$ was named "Schwertmannite" by the "Commission of New Minerals and Mineral Names" in honour to Prof. Dr. U. Schwertmann.

In a natural environment this mineral normally forms as a product of iron sulfide or pyrite weathering. This complex process of the FeS_2 oxidation was investigated in numerous works (Evangelou & Zang, 1995; Nordstrom et al, 1998) and can be described by several chemical equations. Ultimately the reaction [1-1] of one mol pyrite (FeS_2) with water and oxygen results in the formation of one mol iron hydroxide and two mol sulfuric acid.

$$FeS_2 + 3.75\ O_2 + 3.5\ H_2O \leftrightarrow Fe(OH)_3 + 2\ H_2SO_4 \qquad [1\text{-}1]$$

Thereby the expression "$Fe(OH)_3$" represents a collective term for various Fe(III) oxides, hydroxides and (in the case of simultaneously precipitated sulfate) Fe(III) sulfates which are considered as “secondary minerals of the pyrite oxidation”. Depending on the chemical environment, e.g. the minerals goethite, jarosite, akaganéite, ferrihydrite or schwertmannite can crystallise.

During the last 12 years schwertmannite has been discovered in numerous natural and anthropogenically affected systems. Predominantly, it has been proven in AMD deposits (e.g. Bigham et al., 1994; Yu et al., 1999, Childs et al., 1998). In addition, schwertmannite has been identified in some Australian soils (Cat Clays) by Fitzpatrick & Self (1997) as well as in sediments of an alpine stream in the Zillertaler Alps of Austria (Schwertmann et al., 1995, Ruede et al., 2000). Even assumptions that the red soils of the planet Mars contain schwertmannite can found (Bishop, 1996). In 1998 Peine and Peiffer proved the existence of this mineral in the sediment of an acidic lignite open-cast lake (ML 77, Lausitz) and set up the

hypothesis that it has great importance in this lake as a buffer for the pH value. Among other things this assumption is questioned in this study.

Characteristics

Schwertmannite is a mineral of "weak crystallinity" which affects its difficult identification. This can be explained by its crystal structure as described by Bigham et al. (1990) which was found to be isostructural to the mineral akaganéite (β-FeOOH). This structure consists of chains of iron(III)oxide- and hydroxide-octahedra which are partly connected in a certain manner to form cavities between them. (An exact description of the crystal structure is presented in the introduction of chapter II.2, pp. 8-10.) In these cavities anions are stored which predominantly consist of chloride in the case of akaganéite and of sulfate in the case of schwertmannite. The storage of sulfate causes a small shift in lattice constants or in preferential crystal growth direction, respectively. Thereby a "new" mineral forms which can be distinguished from akaganéite (in chapter II.2 of this thesis, the crystal structure of schwertmannite is described in detail).

The specific characteristics of schwertmannite, enumerated in the following section can be explained by its crystal structure (Bigham et al., 1990). They form the basis for the questions and interpretations in my thesis.

- **Sulfate Substitution:** The cavities within the structure of schwertmannite are normally occupied by sulfate which can (probably) be exchanged by other oxyanions.
- **Morphology and Surface:** Due to the preferred crystal growth direction, the schwertmannite crystals are extremely thin and needle shaped. They agglomerate to "hedge-hog" particles with a diameter of ~ 200 nm and a large surface area of 125 to 250 $m^2 \cdot g^{-1}$.
- **Adsorption Capacity and Solubility:** The high surface area and small particle size result in a high surface reactivity. About 30 % of schwertmannite sulfate is surfacially bound.
- **Chemical Environment:** The formation of schwertmannite in a Fe(III) solution requires a sulfate rich (> 5 $mmol \cdot l^{-1}$) as well as an oxic and acidic (pH 2.5 to 4.5) milieu.
- **Metastability:** Depending on both, time and pH of a schwertmannite suspension, this mineral either dissolves [1-2] or transforms into the thermodynamically more stable mineral goethite [1-3] (Bigham et al., 1996). Therefore, in natural systems, schwertmannite is usually associated with goethite (FeOOH) and is not be found in older sediments (> 10 a).

$$Fe_8O_8(OH)_6SO_4 + 22\ H^+ \rightarrow 8\ Fe^{3+} + SO_4^{2-} + 14\ H_2O \qquad [1\text{-}2]$$

$$Fe_8O_8(OH)_6SO_4 + 2\ H_2O \rightarrow 8\ FeOOH + 2\ H^+ + SO_4^{2-} \qquad [1\text{-}3]$$

The denotation “stability range” of schwertmannite marks the pH range within which schwertmannite can form and within which this mineral is most stable for a long period of time (few years).

2. OBJECTIVES

In this dissertation the mineral schwertmannite is characterised with respect to the following aspects:

- It can be assumed that schwertmannite is able to enrich a multiplicity of (potentially toxic) compounds by sulfate substitution and/or adsorption. Thus this mineral could be of great importance as a sink in acidic waters. However, as a consequence of ageing or due to changes of the hydrochemical environment, schwertmannite dissolves or transforms into another mineral. Thereby schwertmannite could release the previously enriched elements and thus (also) act as source for these potentially toxic compounds. Consequently, a neutralisation of acidic waters could entail an increase of their toxicity. Therefore one object of this study was to describe and quantify the geochemical interactions between schwertmannite and the toxic anions arsenate and chromate.

- Schwertmannite forms in the hydrochemical environment of acidic iron- and sulfate-containing waters. These conditions frequently exist in lignite mining opencast lakes. In Germany large areas are confronted with the consequences of lignite mining. Therefore for some years the exploration of the processes in these lakes have been the object of many research projects. The goal of my study was to characterise the formation process and the formation probability of schwertmannite in these acidic mining lakes (ML). In a broader sense the general processes of crystallisation, dissolution and transformation of schwertmannite should be analysed.

3. ARRANGEMENT OF THIS WORK

This thesis consists of two sections (II. and III.) in which different aspects of the schwertmannite characterisation are considered.

Section II concerns itself with the geochemical interactions between schwertmannite and the oxyanions chromate and arsenate. Firstly, the general importance of arsenate and chromate (**chapter II.1**) are introduced. Subsequently, (**chapter II.2**) the extent to which arsenate and chromate can be taken up from schwertmannite and the corresponding effects and changes on its crystal structure and stability are considered. These investigations were accomplished almost exclusively in the laboratory using synthetic schwertmannite. The characterisation of schwertmannite is predominantly based on measurements of powder X-ray diffraction.

In coprecipitation- and adsorption-experiments the enrichment of arsenate and chromate in schwertmannite was examined and long-term stability experiments should supply evidence about the release of toxic oxyanions. In order to investigate the significance of schwertmannite as sink or source for arsenic and chromium in the environment, schwertmannite precipitates were sampled from acidic mine drainage waters of two former ore mines and analysed for their arsenic and chromium content.

Chapter II.3 monitors investigations about the mode of the oxyanion binding to schwertmannite using the method of FTIR spectroscopy. C**hapter II.4** presents the results of a preliminary study which examined the incorporation of arsenite into schwertmannite.

The research presented in **chapter II.5** concerns the reduction of Fe(III) in schwertmannite under anoxic conditions by micro-organisms. In former studies bacteria (*acidiphilium cryptum* JF-5) were isolated from sediment samples and schwertmannite reduction in the natural environment was investigated (Kuesel et al., 1999 and Peine et al., 2000). It has been stated that these bacteria use the easily available Fe(III) of schwertmannite as an energy supplier. In my examinations the influence of arsenate and chromate incorporation in schwertmannite on the bacterial Fe(III) reduction of the mineral were analysed.

Investigations on the surface properties of schwertmannite are presented **in chapter II.6**. For comparison, most experiments in this study were performed with synthetic goethite, too. The mineral surfaces were characterised using different methods as BET-surface measurements, scanning electron microscopy (SEM) and electrophoretic measurements of surface potential. Additionally acid-base titration in batch attempts were performed. Thereby adsorption isotherms were constructed as a function of adsorbate and adsorbent concentrations as well as depending on the pH value.

The second focus of my work which involves investigations on the formation and stability of schwertmannite in the geochemical environment of acidic lignite opencast lakes, is presented in **section III.**

Based on the thesis of Ariane Peine (1998) in which schwertmannite was proven for the first time in one lignite mining lake (ML 77, Lausitz), in my study a multiplicity of mining lakes (18) were examined for schwertmannite.

Thereby the object was to find out under which conditions schwertmannite forms, which mechanisms control its crystallisation, how frequently it occurs in the mining lakes and which importance schwertmannite possesses as a buffer for the pH-value in nature. Beside extensive sampling and the analysis of water and sediment, this part of my thesis contains a geochemical modelling to calculate the (expected) iron(III) solid phase.

The metastability of schwertmannite referring to goethite has been characterised in the sediment of one lake ("ML 77") and compared to results of a long-term stability experiment with synthetic schwertmannite in order to contrive information about the kinetics of schwertmannite transformation.

Finally (**IV**), a summary and a conclusion of all obtained results, including a short outlook for future necessities and suggestions of research, are presented.

II. GEOCHEMICAL INTERACTIONS BETWEEN SCHWERTMANNITE, CHROMATE AND ARSENATE

1. MOTIVATION TO INVESTIGATE ARSENATE AND CHROMATE

Part II of this thesis illustrates the geochemical interactions between the mineral schwertmannite and the oxyanions arsenate and chromate. This chapter (II.1.) gives a short characterisation of these ions and explains thereby the motivation why arsenate and chromate were chosen for investigations referring to schwertmannite.

It is well known that hydrous oxides of iron are important sorbents for toxic anions in soils and water. As will be explained in the following, schwertmannite probably is one of the most significant immobilisers of some of these hazards. The Fe(III)-sulfate mineral schwertmannite approximately contains 12 wt.-% of sulfate (Bigham et al., 1990). Two thirds of this amount are directly incorporated into its crystal lattice, i.e. it is covalently bound to the iron hydroxide and called “structural sulfate”. The other third is specifically and/or unspecifically adsorbed to the mineral surface. This study is bound to answer the question if the structural and the surface bound sulfate, respectively, can be exchanged with other oxyanions by substitution or adsorption. In case of an enrichment of the toxic oxyanions arsenate and chromate, schwertmannite could function as a sink for these substances and by inhibiting their mobility, it would have great significance in natural waters.

Arsenic and chromium are two important poisons that enter the environment primarily due to anthropogenic activities. In Table II.1-1 some characteristics of As and Cr are listed. As schwertmannite they frequently occur in the environment of acid mine drainage. In oxygenated systems they dominante as AsO_4^{3-} and CrO_4^{2-} and thus are as tetrahedrally coordinated (Fig. II-1) as sulfate which is, as mentioned above, a part of the crystal structure of schwertmannite. Since they have a similar ionic radius as sulfate (0.23 nm, Tab. II-1), it was assumed that these ions can substitute the sulfate in schwertmannite.

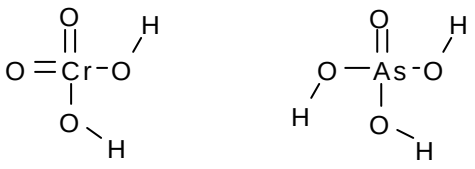

H_2CrO_4 H_3AsO_4

Fig. II.1-1 Coordination of the molecules chromate (or sulfate) and arsenate (or phosphate).

Because of the hazards invoked by arsenate and chromate - both oxyanions are potentially carcinogen - processes that remove these species from the aqueous phase and limiting their bioavailability are desirable.

Table II.1-1 Selection of some ecological-relevant characteristics of arsenic and chromium.

	As	Cr	Reference
mean content in the earth crust	1.8 (ppm)	100 (ppm)	Mason & Moore, 1990
occurrence in minerals	arsenopyrite (FeAsS), realgar (As_4S_4), oripiment (As_2S_3), frequently contained in pyrite (FeS_2)	chromite ($FeCr_2O_4$), frequently Cr^{3+} substitutes Fe^{3+} in iron minerals	Matthes, 1996
background value for soils	20 (ppm)	100 (ppm)	Hollandliste (1988)
limit in water	0.01 (ppm)	0.05 (ppm)	TrinkwV (1990)
damage for humans	carcinogenic for skin, lung (liver, mark), enrichment in the body	carcinogenic for skin, lung (liver, mark)	Fendorf et al., 1997
environmental input	pesticides, AMD, geogen	industries of paints and textiles, AMD	
toxic oxyanions	AsO_4^{3-} (arsenate), AsO_3^{3-} (arsenite, ~10-fold more toxic than arsenate)	CrO_4^{2-} (chromate), $Cr_2O_7^{2-}$ (dichromate)	
Ionic radius	AsO_4^{3-}: 0.248 nm	CrO_4^{2-}: 0.24 nm	Wilkinson, 1987
mobility of oxyanions in soils	arsenate: low mobile; increased mobility during reduction to arsenite	very mobile: low retention in soils, hardly biologic. degradable	Fendorf et al., 1997
miscellaneous		strong oxidant, corrosive	WHO, 2000

Other oxyanions of As and Cr occurring in natural environments

At a low pH chromate partly dissociates to **dichromate** ($Cr_2O_7^{2-}$) and in the environment of schwertmannite formation (pH 2.5-4) about 50 % of Cr(VI) is present as dichromate. The dichromate molecule consists of 2 chromate tetrahedra, linked by a joint oxygen atom (Holleman & Wiberg, 1985). Both anions are strongly toxic (WHO, 2000), form hardly soluble complexes with divalent cations and act as oxidising agents in acidic solutions. In this study the two anions of Cr are not distinguished because they differ only slightly and it was not possible to quantify $Cr_2O_7^{2-}$ (by photometry) in schwertmannite extracts. Therefore results represented in this study concerning chromate, include always the sum of both Cr(VI)-salts.

In As-polluted systems, additionally to arsenate, the more toxic and very mobile, trivalent **arsenite** (AsO_3^{3-}) is of great importance. In the oxic environment of schwertmannite-formation, arsenate should actually dominate. However, due to the slow oxidation kinetics of arsenite, it possibly could occur together with schwertmannite. Therefore, it was considered in some experiments of this study. The results are summarised in chapter II.4.

2. EFFECTS OF ARSENATE AND CHROMATE INCORPORATION ON THE SCHWERTMANNITE STRUCTURE

2.1 Introduction

Iron(III)oxides and hydroxides in soils and sediments are of major environmental importance, because they often bind toxic elements and thus reduce their mobility and availability (Scheffer & Schachtschabel, 1992). This is why they are frequently present as very small crystals (< 100 nm in size) with a large and reactive surface area (Schwertmann & Fitzpatrick, 1992). At their surface they carry functional groups which can adsorb lots of ions and molecules (Stumm & Morgan, 1996) and thus function as a filter for hazardous materials. Schwertmannite, an oxyhydroxysulfate of iron, is particularly suitable for acting as a sink for toxic oxyanions, because additionally to its large surface (100-200 $m^2 \cdot g^{-1}$, Bigham et al., 1994) it has a special crystal structure which could favour their incorporation.

2.1.1. Schwertmannite Structure and Formation

Schwertmannite is of weak crystallinity and therefore difficult to identify and was therefore unknown until few years ago. Based on X-ray diffraction (XRD), Mössbauer and Infrared spectroscopy, Bigham et al. (1990) described its structure as isostructural to the mineral akaganéite (β-FeOOH). This seems obvious when the XRD patterns of schwertmannite and akaganéite are compared (Fig. II.2-1).

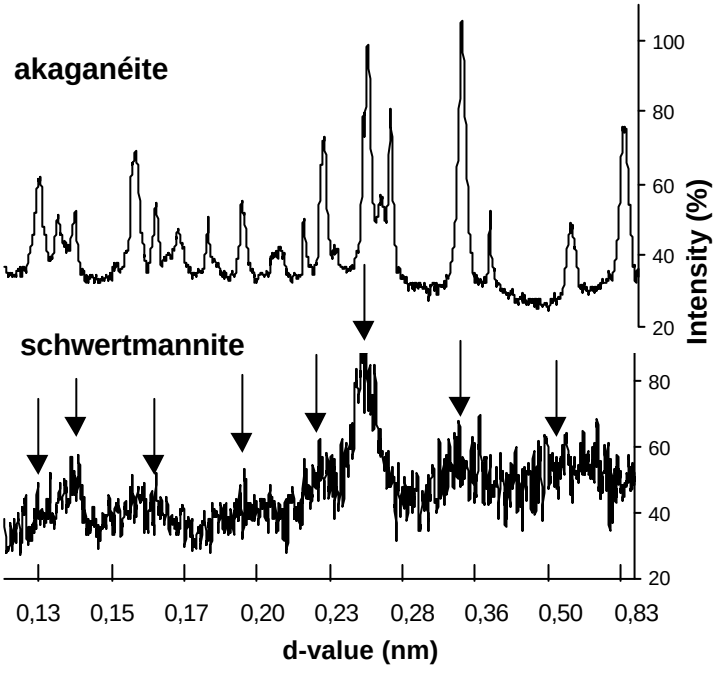

Fig. II.2-1 Powder X-ray diffraction pattern of synthetic akaganéite and schwertmannite. Arrows mark the positions of the eight XRD-peaks of schwertmannite as described by Bigham et al. (1990).

The diffractogram of schwertmannite consists of eight broad peaks which are located at the same positions as those of akaganéite. Therefore, it was assumed that the structure for both minerals is almost the same (Bigham et al., 1990). The akaganéite structure is well known and was described by Murad (1979) based on a crystallographic tetragonal unit cell (cell parameters: a_0=1.054, c_0= 0.303 nm). Other authors described the unit cell as monoclinic (Table II.2-1) with a monoclinic angle of 90.63° (Cornell & Schwertmann, 1996). Anyway, the unit cell consists of 8 $FeO_3(OH)_3$-octahedra forming double chains which are shared over edges and run parallel to the b-axis. They share corners with adjacent chains and thus enclose cavities (Fig. II.2-2). There is one tunnel cave per unit cell with a diameter of 0.5 nm^2 into which anions with a maximum diameter of 0.35 nm (normally chloride) are incorporated. However, also large sulfate molecules (0.46 nm in diameter) can be incorporated as confirmed by infrared studies. By this method the formation of bridged bidentate complexes (-Fe-O-SO_2-O-Fe-) inside these structures were proven. It was assumed (Bigham et al., 1990) that two of the oxygen atoms of sulfate get directly connected to the oxygen atoms of the Fe octahedra (Fig.II.2-2), whereas sulfur and the two “free” oxygen atoms occupy consecutive cavities parallel to the tunnel axis (b-axis) (Bigham et al., 1994).

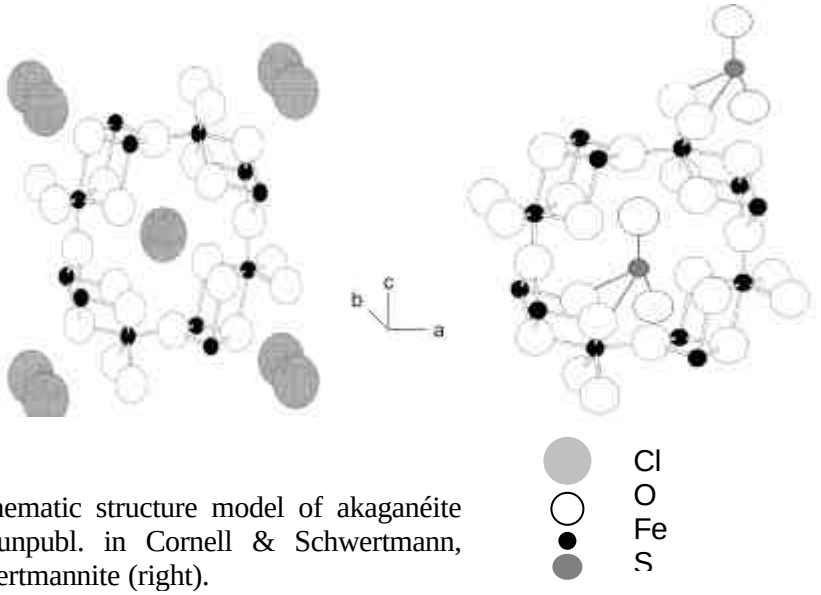

Fig. II.2-2 Schematic structure model of akaganéite (left; Stanjek, unpubl. in Cornell & Schwertmann, 1996) and schwertmannite (right).

Due to the larger size of the sulfate the structure distorts in the a-dimension and consequently the c_0-unit in the tetragonal unit cell doubles from the b_0-unit 0.303 nm in monoclinic akaganéite and becomes a 0.604 nm c_0- unit in tetragonal schwertmannite, as shown in Table II.2-1. The unit cell distortion also results in a limited crystal growth direction which affects a length growth (up to 200 nm) parallel to the c-axis and perpendicular to a thickness of only

some nm. Accordingly, the habit of schwertmannite crystals is marked by long, thin needles which agglomerate to “hedgehog” -similar particles with the mentioned very high surface area and corresponding high reactivity. This results in the characteristic features of schwertmannite as high adsorption capacity, good solubility and metastability. Sulfate is as well bound into the structure of schwertmannite (“tunnel sulfate”) as adsorbed onto its surface in a ratio of ~ 3:1 (Bigham et al., 1990).

Table II.2-1 Crystallographic cell parameters of schwertmannite, akaganéite, goethite and chromated schwertmannite (sample Sh-Cr-10).

mineral	**crystallographic system**	**dimension of the unit cell (nm)**			**reference**
		a	**b**	**c**	
schwertmannite	tetragonal	1.066	1.066	0.604	Bigham et al. (1994)
akaganéite	monoclinic (β: 90.63°)	1.056	0.303	1.048	Cornell & Schwertmann (1996)
	tetragonal	1.054	1.054	0.303	Murad (1979)
goethite	orthorhombic	0.461	0.996	0.302	Cornell & Schwertmann (1996)
Sh-Cr-10	tetragonal	1.044	1.044	0.302	this study

The XRD pattern of schwertmannite reflects its weak crystallinity which is caused by its limited crystal growth. Compared to the pattern of akaganéite, the total peak intensity (or the X-ray diffraction interferences) in the schwertmannite pattern is much lower and the width of the peaks is broader. Moreover, some differences in peak location (the d-values) between the two minerals can be observed in their X-ray diffraction patterns (Table II.2- 2, Fig.II.2-1).

Bigham et al. (1990) interpreted these changes as a consequence of sulfate incorporation in the akaganéite structure. Thereby the akaganéite characteristic peak at the d-value of 0.739 nm disappears and the peak located at 0.53 nm in akaganéite shifts to 0.471 nm in schwertmannite.

Other ions instead of and in addition to sulfate can be enriched in schwertmannite. This has been previously established for the high adsorption capacity of heavy metals by Webster et al. (1998). Anions probably adsorb in higher amounts due to the generally positive charge of iron minerals (Cornell & Schwertmann, 1996).

Bigham et al. (1990) showed that a total substitution of selenate, an oxyanion similar to sulfate in ionic radius and charge, is possible. Therefore it was hypothesised that other comparable oxyanions have the same effect. In this study the exchange of structural and adsorbed sulfate by the toxic oxyanions arsenate and chromate is investigated.

Table II.2-2 X-ray diffraction data of akaganéite and schwertmannite (Cornell & Schwertmann, 1996) compared to chromated schwertmannite (Sh-Cr-10), measured by H. Stanjek (TU-Munich). Peak position: d-value (d) in nm, crystallographic interpretation (hkl) and relative peak intensity (I) in %.

akaganéite			schwertmannite			sample Sh-Cr-10		
d	**hkl**	**I**	**d**	**hkl**	**I**	**d**	**hkl**	**I**
0.740	110	100	0.194	411	60			
0.525	200	40	0.185	440	10	0.486	200, 111	37
0.370	220	10	0.175	600	40	0.339	310	46
0.331	310	100	0.172	501, 431	10	0.255	212	100
0.262	400	40	0.163	521	100	0.228	302	23
0.254	211	80	0.151	002	40	0.195	412	12
0.234	420	20	0.149	611	20	0.166	522	21
0.228	301	40	0.148	112, 710	20	0.151	004	24
0.209	321	20	0.146	640	10	0.146	204, 542	18
0.206	510	20	0.142	541	80			
			0.137	730	40			

sample Sh-Cr-10		
d	**hkl**	**I**
0.738	110	56.7
0.522	200	43.5
0.330	310	100
0.247	400	49.1
0.228	212	97.8
0.194	301	34.6
0.163	521	29.3
0.151	002	11.1
0.143	541	5.6

Schwertmannite forms under oxic, acid, sulfate- and iron- rich conditions (Bigham et al., 1994). At pH values between 2.5 and 4.5 the Fe(III) in water is predominantly available as a Fe(III)sulfate complex (Music et al., 1981) promoting the crystallisation of schwertmannite. The requirements for schwertmannite formation are frequently given in environments influenced by acid mine drainage, because their chemical conditions are a consequence of pyrite (FeS_2) oxidation (Evangelou & Zhang, 1995). Schwertmannite is a metastable mineral which means that by time or in consequence to changes in pH a dissolution or transformation to goethite can be expected (Bigham et al., 1996). Thereby, potentially enriched toxic elements will be released.

2.1.2. Investigated Oxyanions

Arsenic and chromium are two environmental poisons, frequently occurring in combination with acid mine drainage, in natural systems. Both are often found included in pyrite. Arsenic additionally forms sulfidic minerals associated to pyrite, such as arsenopyrite (FeAsS), realgar (As_4S_4) or orpiment (As_2S_3) (Matthes, 1996) which oxidise in a similar way as described for pyrite. Sulfide weathering results in a release of incorporated toxic elements. Arsenic and chromium occur in the redox environment of schwertmannite mostly in their highest oxidation level as AsO_4^{3-} and CrO_4^{2-}. In these forms they are tetrahedrally coordinated and their ionic radius and charge is similar to SO_4^{2-} (Table II.2-3).

Due to this similarity they could either completely or partly substitute the sulfate in schwertmannite. It has been hypothesised that schwertmannite immobilises these oxyanions by adsorption or substitution. In addition to chromate and arsenate, some experiments were performed with phosphate (PO_4^{3-}) and molybdate (MoO_4^{2-}) to gain more exact information on the influence of ionic radius and charge for the substitution. The geometric features of these ions are presented in Table II.2-3.

Table II.2-3 Ionic charge and radius of certain anions (Wilkinson, 1987; Gmelin, 1954).

anion	**Cl^-**	**SO_4^{2-}**	**CrO_4^{2-}**	**AsO_4^{3-}**	**PO_4^{3-}**	**MoO_4^{2-}**
charge	-1	-2	-2	-3	-3	-2
ionic radius (nm)	0.18	0.23	0.24	0.248	0.238	0.246

However, arsenate and chromate were predominantly investigated because of their high toxicity to organisms (both are highly carcinogenic). Chromate is very mobile, only slightly retentionable in soils and it is hardly available for micro organisms. Its input is mainly caused by industries of paints and lacquers or mining activities (WHO, 2000). In the environment arsenate frequently occurs due to human activities (pesticides, paints or mining) or in a consequence to geogen conditions. Arsenic represents an acute problem for the drinking water quality in many countries as described for lots of regions world wide, for example Western India, Bangladesh or Taiwan (Chatterjee, et al., 1995; Chowdhuri et al., 2000; Lu, 1990).

The object of this study is to characterise the geochemical interactions between schwertmannite and the anions arsenate and chromate with regard to their substitution, adsorption and time depending stability. Arsenate and chromate incorporation in schwertmannite should have been quantified and compared to resulting changes in crystal structure. Examinations of the processes during schwertmannite formation and changes of its structure over time in dependence to the incorporated oxyanions, should explain the type (structural or adsorptive) and influence of the oxyanion bonding on schwertmannite stability.

2.2. Materials and Methods

2.2.1. Mineral Synthesis

Schwertmannite was synthesised by two methods: (1) According to Bigham et al. (1990), 2 L of deionised water were heated in an oven to 60°C. After adding 10.8 g $FeCl_3 \cdot 6H_2O$ (~ 40 mM Fe^{3+}) and 3 g Na_2SO_4 (~ 10 mM SO_4^{2-}) the solution was kept for further 12 minutes at 60 °C. The suspension was cooled down to room temperature and dialysed (Serva dialysis bags, pore radius of 2.4 nm) against deionised water (~ 4 L) which was renewed on a daily basis over a period of 33 days. After this time the measured electric conductivity in this "dialysis water" was constantly < 5 µS indicating that no further ionic exchange had taken place. The produced amount of schwertmannite, weighed after freeze drying, was 1.9 g. In this study this technique was termed "synthesis in Fe(III)-solutions ". The other schwertmannite synthesis-method (2) after Pentinghaus (pers. commun.) was termed the "oxidative synthesis". $FeSO_4$ was dissolved in deionised water (several grams per L) and some mL of H_2O_2 (32 %) were added to accelerate the oxidation of Fe^{2+} to Fe^{3+}. The precipitated orange coloured solid consisted of pure schwertmannite. Variation of the two synthesis methods was reached by the addition of different concentrated oxyanions (Na_2CrO_4, $Na_3PO_4 \cdot 12\ H_2O$ und $Na_2HAsO_4 \cdot 7\ H_2O$) into the synthesis solution. In Table II.2-4A, -4B and -4C the different synthesis solutions are presented.

The mineral formation process for the "synthesis in Fe(III) solutions" was observed in several samples over time by continuously measuring the pH and the concentrations of iron(tot), sulfate, arsenic, chromium and phosphate in the synthesis solution. Thereto each few days aliquots of 5 mL were taken from the suspensions in the dialysis bags and analysed. After 10 and after 18 days volumes of 50 mL were removed, filtrated and the filter residue was examined by X-ray diffraction (see below).

Synthetic goethite (α-FeOOH) was produced by adding 180 mL 5 M KOH to 100 mL 1 M $Fe(NO_3)_3$ solution (Cornell & Schwertmann, 1996). Thereafter the suspension was diluted to 2 L with bidestilled water and held in a closed glass vessel in an oven at 70 °C for 60 h. Finally the yellow precipitate was washed twice and dried at 50 °C.

To precipitate akaganéite (β-FeOOH) 2 L of a 0.1 M $FeCl_3$ solution were kept in a closed vessel at 70°C for 48 h. During this time the pH value dropped from 1.7 to 1.3 and ~5 g of the yellow mineral akaganéite was formed (Cornell & Schwertmann, 1996).

Bigham et al. (1994) determined the water content in schwertmannite to ~ 0.63 mol H_2O per mol Fe. This amount is not constant and could disturb some measurements. Therefore, it was completely eliminated by freeze drying all samples in my experiments. A comparison of the XRD patterns showed no differences between the water free and the hydrated samples.

2.2.2. Analytical methods

The synthesised samples, ground to a homogeneous powder, were mineralogically identified by powder X-ray diffraction (XRD) using a Co-K$\alpha_{1,2}$ radiation with a Siemens D 5000 X-ray goniometer (40 kV, 40 mA) and with silicon as internal standard. The specimen were step scanned from 10° or 20° to 80° 2θ in increments of usually 0.02° θ with 2 or 8 s counting time. The peak maxima were directly read from the diffractogram. Mineral components were determined by the library evaluation programme DiffracAT Vers. 3.3. Schwertmannite was identified by comparison with a synthetic schwertmannite standard. This reference-diffractogram was identical to the one described for schwertmannite according to Bigham et al. (1990). The program winfit (beta release 1.2.1) was used for further processing of the diffractograms. The unit cell edge-lengths of the sample Sh-Cr-10 were calculated by H. Stanjek, TU Munich with the program GITTER.
Scanning electron micrographs (SEM) were obtained by a Leo 1530 electron microscope (zircon oxide radiation source on wolfram wire) which had an optical resolution of few nm. The samples were covered with a platinum layer before measurement.

The chemical composition of the solid samples with the crystal structure of schwertmannite was determined after extraction in 1 M HCl (1 $g \cdot L^{-1}$). In the extracts and in the aquatic phase Fe(tot) was measured by flame atomic absorption spectrometry (Varian/Spectr-AA-20), S(tot) and P(tot) by ICP-AES (Integra-XMP-GBC) and As(tot) and Cr(tot) by graphite tube AAS (Varian/Spectr-AA-30, GTA-96). Detection limits were 0.5 ppm for Fe(tot), 0.2 ppm for S(tot), 0.3 ppm for P(tot) and each 5 ppb for As(tot) and Cr(tot). In the aquatic phase sulfate and phosphate were determined by ionic chromatography (Metrohm IC Separation Center 733) with a detection limit of 30 $\mu mol \cdot L^{-1}$.

2.2.3. Stability Experiment

Samples of schwertmannite and of schwertmannite containing arsenate, chromate and phosphate (Sh, Sh-S-As-1, Sh-S-P-1, Sh-S-Cr-1, Sh-Cr-10) were prepared by the synthesis in

Fe(III)-solutions (the compositions are presented in Table II.2-4A). After 30 days of dialysis, the suspensions were filled from the dialysis bags into glass vessels. Each two parallels of the five different suspensions were produced. Subsequently, pH values of 2 and 4, respectively, were adjusted by adding of different amounts of HNO_3 or NaOH in each of the parallels. Table II.2-5 (page 24) shows the titrated concentrations and the pH for each sample. The closed vessels were homogeneously stirred at 20 °C (± 0.1 °C). On a daily basis the pH was controlled and adjusted to constant values of 2 or 4 by adding of acid or base. The added concentrations were reported. Occasionally (every few days) certain volumes of the suspensions (either 10 or 50 mL) were taken for analysis. After the defiltration of the solid part (blue ribbon filter), sulfate, iron, arsenic and chromium were measured in the filtrate. Ionic activities were calculated by the Davies approximation. The crystallinity of the ten samples was analysed by XRD at the end of the experiment. About every two weeks FTIR-spectra of the filtrated solid were recorded with a Fourier Transform infrared (FTIR) spectrometer between 7500 and 370 cm^{-1} and with 1 cm^{-1} resolution. Samples were measured as KBr pellets (1 % sample).

Measured concentrations obtained during this study at pH 2 were used to determine the ionic activity product (IAP) of schwertmannite in dependence on its composition. It was calculated (eq. 2-1) in analogy to the solubility window according to Bigham et al. (1996).

$$Fe_8O_8(OH)_x(SO_4)_y + (24-2y)H^+ \rightarrow 8\ Fe^{3+} + y\ SO_4^{2-} + (24-2y+x)/2\ H_2O \qquad [2\text{-}1]$$

$$\text{Log } K_{Sh} = 8 \text{ Log } aFe^{3+} + y \text{ log } aSO_4^{2-} + (24-2y)\cdot pH\ ; \qquad IAP_{Sh} = 18.0 \pm 2.5$$

2.2.4. Adsorption Experiment

The specific surface area of the synthetic samples was measured by N_2 adsorption with a Gemini 2370 V1.02. according to the BET-method (Brunauer et al., 1938).

In order to investigate the adsorption capacity of schwertmannite, aliquots (25 mL) were produced containing 10^{-4} M or 10^{-3} M chromate or 10^{-4} M, 10^{-3} M or $5\cdot10^{-3}$ M arsenate and KNO_3 (c=0.1 M) as inert electrolyte. Therein 1 or 4 $g\cdot L^{-1}$ freeze dried schwertmannite samples were suspended. Subsequently different pH values were adjusted by addiing of HNO_3 or NaOH. During the addition of the components the vessels were gazed with N_2 to prevent sorption of carbonate or hydrogencarbonate to the surfaces. Samples were constantly shaken at 20 °C over 24 h. Finally, the suspensions were filtrated (0.45 µm) and sulfate, arsenate and chromate were measured in the filtrate.

2.2.5. Natural Specimens

Samples of water and precipitate were collected in the summer 2000 from two different mines in which ores were exploited over centuries. The geology of both mines is marked by palaeozoic, crystalline rocks with veins of sulfidic ores such as pyrite, chalkopyrite or arsenopyrite. As secondary minerals in high concentrations sulfates were found, such as gypsum, diadochite or barite (Rüger, et al., 1994, Maly, 1999).

The former alaun-schist mine "Saalfelder Feengrotten" is located in Thuringia (Germany) in the south of Saalfeld/ Saale (Fig.II.2-3). The pyrite rich schists (under silur) are located as inter-bedded strata with quartzite. The mining area "Prybyslav" where predominantly silver has been exploited during the middle ages is located 50 km NE of Jihlava (Czech Republic, Fig. II.2-3). The sulfidic ores are contained in moldanubic tectonically stressed paragneisses (Maly, 1999).

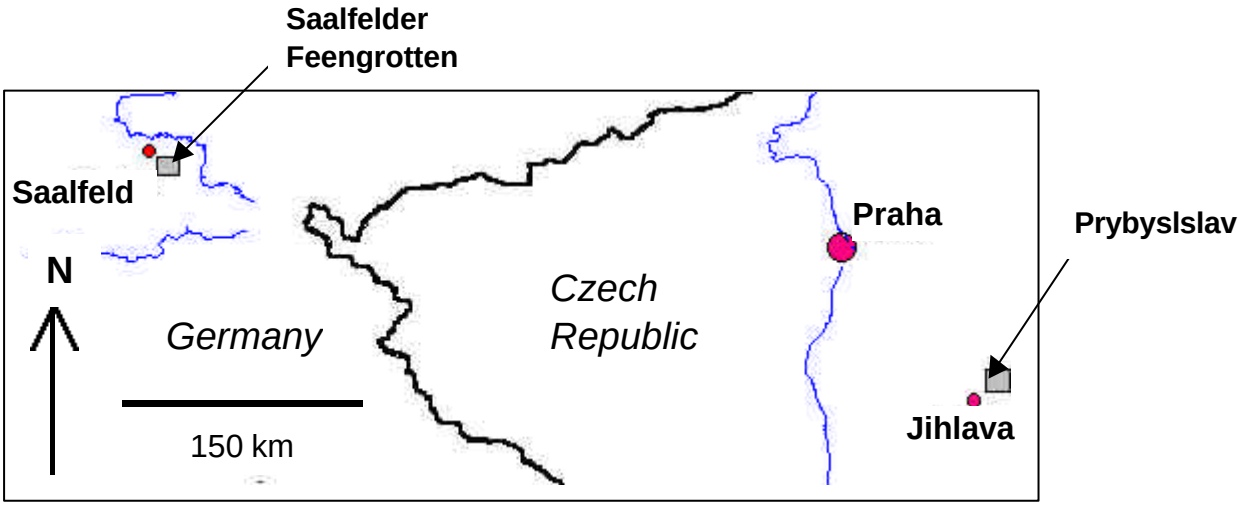

Fig. II.2-3 Location map of the sampling sites: The two former mines "Saalfelder Feengrotten" in Germany and "Prybyslav" in the Czech Republic.

Samples of orange-red precipitates occurring as crusts and stalactites, as well as drainage water, were taken in each mine at about 10 different locations.

In the laboratory precipitates were freeze dried and their mineralogical composition analysed by XRD. In case of the schwertmannite identification, the samples were extracted over 15 min with NH_4 oxalate (pH = 3) in the absence of UV radiation of light in order to dissolve solely the weak crystalline Fe(III) mineral (Carlson & Schwertmann, 1981, Bigham et al., 1990). In the extracts the total concentrations of Fe, S, As and Cr were measured.

2.3. Results

2.3.1. X-Ray Diffraction Data

The method of powder X-ray diffraction (XRD) was used to prove schwertmannite formation and to describe changes in its crystal structure which could be a result either of the used synthesis method or the different synthesis solution composition. No differences were observed between samples produced by the "oxidative synthesis" and the "synthesis in Fe(III)-solutions". Both diffractograms showed the characteristic schwertmannite pattern, marked by eight broad peaks (Fig. II.2-1).

Variation in the sample composition was reached by adding of different amounts of arsenate, chromate, phosphate and molybdate into the synthesis solution. In Table II.2-4 these compositions are presented. Incorporation of arsenate during the precipitation of schwertmannite strongly influenced the XRD pattern of the resulting sample. As shown in Fig. II.2-4, an increasing ratio of As:S in the synthesis solution or in the resulting solid sample (Sh-S-As-1, S-As-2.5, S-As-5 and As-10) effected the disappearance of all schwertmannite-characteristic peaks.

While the diffraction pattern of the sample Sh-S-As-1 (with 5.6 wt-% As and 2.77 wt.-% S) was still identical to pure (As-free) schwertmannite, sample S-As-2.5 already showed some differences:

the XRD-peaks were broader, the background noise were stronger and a new broad peak with a maximum at 0.32 nm formed. Further addition of arsenate enhanced this effect: the schwertmannite structure disappeared and two new peaks (0.32 and 0.16 nm) developed.

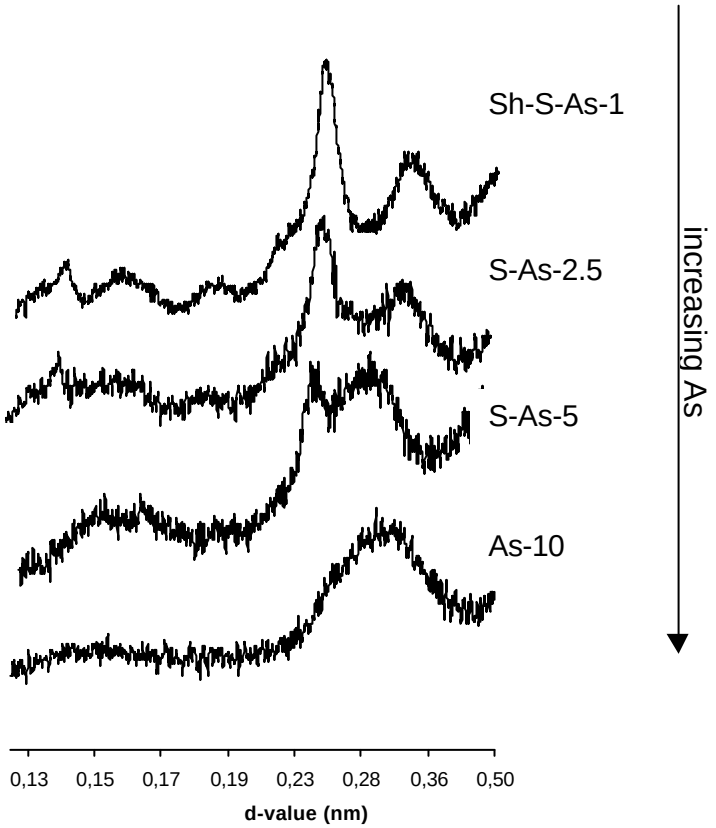

Fig. II.2-4 X-ray powder diffraction pattern of samples, nthesized with increased As:S-ratio in the synthesis solutions.

This indicated the formation of a new solid iron-arsenate phase of very low crystallinity.

Therefore, the prefix “Sh” in front of the sample name which indicated an evidence of schwertmannite crystallinity by XRD, was not used for samples with high arsenic content. The maximum content of arsenate in a synthesis solutions still resulting in the formation of schwertmannite probably amounts to between 0.8 and 1 mmol·L^{-1}.

An increased phosphate concentration in the synthesis solution of schwertmannite had the same effect in the XRD pattern as demonstrated for arsenate. The schwertmannite crystallinity decreased and two new peaks formed at the same location as demonstrated for the arsenated samples (see appendix A).

In contrast to phosphate and arsenate, a complete exchange of sulfate by chromate in the synthesis solution of schwertmannite provoked the characteristic XRD pattern of schwertmannite (Fig. II.2-5). Merely a slightly increasing background noise in the chromated samples was observed.

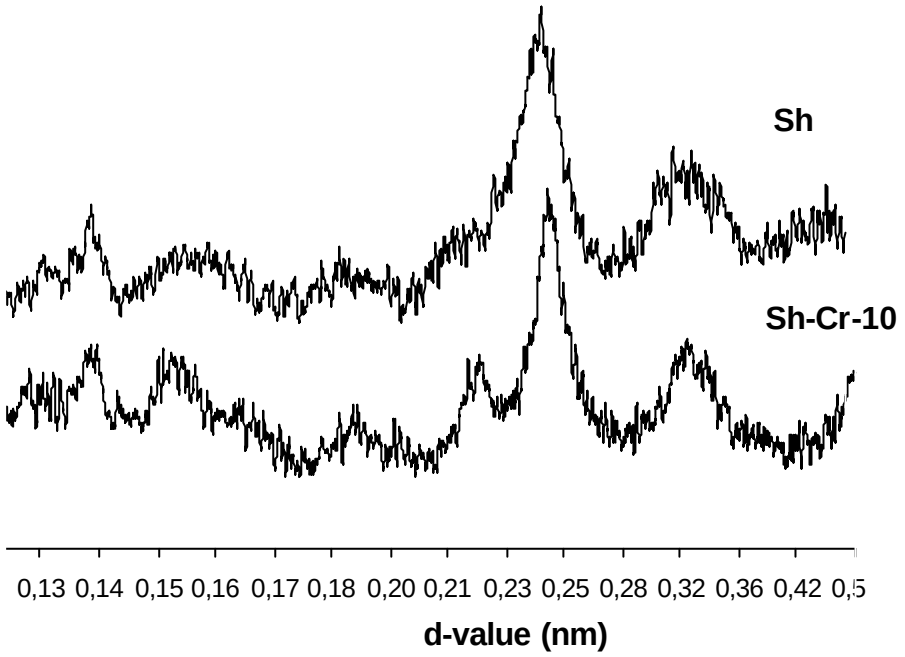

Fig. II.2-5 X-ray powder diffraction pattern of schwertmannite containing sulfate (above) and chromate (below) in its structure.

Unit-cell edge lengths were calculated with the program “winfit” (H. Stanjek, Technical University of Munich) of the sample Sh-Cr-10 which contained chromate instead of sulfate. In Table II.2-1, the calculated results are compared to the cell parameters of pure schwertmannite. Both are of tetragonal symmetry, but the unit cell parameter of c_0 in chromated schwertmannite was with 0.3 nm only half as long as that observed in pure schwertmannite.

A complete exchange of sulfate by molybdate, another tetrahedrally coordinated oxyanion with a hexavalent cation (similar to chromium and sulfur) in schwertmannite was not possible as XRD measurements demonstrated (Fig. II.2-6).

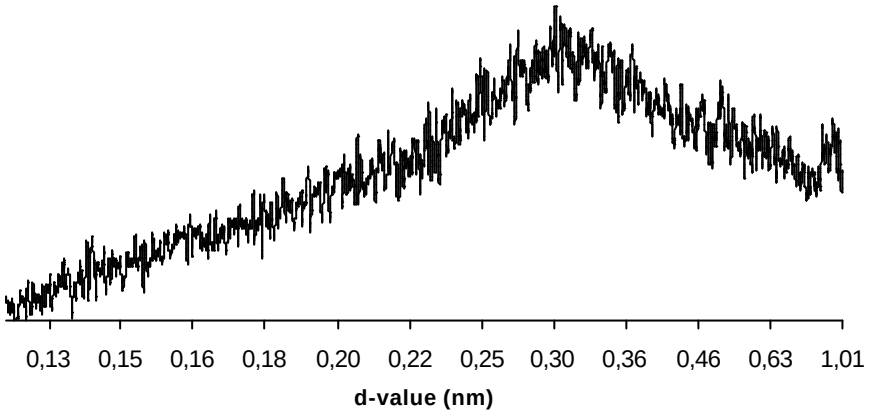

Fig. II.2-6 X-ray powder diffraction pattern of an iron(III)-molybdate precipitate. The synthesis occurred analogue to schwertmannite with molybdate instead of sulfate in the synthesis-solution.

2.3.2. Processes and Products of Schwertmannite Synthesis

The chemical processes which occurred during schwertmannite synthesis were examined for both methods: the "synthesis in Fe(III)-solutions" and the "oxidative synthesis".

Synthesis in Fe(III)-solutions

The formation of schwertmannite by the reaction of 40 mM iron(III) and 10 mM sulfate in a dialysis bag was completed after ~ four weeks. The precipitate had a dry weight of 1.93 g. The analysis of its chemical composition (Table II.2-4A) suggested that the total amount of iron, but only 40 % of the sulfate, were consumed for the schwertmannite production. Equation II.2-2 quantifies this reaction (data in mM).

$$40\ FeCl_3 \cdot 6\ H_2O + 10\ Na_2SO_4 \rightarrow 2.5\ Fe_{16}O_{16}(OH)_{10.9}(SO_4)_{2.55}$$
$$+20\ Na^+ + 120\ Cl^- + 3.6\ SO_4^{2-} + 107\ H^+ + 172\ H_2O \qquad \text{[II.2-2]}$$

During the dialysis Na^+, Cl^-, a bulk of SO_4^{2-} and protons gradually diffused out of the dialysis bag into the deionised and daily changed water which surrounds the bags. After the electric conductivity in this water was constantly < 5 µS, the reaction was completed.

The suspensions inside the dialysis bags were analysed (from the samples Sh, Sh-S-As-1, S-As-5, Sh-S-Cr-1, Sh-S-Cr-5, Sh-S-P-1, and P10) by periodic measurements of pH, Fe(tot), SO_4^{2-} As(tot) and Cr(tot) and the precipitated solid phase was examined after 10 and 18 days by XRD.

In all synthesis solutions the dissolution of $FeCl_3$ salt or the hydrolysis of iron(III) resulted in a similar release of acid. The starting pH was 1.5 and during the following weeks of dialysis it increased up to 4 (Fig. II.2-7).

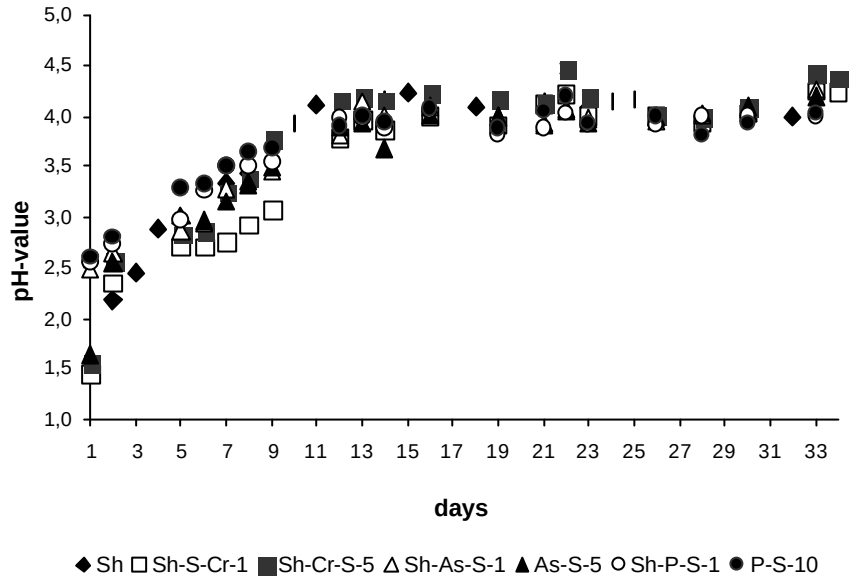

Fig. II.2-7 Variation of pH as a function of time during the formation of the samples Sh, Sh-S-As-1, S-As-5, Sh-S-Cr-1, Sh-S-Cr-5, Sh-S-P-1, S-P-10 in the synthesis-suspensions inside the dialysis-bags.

The precipitation rate of the oxyanions (from solution into solid) was highest for arsenate, because after 5 to 6 days 99 % were displaced from solution. The removal of chromate lasted 2 - and that of sulfate about 10 more days (Fig.II.2- 8). Dissolved iron was in all suspensions below the detection limit.

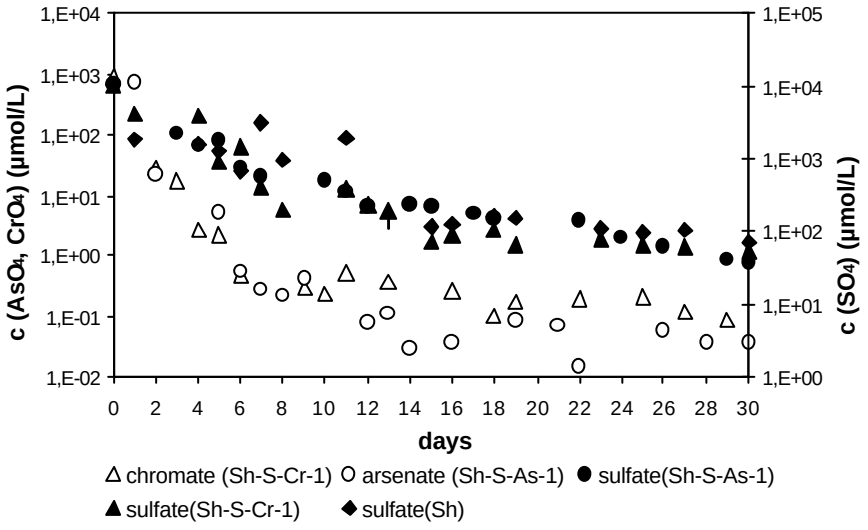

Fig. II.2-8 Variation of the oxyanion-content as a function of time during the formation of the samples Sh, Sh-S-As-1, Sh-S-Cr-1 in the synthesis-suspensions inside the dialysis-bags.

The XRD pattern of the filtrated solid (sample Sh) hardly showed the characteristic peaks of schwertmannite after ten days. After 18 days the complete schwertmannite pattern was visible (Fig. II.2-8).

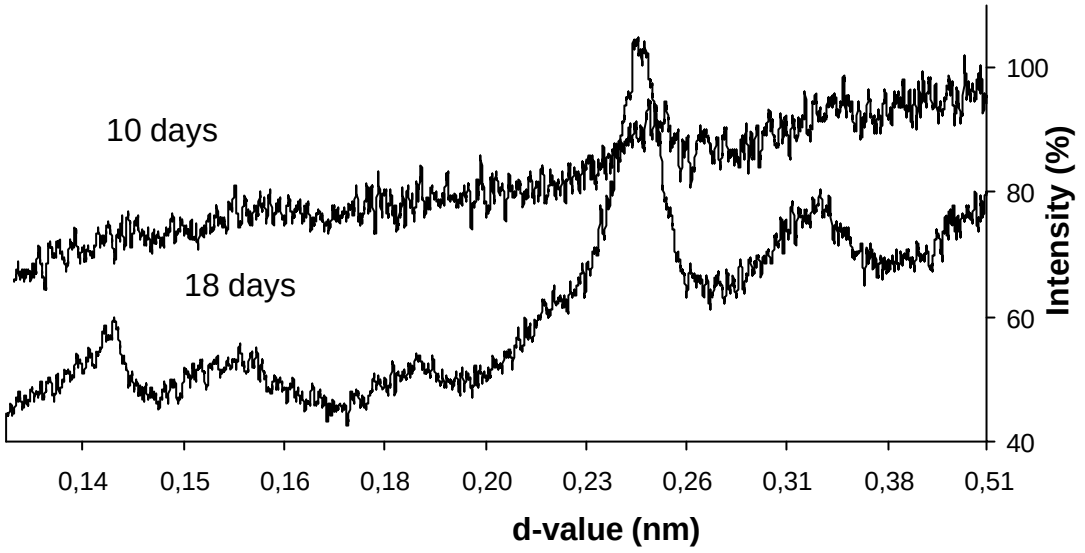

Fig. II.2-8 X-ray powder diffraction pattern of two evolution phases of schwertmannite formation (after 10 and 18 days of dialysis-start).

Depending on the composition of the synthesis solution, differently composed solids with the crystallinity of schwertmannite (mineralogical evidence by XRD) were produced.

Table II.2-4A shows the concentrations of the dissolved salts added to the synthesis solutions and the composition of the resulting schwertmannite solids. Besides the calculated chemical formulas, the ratio of iron to the sum of the oxyanions is presented which is a characteristic value for iron-sulfate minerals. Pure schwertmannite has a value of eight, if no oxyanions are adsorbed to its surface. Accordingly, a value of five in schwertmannite means that 33 % of total sulfate is adsorbed and a value of eight that no sulfate is adsorbed but only structurally incorporated. The calculated chemical formulas of the resulting schwertmannite samples demonstrate a competition of the oxyanions to incorporate into the structure. E.g., in sample Sh-S-Cr-10, similar amounts of sulfate (10 mmol L^{-1}) and chromate (8.6 mmol L^{-1}) were added to the solution and in the end more chromate was incorporated in schwertmannite (unit cell formula: $Fe_{16}O_{16}(OH)_{11.5}(SO_4)_{0.7}$ $(CrO_4)_{1.5}$). The affinity is highest for arsenate and phosphate, followed by chromate and finally sulfate.

Table II.2-4 Schwertmannite-synthesis experiments

A) Precipitates with schwertmannite structure (evidence by XRD), produced by "synthesis in Fe(III) solutions". Composition of the synthesis solution and the formed solid (ref. to dry weight) after 30 days.

sample name	composition of the synthesis solution ($mmol \cdot L^{-1}$)	composition of the schwertmannite solid (wt. %)						chemical formula	Ratio of Fe/Oxyanion
		Fe	± s	S	± s	As/P/Cr	± s		
Sh	40 Fe + 10 SO_4	44.1	0.8	4.1	1.1	-	-	$Fe_{16}O_{16}(OH)_{10.9}(SO_4)_{2.6}$	6.3
Sh-S-As-1	40 Fe + 10 SO_4 + 0.72 AsO_4	43.3	1.2	2.8	0.6	5.6	0.3	$Fe_{16}O_{16}(OH)_{7.8}(SO_4)_{1.8}(AsO_4)_{1.5}$	4.8
Sh-S-P-1	40 Fe + 10 SO_4 +1.05 PO_4	33.3	1.7	1.5	0.7	3.7	0.9	$Fe_{16}O_{16}(OH)_{10.3}(SO_4)_{1.2}(PO_4)_{1.1}$	6.9
Sh-S-Cr-1	40 Fe + 10 SO_4 + 0.86 CrO_4	32.9	0.5	2.4	1.4	0.8	0.7	$Fe_{16}O_{16}(OH)_{11}(SO_4)_2(CrO_4)_{0.4}$	6.5
Sh-S-Cr-2.5	40 Fe + 10 SO_4 +4.15 CrO_4	31.5	1.9	1.9	1.6	1.1	0.4	$Fe_{16}O_{16}(OH)_{11.5}(SO_4)_{1.6}(CrO_4)_{0.6}$	7.2
Sh-S-Cr-5	40 Fe + 10 SO_4 + 4.31 CrO_4	36.3	3.6	2.1	0.8	2.5	1.1	$Fe_{16}O_{16}(OH)_{10.43}(SO_4)_{1.6}(CrO_4)_{1.2}$	5.7
Sh-S-Cr-10	40 Fe + 10 SO_4 + 8.62 CrO_4	39.6	1.1	1	0.7	3.6	1.4	$Fe_{16}O_{16}(OH)_{11.5}(SO_4)_{0.7}(CrO_4)_{1.5}$	7.2
Sh-Cr-10	40 Fe + 8.62 CrO_4	41.2	1.8	0	0	6.9	0.5	$Fe_{16}O_{16}(OH)_{10.2}(CrO_4)_{2.9}$	5.7
Sh-S-As-Cr	40 Fe + 10 SO_4 + 0.72 AsO_4 + 0.86 CrO_4	40.3	-	2.6	-	As: 5.2 Cr: 0.9	-	$Fe_{16}O_{16}(OH)_{7.2}(SO_4)_{1.8}(AsO_4)_{1.5}(CrO_4)_{0.4}$	4.6
Sh-S-As-P	40 Fe + 10 SO_4 + 0.72 AsO_4 + 1.05 PO_4	40.4	-	2.2	-	As: 3.8 P: 2.8	-	$Fe_{16}O_{16}(OH)_{9.6}(SO_4)_{1.5}(AsO_4)_{1.1}(PO_4)$	6.1
Sh-S-As-P-Cr	40 Fe +10 SO_4 + 0.72 AsO_4 + 1.05 PO_4 + 0.86 CrO_4	41.9	-	1.9	-	As:3.7 Cr:0.8	-	$Fe_{16}O_{16}(OH)_{9.6}(SO_4)_{1.3}(AsO_4)_{1.1}(CrO_4)_{0.3}(PO_4)$	5.9
Sh-As-Cr	40 Fe+0.72 AsO_4+ 8.6 CrO_4	42.9	-	0	-	As: 3.8 Cr: 5.8	-	$Fe_{16}O_{16}(OH)_{8.2}(AsO_4)_{1.04}(CrO_4)_{2.3}$	4.8

In Table II.2-4B the compositions of the synthesis solutions are presented which did not form schwertmannite after dialysis, as XRD measurements prove (demonstrated for example in Fig.II.2-4). The synthesis solutions of these X-ray amorphous samples contained high amounts of arsenate, phosphate or molybdate.

Table II.2-4 Schwertmannite synthesis experiments

B) Precipitates with no definable structure (evidence by XRD) produced by "synthesis in Fe(III)solutions". Composition of the synthesis solution after 30 days.

sample name	composition of the synthesis solution ($mmol \cdot L^{-1}$)
As-S-2.5	40 Fe + 10 SO_4 + 1.8 AsO_4
As-S-5	40 Fe + 10 SO_4 + 4.6 AsO_4
As-10	40 Fe + 7.2 AsO_4
P-S-4.4	40 Fe + 10 SO_4 + 4.63 PO_4
P-10	40 Fe + 10.52 PO_4
Mo-10	40 Fe + 10 MoO_4

Synthetic schwertmannite with different amounts of sulfate and arsenate is of orange-red colour. Increasing amounts of chromate darken the solid insofar as Sh-Cr-10 which consists of chromate as single oxyanion is coloured in dark brown.

The surface area of the produced schwertmannite samples varied with the chemical composition between 160 $m^2 \cdot g^{-1}$ and 300 $m^2 \cdot g^{-1}$. However, no direct dependency of the surface area on the mineral composition was observed (more exact results are presented in II.6.1). Similarly, no significant differences of the precipitates were observed by the analysis

of the particle morphology using SEM: all the graphs showed spherical and fluffy schwertmannite particles with a size of ~ 0.5 µm in diameter (see appendix D).

Oxidative synthesis

Schwertmannite formation in a solution of Fe(II) sulfate with H_2O_2 as oxidant was approximately quantified by the equation II.2-3 (data in mM):

$$20\ FeSO_4 + 11.85\ H_2O_2 \rightarrow Fe_{16}O_{16}(OH)_{7.7}(SO_4)_{4.1} + 15.9\ SO_4^{2-} + 16\ H^+ + 4\ Fe^{3+} \qquad [II.2\text{-}3]$$

After several hours a constant pH value of 2.4 was measured.

The resulting precipitate of schwertmannite contained more sulfate compared to schwertmannite produced by dialysis (Table II.2-4C and II.2-4A). This was explained by the higher input of sulfate (the ratio of Fe:S is 1:1) and the reaction in a closed system. Due to the sulfate excess, no exchange experiments with other oxyanions as described for the "synthesis in Fe(III)-solutions " were possible. Addition of arsenate into the iron-sulfate solution resulted in a similar high arsenic incorporation into schwertmannite (4.99 wt.-%) as described for the synthesis in Fe(III)-solutions (5.6 wt.-%). The incorporation capacity for chromate was more limited (< 1.6 wt.-% Cr).

Table II.2-4 Schwertmannite synthesis experiments

C) Precipitates with schwertmannite structure (evidence by XRD) produced by the "oxidative synthesis". Composition of the synthesis solution and the resulting solid (ref. to dry weight).

sample name	composition of the synthesis solution ($mmol \cdot L^{-1}$)	composition of the schwertmannite solid (wt.-%)						chemical formula	Ratio of Fe/Oxyanion
		Fe	± s	S	± s	As/Cr	± s		
Sh-H_2O_2	20 $FeSO_4$	41	1.06	5.9	1.7	-	-	$Fe_{16}O_{16}(OH)_{7.7}(SO_4)_{4.1}$	4.8
Sh-H_2O_2-As	20 $FeSO_4$ + 1AsO_4	40.7	-	6.7	1.9	As: 4.99	1.1	$Fe_{16}O_{16}(OH)_{4.14}(SO_4)_{4.62}(AsO_4)_{0.87}$	4.9
Sh-H_2O_2-Cr	20 $FeSO_4$ + 1CrO_4	38.7	-	6.4	2.0	Cr: 1.56	0.9	$Fe_{16}O_{16}(OH)_{6.78}(SO_4)_{4.61}(CrO_4)_{0.69}$	4.0

Compared to the samples produced by the "synthesis in Fe(III) solutions", a big difference was found by measurements of the surface area. This turned out to be nearly 10 times smaller for samples synthesised by "oxidative synthesis" (~ 25 $m^2 \cdot g^{-1}$). Investigations by SEM confirmed this observation, because the particles were formed (or agglomerated) to smooth nuggets with no crystalline shape (shown in appendix D).

Due to these differences, all further examinations of schwertmannite (adsorption, stability) were conducted with samples produced by "synthesis in Fe(III) solutions".

2.3.3. Changes in Schwertmannite Suspensions over Time at pH 2 and 4

Release of Iron, Sulfate, Arsenate and Chromate

Suspensions of arsenated, chromated, phosphated and pure schwertmannite (samples Sh-S-As-1, Sh-S-Cr-1, Sh-Cr-10, Sh-S-P-1, Sh) were kept at constant temperature (20 °C) and constant pH (each at 2 and 4) in closed vessels over 362 days. The release of iron, sulfate and the other oxyanions from the solid to the aqueous phase were continuously determined. Table II.2-5 is representing the activities of these ions (except of phosphate which was not measured) in the end of the experiment.

Table II.2-5 Composition of the suspensions kept at constant pH of 2 or 4 in the beginning and in the end of the stability experiment. In the beginning, the solid dry weight in all samples was 0.75 $g \cdot L^{-1}$ with an iron content of c = 7.76 mM.

Sample name	pH	SO_4^{2-} in solid ($mmol \cdot g^{-1}$)	CrO_4^{2-}, AsO_4^{3-}, PO_4^{3-}, in solid ($mmol \cdot g^{-1}$)	added NaOH (mM)	added HNO_3 (mM)	release after 360 days (activity)		
						Fe (mM)	SO_4^{2-} (mM)	Σ Ox.(mM)[1]
Sh	2	1.281	-	-	9.88	2.913	0.737	0.737
Sh	4	1.281	-	1.11	0.05	< 0.01	0.213	0.213
Sh-S-As-1	2	0.838	AsO_4^{3-}: 0.756	-	10.51	2.603	0.425	0.571
Sh-S-As-1	4	0.838	AsO_4^{3-}: 0.756	0.11	0.005	< 0.01	0.236	0.236
Sh-S-P-1	2	0.464	PO_4^{3-}: 1.201	-	11.9	1.985	0.481	n.m.[2]
Sh-S-P-1	4	0.464	PO_4^{3-}:: 1.201	0.06	-	< 0.01	0.184	n.m.[2]
Sh-S-Cr-1	2	0.755	CrO_4^{2-}: 0.016	-	10.24	3.132	0.427	0.496
Sh-S-Cr-1	4	0.755	CrO_4^{2-}: 0.016	0.035	-	< 0.01	0.246	0.257
Sh-Cr-10	2	-	CrO_4^{2-}: 1.333	-	9.60	3.042	-	0.354
Sh-Cr-10	4	-	CrO_4^{2-}: 1.333	0.008	-	< 0.01	-	0.155

[1] total amount of released oxyanions (sulfate + arsenate + chromate); [2] phosphate was not measured

At pH 2 high activities of iron in all suspensions indicated a dissolution of the solid. The highest dissolution was observed for pure and chromated schwertmannite (release of 2900-3100 µM Fe), whereas dissolution of arsenated and phosphated schwertmannite was obviously minor (1900-2600 µM Fe). The total release of oxyanions (sulfate + chromate + arsenate) was lowest for chromated schwertmannite (without sulfate) as shown in Table II.2-5. However, arsenate is the lowest concentrated oxyanion (Fig. II.2-10). Moreover, the releasing rates of arsenate and chromate differed: while at pH 2 the released arsenate gradually amounted until ~ 120 days after the beginning of the experiment and finally reached a maximum of 150 µM, the released concentrations of chromate were at the same pH already after ~100 days at a constant maximum of about 350 µM (Fig. II.2-10). In all solutions kept at pH 4 no iron, small amounts of sulfate (200 –250 µM) and chromate (< 120 µM) and hardly any arsenate (< 0.1 µM) were detected over time (Table II.2-5 and Fig. II.2-10).

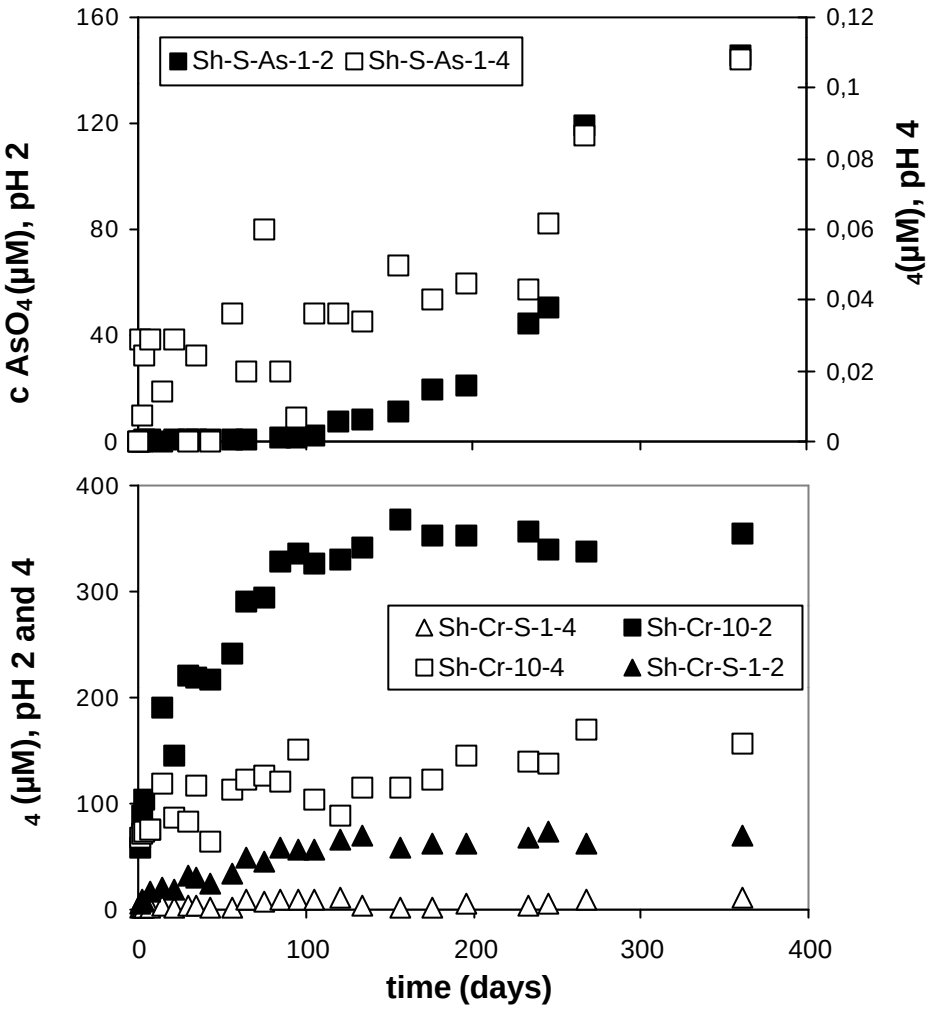

Fig. II.2-10 Variation of arsenate- and chromate- concentrations as a function of time during the suspension of schwertmannite samples (Sh-S-As-1, Sh-S-Cr-1, Sh-Cr-10) at constant pH of 2 or 4 (the appendix "-2" or "-4" mark the pH-value).

Variation in Crystal Structure

All XRD patterns of precipitates obtained from the suspensions kept at pH 4 showed the characteristic features of schwertmannite in the end of the experiment after 362 days (Fig.II.2-11). As opposed to arsenated, chromated and phosphated schwertmannite solely in the sample of pure schwertmannite other peaks (e.g. at 0.418 nm) appeared and the intensity of the peak at 0.156 nm increased. In chromated, arsenated and phosphated samples these changes were not observed.

In the suspensions kept at pH 2, a considerable part of the solid (~ 40 %) dissolved over time. The small residues showed features of schwertmannite in their XRD pattern but some peaks partly disappeared.

These results were confirmed by FTIR spectroscopic investigations of the solid samples performed every several weeks during the experiment: At pH 4 all solids except that of pure schwertmannite showed approximately the same pattern as in the beginning of the experiment (the same as described for schwertmannite by Bigham et al., 1990). At pH 2 the complete schwertmannite IR spectrum was unchanged in all samples after one year.

2.3.4. Adsorption Capacity for Arsenate and Chromate

The surface of pure schwertmannite, prepared after the synthesis method, had an area of 195 $m^2 \cdot g^{-1}$. In this study, quantitative adsorption of arsenate and chromate to schwertmannite in dependence on pH (between 2.5 and 4.5), concentration of adsorbate ($1 \cdot 10^{-4}$ M, $1 \cdot 10^{-3}$ M and partly $5 \cdot 10^{-3}$ M) and adsorbent (1 $g \cdot L^{-1}$ and 4 $g \cdot L^{-1}$) was examined. The adsorption in the investigated range of pH, was of little pH dependence. Table II.2-6 shows the maximum amount of adsorbed oxyanions, the amount of simultaneously released sulfate and the corresponding pH.

Table II.2-6 Schwertmannite adsorption capacity (maximum value) for arsenate and chromate, corresponding pH and release of sulfate in dependence on the concentrations of adsorbate and adsorbent (concentrations in mM).

		1 $g \cdot L^{-1}$			4 $g \cdot L^{-1}$		
adsorbate addition		**pH**	**adsorbed AsO_4/ CrO_4**	**SO_4 release**	**pH**	**adsorbed AsO_4/ CrO_4**	**SO_4 release**
0.1	**AsO_4^{3-}**	3.9	0.099	0.39	3.6	0.099	0.66
1	**AsO_4^{3-}**	3.9	0.969	0.63	4.1	0.999	1.35
5	**AsO_4^{3-}**	4.0	4.775	0.59	-	-	-
0.1	**CrO_4^{2-}**	4.4	0.098	0.18	3.9	0.099	0.93
1	**CrO_4^{2-}**	3.5	0.883	0.30	4.3	0.975	0.69

1 $g \cdot L^{-1}$ schwertmannite adsorbed from a solution of $c=10^{-4}$ M chromate or arsenate nearly 100 %. From a 10^{-3} M adsorbate solution, 1 $g \cdot L^{-1}$ schwertmannite adsorbed nearly 100 % arsenate and 88 % chromate. A further increase of the arsenate concentration to $c = 5 \cdot 10^{-3}$ M showed that even 4.7 $mmol \cdot g^{-1}$ arsenate were enriched in schwertmannite.

To quadruplicate the amount of schwertmannite (4 $g \cdot L^{-1}$), nearly 100 % of both oxyanions from a $c=10^{-3}$ M were adsorbed. Outside the observed pH range (2.5 to 4.5) of schwertmannite stability, the pH dependency of adsorption for both oxyanions was much

stronger, but due to potential dissolution and transformation reactions of schwertmannite under these conditions (Bigham et al., 1990), quantification was not possible and therefore not further considered in this study.

The suspension of schwertmannite in different adsorbate solutions involves the release of sulfate. The sulfate concentrations which correspond to adsorption maxims are presented in Table II.2-6. The release of sulfate is strongly dependent on pH and increases with increasing pH. Compared to chromate solutions, in arsenate solutions the sulfate release is higher and an increased amount of schwertmannite resulted in slightly higher sulfate concentrations (0.6 to 1.3 $mM \cdot g^{-1}$).

2.3.5. Enrichment of As and Cr in Natural Schwertmannite

Schwertmannite was identified at several locations in both of the two investigated former mines (Fig. II.2-3). The range of arsenic and chromium concentrations, measured in NH_4-oxalate extracts of schwertmannite precipitates and in the drainage water of the corresponding sampling sites are presented in Table II.2-7 (8 to 10 sampling sites of water and schwertmannite precipitate in each mine, see appendix B). Results suggest a strong enrichments of Cr (up to 800 ppm) and As (up to 6700 ppm) in schwertmannite. In contrast to these precipitates, concentrations in water reached only in few cases values > 100 ppb. Concentrations were usually low and partly undetectable.

Table II.2-7 Range of As- and Cr-concentrations determined in AMD waters and in associated schwertmannite containing precipitates (each 8 to 10 measurements) sampled in the former mines "Saalfelder Feengrotten" (D) and "Prybyslav (Cz).

	Mine drainage water		**Precipitate of Schwertmannite**	
	As_{tot} (ppb)	Cr_{tot} (ppb)	As_{tot} (ppm)	Cr_{tot} (ppm)
Saalfelder Feengrotten (D)	0 - 35	0-19	54 - 1594	10 - 296
Prybyslav (Cz)	0 - 235	0 - 174	560 - 6740	812 -100

2.4. Discussion

2.4.1. Tunnel Sulfate, Arsenate or Chromate in Schwertmannite

According to Bigham et al. (1990, 1994), sulfate is incorporated into caves of the schwertmannite tunnel structure. Due to a direct binding of sulfate oxygen atoms to oxygen atoms of the iron-hydroxide octahedra, sulfate is specifically ("structurally") bound to schwertmannite by the formation of bidentate binuclear complexes (Fe–O–S(O_2)–O–Fe, Fig. II.2-2). Recently some authors doubted this theory and stated that sulfate is exclusively bound by inner- and outer-sphere adsorption to akaganéite (β-FeOOH) whose structure is marked by tunnel caves which are either occupied by (outer-sphere bound) chloride or fluoride or are unassigned (Waychunas et al., 2000). The characteristic XRD pattern of schwertmannite (Fig. II.2-1) with different (compared to akaganéite) crystallographic cell parameters (Table II.2-1) obtained in this study, is in accordance with the structure determinations of Bigham et al. (1990) and serves as evidence for structural changes as a result of structurally bound sulfate. Moreover, it seems not probable that high amounts of sulfate (1.25 $mmol \cdot g^{-1}$) in schwertmannite are exclusively adsorbed to the surface (200 $m^2 \cdot g^{-1}$). And only a part of the total sulfate (< 0.6 $mmol \cdot g^{-1}$) was desorbable in highly concentrated arsenate (c= 5 mM) solutions. Therefore, the theory of sulfate bound in tunnel caves of schwertmannite (Bigham et al., 1990) serves as a basis for further argumentation in this study.

Arsenate and chromate enriched in Schwertmannite

The analysis of both, synthetic and naturally formed schwertmannite (Table II.2-4 and Table II.2-7, respectively) have shown that this mineral can incorporate high amounts of arsenic or chromium. Therefore, schwertmannite could act as a sink for these toxic elements in contaminated waters. Similar "cleaning effects" of schwertmannite were already described by Rüde et al. (1999) for a natural stream (Rötlbach, Zillertaler Alps) in which the spring water was highly enriched with arsenic. After the formation of schwertmannite, the arsenic concentration decreased below detection limit in the stream water and As accumulated up to 1000 ppm in precipitates of schwertmannite.

Due to its low stability resulting in dissolution or transformation of this mineral (Bigham et al., 1996) a release of these molecules should be expected by ageing or by change of hydrochemical parameters. Depending on the bonding strength or the bonding type of the oxyanions, the potential resulting contamination could differ. Structural incorporation by sulfate substitution, specific- or non specific adsorption and coprecipitation of a secondary

phase are the possible and presently discussed mechanisms of the incorporation of arsenate and chromate to schwertmannite.

Although incorporation of arsenate and chromate takes place in schwertmannite, produced by both synthesis methods (oxidative synthesis and synthesis in Fe(III)-solutions , Table II.2-4), this discussion only refers to results obtained for samples produced by synthesis in Fe(III)-solutions. Reason for this was the low surface area of the particles (5-20 $m^2 \cdot g^{-1}$) produced by oxidation of $FeSO_4$. Therefore, they are difficult to compare with samples synthesised by dialysis and which show a very high surface area of 100-300 $m^2 \cdot g^{-1}$.

2.4.2. Solid Solution or Coprecipitation of a Secondary Phase

Substitution of Sulfur in Minerals

Solid solutions in minerals generally depend on the particular ionic radii and charge of the substituted compounds (Goldschmidt, 1937). Little differences of these features exist between the anions sulfate, arsenate, chromate, phosphate or molybdate (Table II.2-3). Therefore, exchanges of these anions can be expected in crystal structures. However, a substitution of the tetrahedrally coordinated sulfur by other cations was rarely observed in most sulfate mineral structures described in literature (Hawthorne, et al., 2000). Few exceptions were found in minerals, such as a substitution of sulfur by molybdenum in vergasovaite ($Cu_3O[(SO_4)(Mo,S)O_4)]$) (Berlepsch et al., 1999) or by chromium in hashemite ($Ba[(Cr,S)O_4]$) (Duesler & Ford, 1986). Heterovalent isomorphism as an exchange of S^{6+} by P^{5+} was also observed as described for woodhouseite (Kato, 1977) and svanbergite (Kato & Miura 1977), respectively. The charge balance was then given as $[P^{5+}O_3(OH)]^{2-}$ for $[SO_4]^{2-}$. The same scheme is valid for the sulfur substitution by arsenic in beudantite where the tertahedrally coordinated sites consist of 53.5 % As and of 46.5 % S (Szymanski, 1988). According to these references an exchange of sulfate in schwertmannite by other oxyanions (chromate, phosphate, arsenate or molybdate) seems, at least partly, possible.

Structure and Structural Changes of Schwertmannite and its Solid Solutions

In this study, the mineralogy of both, synthesised and natural solid samples was investigated by XRD analysis. Compared to the XRD patterns of well crystalline minerals with definite peak positions as observed in this and described in other studies (Cornell & Schwertmann, 1996) for the Fe(III) hydroxides goethite (α-FeOOH) or akaganéite (β-FeOOH), the pattern of schwertmannite is, due to its low crystallinity, hardly to identify (Fig. II.2-1). According to Bigham et al. (1990), the XRD pattern of schwertmannite is marked by eight broad peaks.

Their position and corresponding hkl indices are presented in Table II.2-2 and compared to akaganéite.

The results obtained by XRD showed that a complete substitution of sulfate by chromate in schwertmannite is possible (Fig. II.2-5). However, minor differences between the patterns of pure and chromated schwertmannite were observed (Table II.2-1) which can be explained by different ionic radii of the two molecules (Table II.2-3). It was assumed that chromate incorporates similar to sulfate in the tunnel cavities of schwertmannite. However, due to the slightly larger ionic size of chromate, a more enhanced distortion of the crystal unit cell results and therefore crystal growth is more reduced. As a consequence of this minor structural change, the peaks on the diffraction pattern slightly shifts (Table II.2-2) and a change of the unit cell parameters was obtained (the c-dimension halves, (Table II.2-1). It is known that the symmetry of the unit cell influences the crystal growth and correspondingly the macroscopic morphology (Cornell & Schwertmann, 1996). The incorporation of chromate results in a more limited crystal growth and therefore in smaller particles, because the schwertmannite crystal-needles are getting thinner. This was indirectly observed by scanning electron microscopy: The obtained pictures of chromatised schwertmannite became, due to smaller particle size, indistinct (therefore they were just presented in appendix D). However, this is only a presumption, because other factors such as solution chemistry, have a stronger influence in mineral morphology. Compared to the cell parameters of akaganéite and goethite which are mineralogically related to schwertmannite, the differences between sulfated and chromated schwertmannite are very small (Table II.2-1).

A similar solid solution effect, as shown for sulfate by chromate in schwertmannite, was already demonstrated for the anion selenate (SeO_4^{2-}) by Bigham et al. (1990). Therefore, it could be assumed that divalent oxyanions of tetrahedrally coordinated cations, can be incorporated into the schwertmannite tunnel structure. However, in this study it was shown that other factors also influence the substitution, because a complete exchange of sulfate by molybdate (MoO_4^{2-}) in schwertmannite was not possible, as the XRD pattern in Fig.II.2-6 demonstrates. Presumably the larger size of this molecule (Table II.2-3) inhibits ist integration into the structural tunnel positions of schwertmannite.

Incorporation of trivalent oxyanions, such as arsenate and phosphate, is limited as results obtained by XRD show (Fig. II.2-4). Carlson et al. (2001) confirmed a substitution dependency on the oxyanion charge by XRD analysis of similarly produced arsenate schwertmannite samples. Schwertmann et al. (1996) also showed that a nitrate incorporation in schwertmannite is possible.

According to these results, it was assumed that one or two excessive electrons in the molecule permit a complete surrogate of the tunnel sulfate (substitution) in schwertmannite, if their ionic radius is not larger than ~ 0.24 nm. Oxyanions with three excessive electrons in high concentrations prevent this substitution, if the molar ratio sulfate: arsenate lies below 10 : 1. The strong affinity of these anions to iron(III) probably provokes other structures (coprecipitation of a secondary phase).

A comparison to the sulfate-mineral group of jarosite-alunites confirms these results: This group consists of about 40 minerals with the general formula of $DG_3(TO_4)_2(OH,H_2O)_6$ wherein D represents cations with a coordination number ≥ 9 and G and T represent sites with octahedral and tetrahedral coordination, respectively (Smith et al., 1998). Tetrahedra are composed of sulfate (the most frequently occurring jarosite group), phosphate, arsenate, chromate, molybdate or silicate. Each of them forms a different mineral subgroup and substitution of the tetrahedra within a subgroup is limited. The synthetic chromate analogue of jarosite ($KFe_3(SO_4)_2(OH)_6$) is known (Baron & Palmer, 1996a) and substantial amounts of chromate can substitute arsenate in philipsbornite ($PbAl_3[(AsO_4)_2(OH, H_2O)_6]$), as reported by Walenta et al. (1982). These data verify the obtained results for schwertmannite that a complete solid solution between sulfate and chromate is potential, whereas between sulfate or chromate by phosphate or arsenate can be partly possible, but is always limited (due to the high width of the XRD peaks no clear evidence can be given). Correspondingly, the charge of oxyanions seems to have the greatest influence in inhibiting the substitution.

Formation of Schwertmannite and Substitution Affinities

The formation process of schwertmannite in the dialysis suspensions was marked by two phases. During the first ten days, the pH in all solutions arose to a value of 4 (Fig. II.2-7) and nearly all oxyanions (< 90 %) were removed from the solution (Fig. II.2-7). This process was most rapid for arsenate (complete after ~ 6 days). Due to the fact that the total amount of arsenate was finally fixed in the precipitate, a preferred complex formation of arsenate with Fe(III) was assumed.

In the second phase of schwertmannite formation which began after ten days of the synthesis start, the pH remained constant and the solution composition hardly varied. Instead of that, the X-ray diffraction pattern of the solid was altered during the following days. As shown in Fig. II.2-9, the characteristic peaks for schwertmannite in the XRD pattern developed between 10 and 18 days after the synthesis had started.

Due to this observation, and since the crystallisation of other iron (III) minerals in acid media is well described (Schneider & Schwyn, 1987; Music et al., 1982; Aktinson, 1977), it was concluded that schwertmannite forms by this process in the dialysis bags: Firstly, Fe(III) reacted with oxygen, hydroxide, chloride and the oxyanions to form different structural complexes (polynuclears) of varying stability. These precipitated as X-ray amorphous solids during the first 10 days of the experiment. Complexes of lower stability (as iron chlorides) subsequently dissolved and chloride, sodium and high amounts of sulfate and hydronium diffused through the dialysis-bag membranes. Finally, the remaining complexes gradually re-ordered to form polynuclears with the structure of schwertmannite. Therefore, the velocity of schwertmannite formation was controlled by the strength of the complexed species of iron (Fe(III) chloride, Fe(III) sulfate, Fe(III) hydroxide, Fe(III) arsenate…). The process might have been accelerated by more enhanced frequent water changes (deionised water outside the dialysis bags) to eliminate the chloride. Due to the presence of too much arsenate or phosphate in the synthesis solution (more than ~ 0.04 mol per mol Fe), most iron was complexed with these oxyanions and no (or not enough) Fe hydroxide octahedra-chains could form which are requirement for schwertmannite formation.

The trivalent oxyanions arsenate and phosphate were strongly preferred to schwertmannite for structural incorporation, compared to sulfate. Similar amounts of chromate and sulfate in the solutions resulted in a marginal preference of chromate incorporation (2.9 mol chromate per mol schwertmannite) compared to sulfate (2.6 mol sulfate per mol schwertmannite, as shown in Tab.II.2-4A). Substitution preferences in minerals can generally be explained by their crystal structure (or atomic distances within the structure) and by molecule bonding affinities. Konnert et al. (1994) investigated the influence of the crystal structure on substitution in carlosruizite ($K_6(Na,K)Na_6Mg_{10}[(Se,S,Cr)O_4]_{12}(IO_3)_{12}(H_2O)_{12}$). This mineral contains the cations Se^{6+}, S^{6+} and Cr^{6+} which all occur at the same tetrahedrally coordinated site. The formula of the unit cell consists of twelve tetrahedrally coordinated cations. The proportion of Se:S:Cr is given as 6.4:4.4:1.2. The interpretation of this substitution distribution was given by the distances of the cation to the oxygen. For the crystallisation of carlosruizite a mean <(Se,S,Cr)-O> distance of 1.588 Å is required which is given by the shown proportion. In this study, no atomic distances were determined for schwertmannite crystals. Therefore, the optimal composition can not be calculated.

The other factor influencing the substitution preferences is the tendency of these ions to form complexes in homogenous solutions. The affinity of the oxyanions to form complexes with iron(III) was investigated by Dzombak & Morel (1990) for surface complexes with hydrous

ferric oxides (HFO). They calculated the corresponding complexation constants which describe the intensity of the resulting complex. In Table II.2-8, the dominating equilibria at pH 4 are presented. These values demonstrate that the complexes between Fe(III) and arsenate are strongest, followed by Fe(III) and chromate and at last by Fe(III) and sulfate. According to Cornell & Schwertmann (1996), binding constants for surface complexes show the same stability trend as those for equivalent complexation reactions in solutions. Consequently, high surface complexation constants (log K in Tab. II.2-8) correspond to high adsorption and high complexation affinities. Therefore, the oxyanion incorporation affinity in schwertmannite can be explained with the order of these constants: the higher the surface complexation constants, the higher the affinity of iron to react with the corresponding oxyanion and the more stable is the formed complex.

Table II.2-8 Surface complexation constants of anions complexed with hydrous ferric oxide (Dzombak & Morel, 1990). Constants correspond to surface complexes, dominating at pH 3-4.

complex	**reaction at equilibrium**	**Log K**
$\equiv FeSO_4^-$	$K = \frac{\equiv FeSO_4^-}{\equiv FeOH \cdot HSO_4}$	7.78
$\equiv FeCrO_4^-$	$K = \frac{\equiv FeCrO_4^-}{\equiv FeOH \cdot H\ CrO_4}$	10.85
$\equiv FeH_2AsO_4$	$K = \frac{\equiv FeH_2AsO_4^-}{\equiv FeOH \cdot H_2AsO_4}$	29.31
$\equiv FeH_2PO_4$	$K = \frac{\equiv FeH_2PO_4^-}{\equiv FeOH \cdot H_2PO_4}$	31.29

2.4.3. Influence of Arsenate and Chromate on Schwertmannite Stability

Synthesis experiments showed that high amounts of arsenate and chromate can be enriched in schwertmannite. In consequence, schwertmannite acts as sink for these toxic elements and therefore an industrial application to clean contaminated waters seems reasonable. However, the metastable character of schwertmannite results in its dissolution at pH below 2.5 or in transformation to goethite by increasing pH or by time (Bigham et al., 1996). During these processes schwertmannite possibly releases previously bound toxic substances and therefore this mineral could also act as a source of contamination. To investigate the influence of incorporated oxyanions on schwertmannite stability and to quantify the oxyanion release in dependence on time at constant pH (2 or 4), a long term (1 year) stability experiment with schwertmannite and with schwertmannite containing arsenate, phosphate and chromate was performed.

The results suggest that chromate, phosphate and arsenate have a stabilising effect and thus prevent structural variation of schwertmannite caused by time. In suspensions, kept at pH 2, a considerable part of pure schwertmannite at pH 2 was dissolved at the end of the experiment (37 % of total iron and 78 % of total sulfate was released). In contrast, the dissolution process was slowed down in samples containing other oxyanions than sulfate (Table II.2-5). At pH 4 a part of pure schwertmannite transformed to goethite, as observed by XRD (Fig. II.2-11). This was indicated by the formation of a new peak at 0.418 nm reflecting the 110 plane of goethite and by the increased intensity of the peak at 0.156 nm which is typical for both minerals, but of stronger intensity in the goethite XRD-pattern (Cornell & Schwertmann, 1996). No features of goethite were identified in chromated, arsenated and phosphated schwertmannite.

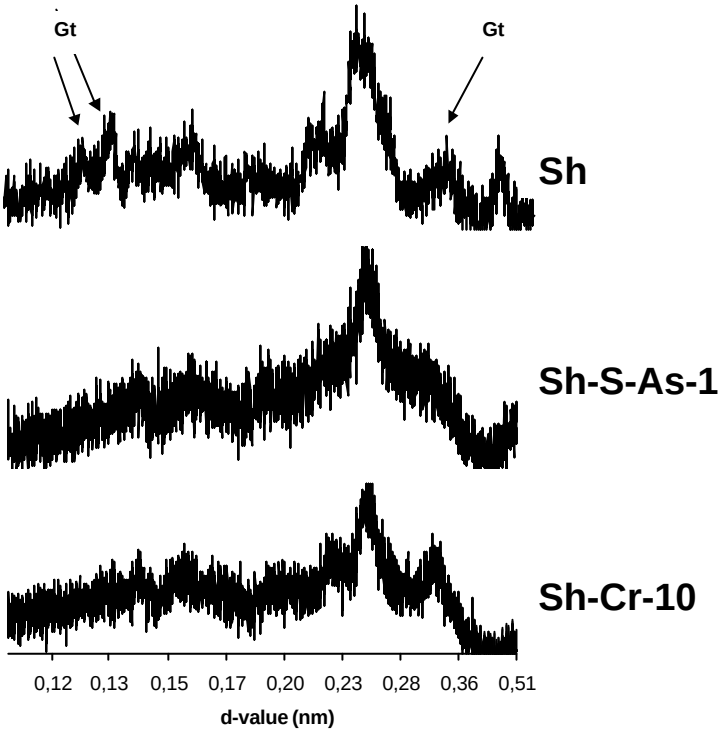

Fig. II.2-11 X-ray powder diffraction pattern of pure-, arsenated- and chromated schwertmannite (samples Sh, Sh-S-As-1 and Sh-Cr-10) after reaction time of 362 days kept at constant pH of 4. All samples show XRD features of schwertmannite. Arrows in sample "Sh" mark peaks of goethite.

Moreover, the total release of arsenate and chromate (0.02 to 0.1 µM AsO_4^{3-} and 100-150 µM CrO_4^{2-}) was lower than the release of sulfate (each ~ 200 µM) during the reaction time. Additionally, differences in the releasing rate of oxyanions indicated the stabilising influence of arsenate (Fig. II.2-10). At pH 2, the release of arsenate (max. 150 µM) steadily increased over the whole time scale, whereas the release of sulfate and chromate (max. 350 µM) was already constant after about 150 days. Due to these results, it was assumed that arsenate and chromate incorporation in schwertmannite retarded dissolution, transformation and the consequent release of toxic elements. Arsenate (and potentially phosphate which was not measured) seemed to have the most stabilising influence, followed by chromate. This stabilising influence is a consequence of the stronger bonding between Fe(III) and arsenate,

compared to chromate or sulfate as explained in the previous chapter on substitution affinities (Dzombak & Morel, 1990; Table II.2-8).

According to Bigham et al. (1996), it is impractical to determine a solubility product constant for schwertmannite because of its inherent compositional variability, the occurrence of sulfate as both, structural and adsorbed species and the apparent instability of the mineral relative to goethite. Therefore they determined an ionic activity product (IAP) for schwertmannite ($\log IAP_{Sh} = 18 \pm 2.5$) which describes a solubility window for schwertmannite and is valid for low pH (otherwise transformation to goethite should be expected) and pure schwertmannite (without arsenate, chromate, etc).

The calculated ionic activity products (IAP) of differently composed schwertmannite determined at pH 2 differed strongly at the end of the experiment (Tab. II.2-9).

Table II.2-9 Calculation of the ionic activity product (IAP) of schwertmannite in dependence on its composition (reaction based on Bigham et al., 1996).

solid composition	**Equation for IAP**	**Log IAP**	
$Fe_8O_8(OH)_{5.45}(SO_4)_{1.26}$	$LogK = 8 \log a(Fe^{3+}) + 1.26 \log a(SO_4^{2-}) + 21.48 \cdot pH$	=18.5	±0.2
$Fe_8O_8(OH)_{3.92}(SO_4)_{0.86}(AsO_4)_{0.77}$	$LogK = 8 \log a(Fe^{3+}) + 0.86 \log a(SO_4^{2-}) + 0.77\ a(AsO_4^{3-}) + 20.74 \cdot pH$	=13.5	±1.2
$Fe_8O_8(OH)_{5.11}(CrO_4)_{1.44}$	$LogK = 8 \log a(Fe^{3+}) + 1.44 \log a(CrO_4^{2-}) + 21.12 \cdot pH$	=16.2	±0.4
$Fe_8O_8(OH)_{5.5}(SO_4)\ (CrO_4)_{0.22}$	$LogK = 8 \log a(Fe^{3+}) + \log a\ (SO_4^{2-}) + 0.22 \log a(CrO_4^{2-}) + 21.56 \cdot pH$	=17.9	±0.5

The log IAP obtained for pure schwertmannite (18) confirmed results of Bigham et al. (1996) who determined a log IAP_{Sh} of 18.5± 2.5. Chromate incorporation debases this log IAP for two units (16.2) and arsenate for five units (13.5), compared to schwertmannite. This indicates the strong stabilising force of these anions to the schwertmannite structure.

A similar effect was described by Baron & Palmer (1995, 1996) for jarosite, an iron(III)sulfate mineral which can substitute sulfate by chromate. Consequently, the chromated jarosite had a clearly lower solubility ($\log K_{SP}$ =-18.4±0.6) compared to sulfate jarosite ($\log K_{SP}$= -11.0±0.3) at 25 °C.

Figure II.2-12 shows the time dependent changes of the calculated IAP which corresponds to the temporal equilibrium setting for the different schwertmannite samples at pH 2. After about 100 days equilibrium was adjusted for pure, chromated and phosphated schwertmannite, whereas the constant log IAP for arsenated schwertmannite (sample Sh-S-As-1) was still not completely reached after 280 days. Therefore, the calculated log IAP of arsenated schwertmannite was possibly slightly underestimated.

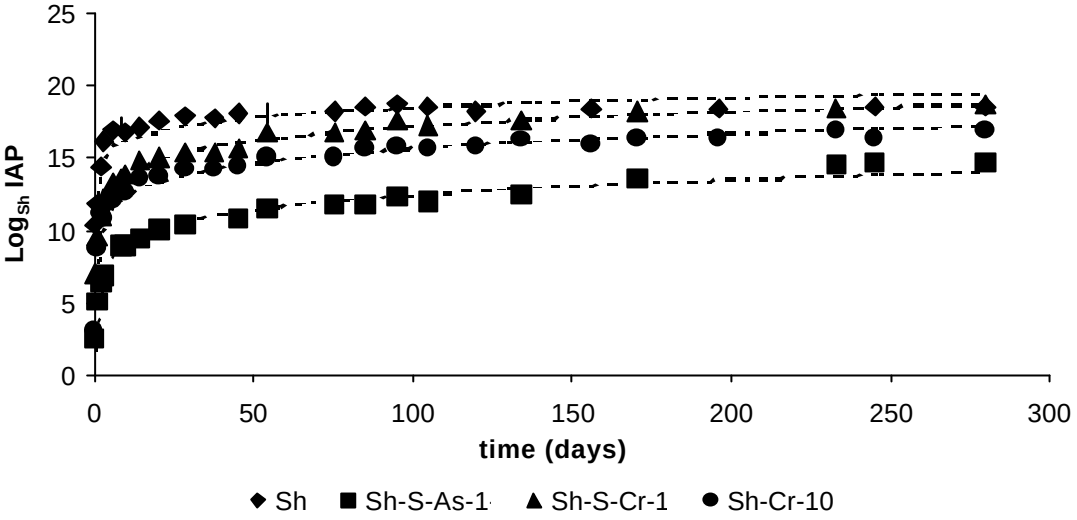

Fig. II.2-12 Variation of the ionic activity product (IAP) as a function of time calculated for schwertmannite with different anionic contents (Sh-S-As-1, Sh-S-Cr-1, Sh-Cr-10) at pH 2.

2.4.4. Adsorption Process

Due to the high surface area (~ 200 $m^2 \cdot g^{-1}$), a high adsorption-capacity of schwertmannite for the investigated anions was assumed. It is known that about 30 % of the total sulfate content of schwertmannite (0.4 to 0.5 $mmol \cdot g^{-1}$) is bound to the surface of that mineral (Bigham et al., 1990). Therefore, the adsorption of oxyanions should be considered for the incorporation of oxyanions in schwertmannite additionally to its substitution. Surface reactions of schwertmannite were investigated in the pH range of its stability, because dissolution at lower values or transformation to goethite at higher values would hint the adjustment of a chemical equilibrium (Bigham et al., 1996).

Simultaneously to the mostly pH independent adsorption of arsenate and chromate, sulfate was desorbed from schwertmannite (Table II.2-6) with a much stronger pH dependency. With increased pH, an excess of sulfate was measured, indicating an addition of base results in an exchange of SO_4^{2-} by OH^- in schwertmannite. Potentially, this replacement at the schwertmannite surface is the first step of transformation to goethite and involves, with increased exchange, the demolition of the mineral structure. It was supposed that the limit between the release of surface sulfate and structurally bound sulfate can be given if the released sulfate exceeds the mentioned 30 % of schwertmannite surface sulfate (which is ~ 0.4 $mmol \cdot g^{-1}$). However, Webster et al. (1998) stated that even 60 wt.-% (~0.8 $mmol \cdot g^{-1}$) of all schwertmannite sulfate is adsorbed and, correspondingly higher amounts of sulfate could get desorbed by an exchange of surface sulfate by OH groups or adsorbates. In this study, sulfate concentration never exceeded this amount indicating that only surface sulfate was released (in the observed pH range). An increased content of suspended adsorbent (4 $g \cdot L^{-1}$ instead of 1 $g \cdot L^{-1}$) resulted in slightly higher sulfate concentrations but not in the expected

quadruplicate amount (Table II.2-6). This indicates that agglomeration of schwertmannite particles in highly concentrated suspensions reduce the surface area.

Compared to the release of sulfate from schwertmannite in chromate solutions (0.3 $mmol \cdot g^{-1}$), more sulfate was released in arsenate ones (0.6 $mmol \cdot g^{-1}$). It was assumed that arsenate displaces the surface sulfate, whereas chromate (mostly) adsorbs additionally to sulfate.

Assuming that on the surface of iron hydroxides 4 OH groups per nm^2 are located (Sigg & Stumm, 1981), the total OH-exchange capacity of schwertmannite (with a surface area of 200 $m^2 \cdot g^{-1}$) should amount 1.33 $mmol \cdot g^{-1}$, if the surface would be exclusively covered with OH groups. These OH^- ions could be replaced by 0.66 $mmol \cdot g^{-1}$ bidentate-bound oxyanions. This amount ranges between the concentrations of adsorbed sulfate determined by Webster et al. (1998) and Bigham et al. (1990). The calculations confirmed that during adsorption experiments only surface sulfate was released. However, measurements of arsenate adsorption have shown that schwertmannite enriched more than 4.5 $mmol \cdot g^{-1}$ arsenate from a 5 mM arsenate solution which could not be exclusively surface bound. Therefore, three other processes additional to adsorption were considered: (1) The exchange of structurally bound sulfate by arsenate in the tunnel caves of the schwertmannite crystal would implicate a release of tunnel sulfate. However, the released sulfate concentration (< 0.63 $mmol \cdot g^{-1}$) hardly exceeded the amount of adsorbed sulfate (0.4 to 0.6 $mmol \cdot g^{-1}$). Therefore no exchange of tunnel sulfate by arsenate was expected. As an other possibility (2), the precipitation of a secondary iron arsenate phase would also imply additional released sulfate, because this process includes the dissolution of a part of schwertmannite to make Fe^{3+} available. More probable (3), though, seemed the diffusion of arsenate into particle pores due to electrostatic effects as it was described by Fuller et al. (1992) for arsenate incorporation into ferrihydrite. This weakly crystalline Fe(III) hydroxide with a high surface area (~ 300 $m^2 \cdot g^{-1}$) enriched 0.1 mol As per mol Fe. They explained the incorporation as a two phase process: After a rapid (some minutes) phase of specific adsorption, a period of gradual arsenate incorporation followed (~ eight days). During this long time, the oxyanions attached to surface places of the colloidal particles within the aggregates bound by electrostatic interactions (diffusive process). No secondary arsenic-containing solid phase was formed as investigations by X-ray spectroscopy (EXAFS) confirmed. A similar process for schwertmannite was assumed, because its colloidal crystals also form loose and porous aggregates, in between which anions could possibly diffuse during the reaction time of 24 h. This was shown by scanning electron microscopy (Bigham et al., 1990, this study: chapter III and appendix D).

2.5. Conclusions

In this study, evidence was given that schwertmannite acts as kind of scavenger for the investigated toxic substances arsenate and chromate. Schwertmannite samples taken in two different, former sulfidic ore mines were highly enriched with arsenic and chromium. In contrast, the concentrations of these elements in associated drainage waters were mostly under detection limit. This indicates a natural cleaning system in AMD affected waters which contain schwertmannite. Even higher amounts of arsenate and chromate were found incorporated in synthetic schwertmannite produced in laboratory.

These high uptake capacities of the mineral schwertmannite can be explained with its crystal structure which is marked by cavities in which oxyanions can be stored. During the formation of schwertmannite, sulfate normally incorporates into these structural cavities. However, this process limits the crystal growth and results in a high particle surface and a low mineral stability. These characteristics were investigated in this study, in order to determine influences of chromate and arsenate incorporation in schwertmannite. It was shown by X-ray diffraction analysis that an exchange of sulfate by chromate in schwertmannite is possible whereas arsenate, though enriched in high concentrations can be found only combined with sulfate or chromate in schwertmannite. Even after synthesis, schwertmannite defiltrates high amounts of chromate and arsenate from a solution. Due to the metastability of schwertmannite, its dissolution or mineral transformation to goethite caused either by time or by changes in the pH, can be expected. This is accompanied with a release of oxyanions which is highest for sulfate, followed by chromate and finally arsenate. Chromate and to a greater extend arsenate have a stabilising influence on the schwertmannite structure and thus they debase the ionic activity product of this mineral which is lowest for arsenated schwertmannite.

In this study the method of XRD was predominantly used for descriptions of changes in the crystal structure of schwertmannite. However, no exact quantitative differentiation was possible between the amounts incorporated in the tunnel caves, adsorbed to the surface or coprecipitated as secondary phase. Other methods as Mössbauer- or EXAFS (extended X-ray absorption fine structure) spectroscopy seem to be reasonable for future examinations of bonding types in schwertmannite.

This mineral can function as sink for arsenate and chromate and therefore should be applied to clean contaminated waters. Furthermore, schwertmannite can potentially enrich other toxic compounds and investigations with industrially produced schwertmannite and its use, optimally dosed, in drinking water conditioning systems could be suggestive.

3. A FTIR SPECTROSCOPICAL STUDY TO EXPLAIN BONDING STRUCTURES OF OXYANIONS INTO SCHWERTMANNITE

3.1. Introduction

Schwertmannite is an oxyhydroxysulfate of iron with the general formula $Fe_8O_8(OH)_ySO_z \cdot n\,H_2O$, where 8-y =z and $1.0 \leq z \leq 1.75$. Due to its weak crystallinity, it is hard to identify (Bigham et al., 1994). Just by a combination of X-ray diffractometry (XRD), Mössbauer- and Infrared-spectroscopy a characterisation of its structure was possible (Bigham et al., 1990). This structure was described to be akin to that of akaganéite (β-FeOOH) which was described in literature to consist of double chains of ironoxide- and hydroxide-octahedra, sharing corners to yield square tunnels in which (in the case of schwertmannite) sulfate is incorporated (Bigham et al., 1990). Additionally to this structurally bound sulfate, high amounts of this anion (~ 30 % of the total sulfate content) can also be adsorbed to its large surface, which is ~ 200 $m^2 \cdot g^{-1}$ (Bigham et al., 1990).

It was supposed that schwertmannite can enrich arsenate and chromate instead of, and in addition to, sulfate. Compared to sulfate, these toxic oxyanions are also tetrahedrally coordinated and have nearly the same ionic radius, which is approx. 0.25 nm. Due to this similarity they could, either completely or partly, substitute the sulfate in schwertmannite. In this study this should be confirmed by XRD. Moreover, it was hypothesised that any incorporation of oxyanions results in changes of the Fourier-Transformed infra red (FTIR) spectrum of schwertmannite, which should be used to distinguish between the types of oxyanion bondings (adsorptive and structural). Therefore, the object of this study was to investigate bonding structures of arsenate and chromate associated with schwertmannite by the method of FTIR spectroscopy similarly as described for sulfate (Bigham et al., 1990).

Vibration spectroscopy of schwertmannite and sulfate

Bigham et al. (1990) characterised the structure of schwertmannite by IR spectroscopy. The spectrum of schwertmannite consists of seven to eleven IR-active bands (Tab.II.3-1), five of which correspond to sulfate vibrations and were differentiated in structural and adsorptive bonding.

Tab.II.3-1 Position of absorption bands in the FTIR spectrum of schwertmannite: Measured data compared to literature data (position and interpretation according to Bigham et al., 1990).

Position (cm^{-1}) this study	**Position (cm^{-1}) (Bigham et al., 1990)**	**Interpretation (Bigham et al., 1990)**
485	483	ν-FeO
608	608	ν_4 SO_4 [1]
704	704	ν-FeO
790-885	800-880	δ-OH
976	976	$\nu_1 SO_4$ [2]
1055, 1130, 1195	1038, 1124, 1186	$\nu_3 SO_4$ [1]
1634	1634	H_2O
3300	3300	ν-OH

[1]structural -/ inner-sphere bonding; [2]outer-sphere bonding

Molecules of tetrahedral symmetry as SO_4^{2-} vibrate in four modes after being activated by electromagnetic radiation. Two vibrations (ν_1 and ν_2) are symmetric (=IR inactive) and therefore normally (besides some exceptions) not observable in the IR spectrum. Depending on the coordinative environment of the molecule, the IR-active asymmetric vibrations (ν_3 and ν_4) can split and with increasing complexation the number of "absorption bands" in the IR spectra also increases (Gottwald & Wachter, 1997, Peak et al., 1999).

Four of the five sulfate absorption bands detected in schwertmannite also appear in samples of Fe(III) minerals with sulfate exclusively adsorbed to the surface (Parfitt & Smart, 1978, Bigham et al., 1990, Tab.II.3-3). The schwertmannite specific absorption band of sulfate is located at 608 cm^{-1} in the IR spectrum, and corresponds to a ν_4-vibration (Nakamoto, 1986). Bigham et al. (1990) showed in a series of schwertmannite-akaganéite-mixing samples that, with the appearance of this band in schwertmannite, an OH-vibration at 640 cm^{-1} in akaganéite disappears simultaneously. This indicates that sulfate incorporation affects an exchange of hydroxide groups by sulfate and therefore this band is associated to an exclusively structural bonding of sulfate into the tunnels of schwertmannite crystals.

The three sulfate vibrations between 1000 and 1200 cm^{-1} in the IR spectrum of schwertmannite correspond to a split ν_3-vibration, which is associated with an innerspheric sulfate bonding to iron minerals (Peak et al., 1999). Parfitt & Smart (1978) described this bonding of sulfate to goethite (= α-FeOOH) as a binuclear bridging complex (Fe–O–S(O_2)–O–Fe), which can be attributed to specific adsorption and (in schwertmannite) also to structural bonding in the tunnel structure (Bigham et al., 1990). Both complexes are the same, because incorporation in the tunnels caves requires that the oxygen atoms of sulfate share places with the oxygen atoms of the iron-oxide/hydroxide octahedra to form a binuclear bridging (Bigham et al., 1990). The occurrence of these absorption bands can not be used to

distinguish between structural and adsorptive bonding. However, the highly intense bands of this ν_3-vibration suggests that high concentrations of sulfate are bound by this way to schwertmannite. Casually, in IR spectra of sulfate complexes, additionally to the ν_3 and ν_4 vibrations a weakly active ν_1-band appears, which is located at approx. 975 cm^{-1} and which corresponds to outer-sphere bound sulfate (Peak et al., 1999). With respect to schwertmannite this indicates that sulfate is adsorbed to its surface by both mechanisms. Together with splitting of the ν_3-vibration this is the consequence of lower symmetry of tetrahedral oxyanions due to inner-sphere complexes (Peak et al., 1999).

3.2. Material and Methods

Sample Preparation

Schwertmannite was synthesised after the recipe of Bigham et al. (1990) by the reaction of 40 $mmol \cdot L^{-1}$ Fe(III) (as $FeCl_3 \cdot 6\ H_2O$)·with 10 $mmol \cdot L^{-1}$ SO_4^{2-} (as Na_2SO_4), heated at 60 °C. Subsequently the resulting suspension, cooled to room temperature was dialysed against deionised water for several weeks with a daily exchange of water using cellulose membranes with an average pore radius permeability of 2.4 nm.

This method was partly modified by the addition of different amounts of arsenate (as $Na_2HAsO_4 \cdot 7\ H_2O$) or chromate (as Na_2CrO_4) into the synthesis solution as shown in Table II.3-2. Synthetic goethite (α-FeOOH) was produced according to Cornell & Schwertmann (1996) by titration of ferric nitrate with KOH. After synthesis all precipitates were freeze-dried. Mineral identification occurred by XRD using a Siemens D 5000 X-ray diffractometer with Co-K$\alpha_{1,2}$-anode (2 sec per 0.02 θ). The specific surface area of the samples was determined by N_2 adsorption according to the BET method (Brunauer et al., 1938).

Tab.II.3-2 Composition of the sample synthesis-solution. The prefix "Sh" of the sample name indicates the formation of schwertmannite as proven by XRD.

sample name	**composition of the synthesis solution ($mmol \cdot L^{-1}$)**
Sh	40 Fe(III) + 10 SO_4
Sh-S-As-1	40 Fe(III) + 10 SO_4 + 0.72 AsO_4
As-S-5	40 Fe(III) + 10 SO_4 + 4.6 AsO_4
As-10	40 Fe(III) + 7.2 AsO_4
Sh-S-Cr-1	40 Fe(III) + 10 SO_4 + 0.86 CrO_4
Sh-S-Cr-2.5	40 Fe(III) + 10 SO_4 +4.15 CrO_4
Sh-Cr-10	40 Fe(III) + 8.62 CrO_4

Adsorption of arsenate and chromate to the minerals was obtained by suspending 1 $g \cdot L^{-1}$ schwertmannite or goethite in a AsO_4^{3-}- or CrO_4^{2-} containing solution (c= 5 $mmol \cdot L^{-1}$). The suspensions of schwertmannite had a pH of 4, which was in goethite suspensions adjusted by addition of acid (HNO_3). After shaking over 48 hours at 20°C, the suspensions were filtrated (0.45 µm) and freeze-dried.

IR-Spectroscopic Measurement

Fourier transformed infrared spectra of the materials were recorded using a Vektor 22 Bruker FTIR Spectrometer equipped with a KBr-beamsplitter, LADTGS detector, KBr-window and silicium carbide as radiation source. The uptaken scans ranged in the middle infrared (MIR) between wavenumbers of 7500 and 370 cm^{-1} with 1 cm^{-1} resolution. 32 scans were collected for each measurement and the background spectrum was subtracted automatically from the sample. Samples were measured in transmission as KBr pellets, which were prepared as a homogenous mixture of 3 mg freeze-dried samples and 300 mg KBr and finally pressed to pellets with a hydraulic press at a load of approx. eight tons. This measurement technique could provoke structural changes, induced by pressing or by reactions with the KBr. This was described by Peak et al. (1999) for changes in the protonation degree of adsorbed ions. Therefore, some samples were measured directly either in suspended form or as solid without KBr using the ATR technique (attenuated total reflection). The ATR unit (MIRacle^{TM} Single Reflection) consists of a ZnSe crystal on which the sample was spread on. The range of wavelength for this measurement reaches wavenumbers as low as 650 cm^{-1} with a maximum resolution of 4 cm^{-1} and is therefore not as accurate as the measurements in transmission mode. The obtained spectra were compared to spectra of the same samples measured as KBr pellets and no significant differences were observed between these two techniques indicating that no structural changes should be expected.

The method of spectra subtraction between two measured samples was used to visualise absorption bands which are normally covered by the mineral spectrum. Thereby the FTIR spectrum of pure schwertmannite (or goethite) was subtracted from the schwertmannite (or goethite) samples containing arsenate or chromate and consequently, the appearing residual bands (the difference spectrum) stand for the vibrations of arsenate and chromate molecules.

The recorded absorption band were identified with the measurement program OPUS-NT and the obtained spectra were compared to the library of Farmer (1974) and in case of schwertmannite to the description of Bigham et al. (1990).

3.3. Results

Powder X-Ray Diffraction

The XRD pattern of the samples Sh, Sh-S-As-1 Sh-S-Cr-1, Sh-S-Cr-2.5 and Sh-Cr-10 (Fig. II.3-1) showed the same eight broad diffraction bands as described by Bigham et al. (1990) for schwertmannite. Therefore, the terms “chromated-” and “arsenated schwertmannite” were used for these samples in which evidence for schwertmannite formation by XRD was obtained. In contrast, the samples S-As-5 and As-10 were termed as X-ray amorphous (Fig.II.3-1).

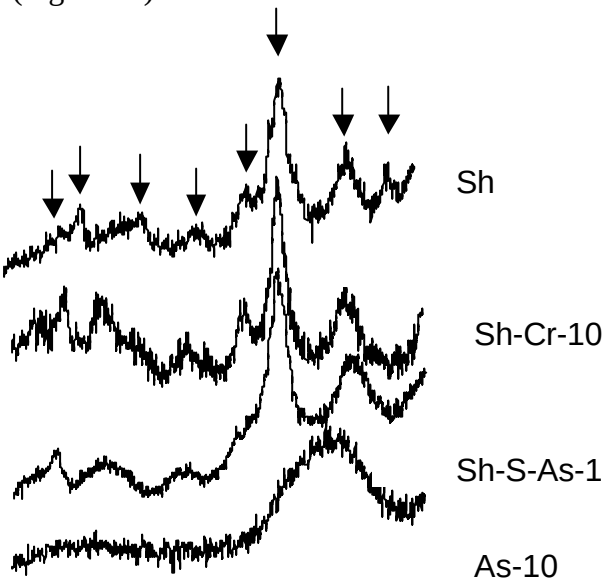

Fig. II.3-1 X-ray powder diffraction patterns of 4 synthesized samples: schwertmannite (Sh), chromated schwertmannite (Sh-Cr-10), arsenated schwertmannite (Sh-S-As-1) and X-ray amorphous iron(III)-arsenate (As-10). Arrows mark the positions of schwertmannite as described by Bigham et al. (1990).

FTIR Spectra of Sulfated Samples

The recorded FTIR spectrum of schwertmannite (sample Sh) was compared to the one described by Bigham et al. (1990) and as shown in Table II.3-1, both spectra are nearly identical. Schwertmannite is marked by five sulfate bands (at 1186, 1124, 1038, 976 and 608 cm^{-1}) and four of them were identified (at 1208, 1129, 1051, 980 cm^{-1}) in spectra of samples with sulfate adsorbed to goethite. Table II.3-3 gives an overview of identified bands of sulfate, chromate and arsenate in our study and a comparison to data in literature.

FTIR-Spectra of Chromated Samples

Fig. II.3-2 shows three difference spectra of chromated schwertmannite with different S:Cr-ratios in the synthesis solutions (samples Sh-Cr-10, Sh-S-Cr-2.5 and Sh-S-Cr-1 as shown in Tab. II.3-2). Chromate absorption bands were found at wavenumbers of 937, 826 and at 767 cm^{-1}.

Increasing chromate concentrations simultaneously result in decreased sulfate absorption intensities. The other IR-absorption bands characteristic to schwertmannite (Tab.II.3-1) were still preserved in the spectra.

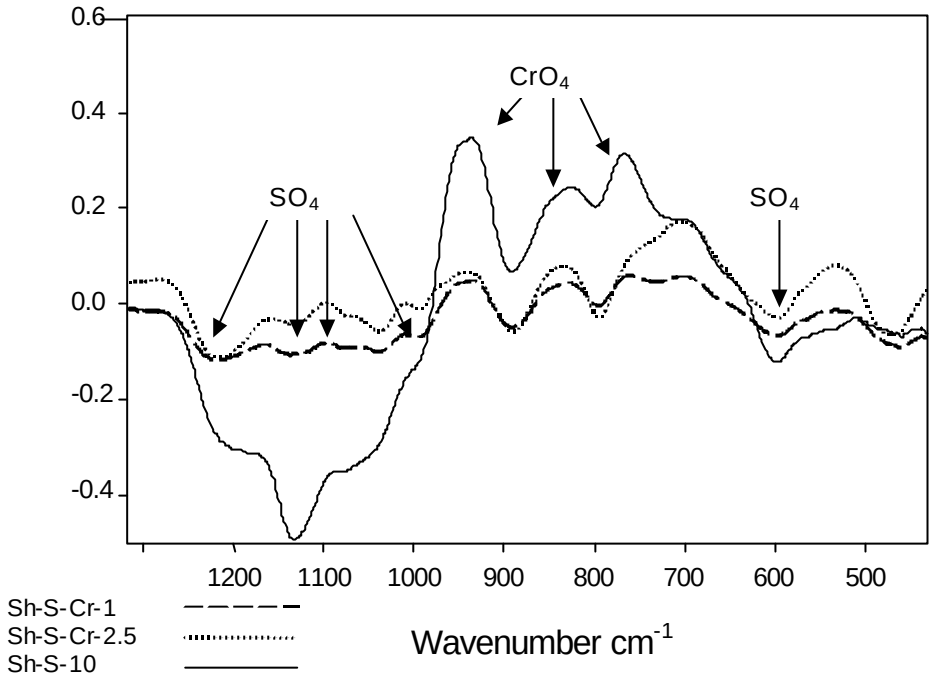

Fig. II.3-2 FTIR-difference spectra of chromated schwertmannite (chromate addition during mineral synthesis) with different amounts of chromate and sulfate (Tab. II.3-2). Marked bands indicate IR-absorption of chromate and sulfate. Sulfate bands are of negative intensity due to subtraction with the schwertmannite spectrum.

Chromate bands in samples with chromate adsorbed after synthesis to schwertmannite (sample Sh-ads-Cr) were similarly located (777, 828, 933 cm^{-1}; Fig. II.3-3), but the sulfate band at 975 cm^{-1} disappeared. In the difference spectrum of samples with chromate adsorbed to goethite two bands (at 743 and 819 cm^{-1}) were identified.

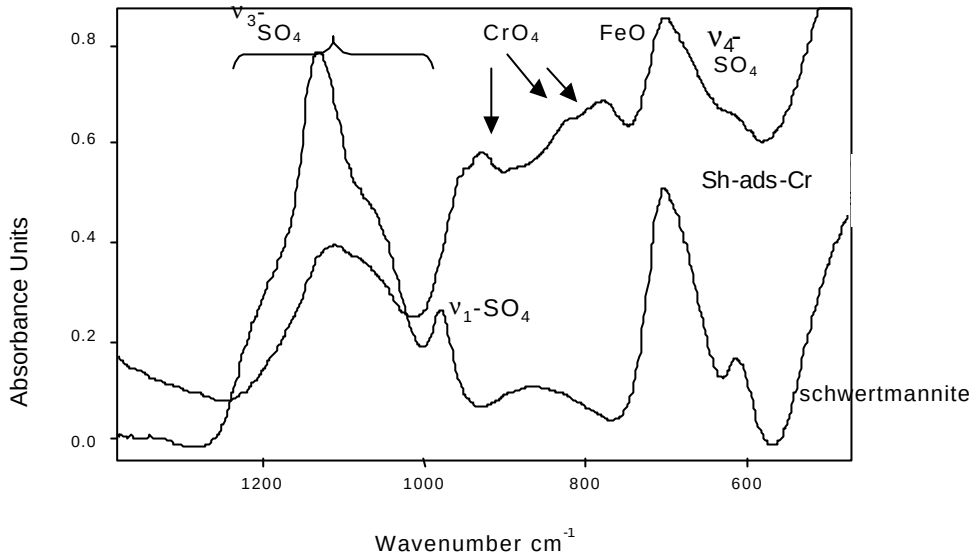

Fig II.3-3 FTIR-spectrum of pure schwertmannite and of schwertmannite with chromate adsorbed after mineral synthesis (Sh-ads-Cr, difference spectrum).

FTIR Spectra of Arsenated Samples

IR spectra, obtained from samples with increasing arsenic content in the synthesis solution of schwertmannite are marked by an increasing disappearance of characteristic schwertmannite absorption bands (e.g. the band at 704 cm^{-1}). Fig.II.3-4 shows the spectra of the samples Sh, Sh-S-As-1, S-As-5 and As-10 with the marked bands of sulfate, FeO and one new vibration occurring in arsenate containing samples at 834 cm^{-1}. An increasing arsenate content caused a decreasing intensity of sulfate- and FeO-vibrations, while the intensity of the arsenate band increases.

The difference spectra of arsenated schwertmannite showed three IR-active bands corresponding to arsenate with maxims at 938, 834 and 760 cm^{-1} (Fig. II.3-5).

The spectrum of schwertmannite with arsenate adsorbed after synthesis was marked by the one broad band at 834 cm^{-1}. The sulfate bands at 608 and 976 cm^{-1} completely disappeared and the split high-intensity sulfate bands between 1000 and 1200 cm^{-1} shrank to one broad band of low intensity. In Fig. II.3-5, a part of this difference spectrum is presented, which shows two shoulders on both sides of the 834 cm^{-1} band, which are located in a similar way to the identified arsenate bands of arsenated schwertmannite (Sh-S-As-1).

The difference spectrum of the sample with arsenate adsorbed to goethite showed three bands, located at 713, 819, 839 cm^{-1}.

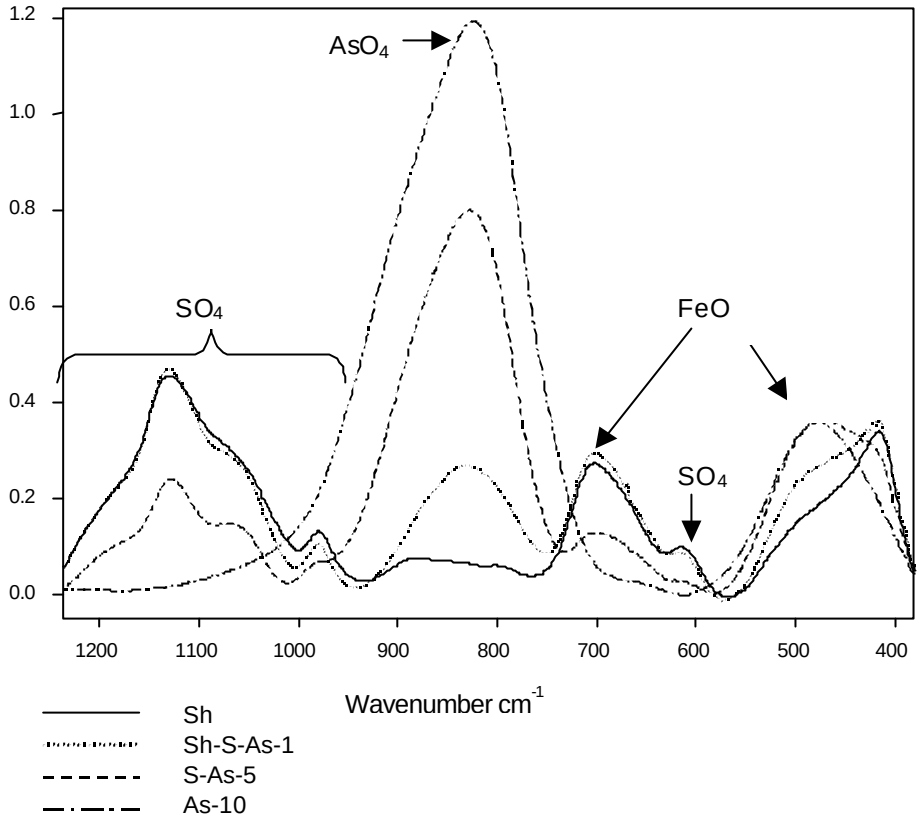

Fig. II.3-4 FTIR-spectra of schwertmannite (Sh) and samples which were synthesized with increasing As:S-ratio in the synthesis solutions (samples: Sh-S-As-1, S-As-5 and As-10, Tab. II.3-2).

3.4. Discussion

IR spectroscopy was used to explain arsenate and chromate bonding in schwertmannite in a similar way as described for sulfate (Bigham et al., 1990). Moreover, this method should confirm and interpret changes in the crystal structure observed by XRD analysis.

3.4.1. Sulfate bound to Schwertmannite

Sulfate incorporation in schwertmannite results in five IR-active vibration modes. The band at 608 cm^{-1} was specific for schwertmannite and corresponds to structural sulfate located in the tunnel caves of the crystals. The band at 976 cm^{-1} is associated with outer-sphere bound sulfate and the three bands between 1000 and 1200 cm^{-1} (ν_3-vibration) with specific sorbed sulfate (Bigham et al., 1990). I assume that this split ν_3-vibration corresponds to both, specific adsorbed and structurally bound sulfate. Due to its high intensity, which is proportional to high concentrations of sorbed sulfate it seems improbable that the large amount of sulfate in schwertmannite (1.2 $mmol \cdot g^{-1}$) is exclusively bound by specific adsorption to the surface. A

rough estimate shows that a surface area of 380 $m^2 \cdot g^{-1}$ is required at minimum to bind all sulfate on its surface if one assumes a large surface density of 4 OH groups per nm^2 of an Fe(III) hydroxide surface (Sigg & Stumm, 1981) of which each two OH ions are replaced by one sulfate ion. However, measurements of the surface area using the BET method resulted in an area of ~200 $m^2 \cdot g^{-1}$. As a consequence, these highly intense bands indicate occurrence of the ν_4-vibration (608 cm^{-1}) structural incorporation of sulfate into schwertmannite.

3.4.2. Chromate bound to Schwertmannite

Three absorption bands, located at 946, 833 and 761 cm^{-1} were identified in this study, which correspond to chromate vibrations (Fig. II.3-1). Two of them were already described by Baron & Palmer (1996) and Barham (1997) in samples of chromatised jarosite and chromatised schwertmannite (substitution of sulfate by chromate in both minerals), as shown in Table II.3-3. Compared to Barham (1997), who found absorption bands at 781 cm^{-1} and at 926 cm^{-1}, in this study chromate bands were slightly shifted to lower wave numbers. This effect can be explained by different protonation, an effect which could cause band-shifts of up to 50 cm^{-1}, as described for arsenate by Myneni et al. (1998).

A complete exchange of sulfate by chromate in schwertmannite was confirmed by XRD (Fig.II.3-1) and therefore similar results should be expected with FTIR spectroscopy of chromated schwertmannite. The spectra of chromatised schwertmannite should be marked by bands of inner-sphere sorption (ν_3-vibration), inner-sphere structural incorporation (ν_4-vibration), and outer-sphere adsorption (ν_1-vibration). However, the absorption band corresponding to a ν_4-vibration of chromate, indicating an exclusively structural incorporation was not found. According to vibration bands of dissolved chromate (Tab. II.3-3), this should be located at a wavenumber of ~ 350 cm^{-1}. Detection limit of the used instrument is > 370 cm^{-1} and therefore this band was not observed and no exact differentiation between adsorptive and structural chromate as described for sulfate was possible. I suppose that all identified chromate bands correspond to a split ν_3-vibration appropriate to the sulfate bands between 1000 and 1200 cm^{-1} identified in schwertmannite. Therefore, this split ν_3-vibration of chromate is equal to sulfate associated with binuclear bridging complexes (Fe-O-Cr(O_2)–O–Fe). Due to high intensities of these bands, they could correspond to specific adsorption and structural incorporation as described for sulfate.

Adsorption of chromate to iron hydroxides was normally described as inner-sphere, binuclear surface-complexation (Hsia et al., 1993).

However, results, obtained by EXAFS measurements showed that different modes of complexes can form by chromate adsorption to goethite, which are both, monodentate-, bidentate-binuclear and bidentate-mononucleare (Fendorf et al., 1997). A similar distinction by IR-spectroscopy was not possible. The bands of chromate identified in the sample Sh-ads-Cr (777, 828, 933 cm^{-1}, Fig. II.3-3) appeared at similar wavelengths as the bands in schwertmannite synthesised in the presence of chromate, indicating that no difference in the bonding mechanism exists between them. Possibly, the lower intensity can be used to distinguish between them. Normally, the intensity of an absorption band depends on both, the amount and the strength of a complex (van-der-Marel & Beutelspacher, 1976). The amount of chromate in sample Sh-S-Cr-1 was quite low (Tab.II.2-2) and the absorption bands clearly stronger than in sample Sh-ads-Cr. Therefore, it was assumed that compared to the structurally bound complexes in Sh-S-Cr-1, Sh-S-Cr-2.5 and Sh-Cr-10, the pure adsorptive chromate complexes in Sh-ads-Cr are less strong and therefore less intense.

The disappearance of the ν_1-sulfate at 975 cm^{-1} in samples with chromate adsorbed after schwertmannite synthesis, indicated that chromate displaces the outer-sphere bound sulfate. Results suggest that a complete differentiation between sorbed- and structural- bound chromate in schwertmannite based on FTIR spectra was not possible.

3.4.3. Arsenate bound to Schwertmannite

IR-spectroscopic investigations of the arsenated samples showed that with increasing arsenate content in the synthesis solution of schwertmannite, nearly all characteristic schwertmannite IR-absorption bands disappeared. As shown in the spectra of Fig. II.3-4, an increased arsenate content resulted in an increased intensity of the band at 834 cm^{-1}, and simultaneously all other bands of schwertmannite shrank independent to the mode of sulfate-molecule bonding (ν_1-, ν_3- or ν_4-vibration) and finally disappeared. Therefore, no preferential exchange of a sulfate-coordination by arsenate was assumed.

The absorption band at 834 cm^{-1} is a characteristic feature for Fe(III)-arsenate vibration and was interpreted for the mineral scorodite ($FeAsO_4 \cdot 2H_2O$) as an As-OFe-bonding (Myneni et al., 1998). This corresponds either to specific adsorption of arsenate to schwertmannite surface or to structural incorporation in the tunnel caves or to coprecipitation of an additional iron-arsenate phase. Arsenate is probably bound by all three mentioned mechanisms to iron in schwertmannite.

In the FTIR difference-spectra (Fig. II.3-5) two additional bands corresponding to arsenate were identified (at 730 and 940 cm^{-1}), which are of low magnitude.

Lumsdon et al. (1984) interpreted the high-intensity band at 834 cm^{-1} as a specific, asymmetric vibration of As-OFe/H, whereas the other two (730 and 940 cm^{-1}) represent symmetric As-OH- and As-OFe vibrations (Tab.II.3-3). According to interpretations of sulfate and chromate bands, it can be supposed that the three bands of arsenate represent a split ν_3-vibration.

Due to the similar location of these arsenate bands compared to arsenate adsorbed to goethite or to other iron hydroxides (Lumsdon et al., 1984, Tab.II.3-3), arsenate potentially is bound in the same way to both minerals (specific, bidentate). Normally, arsenate forms strong complexes with iron hydroxides (Dzombak & Morel, 1991), which are caused by an exchange of two surface OH^- molecules by one AsO_4^{3-} ion (Harrison & Berkheiser, 1982).

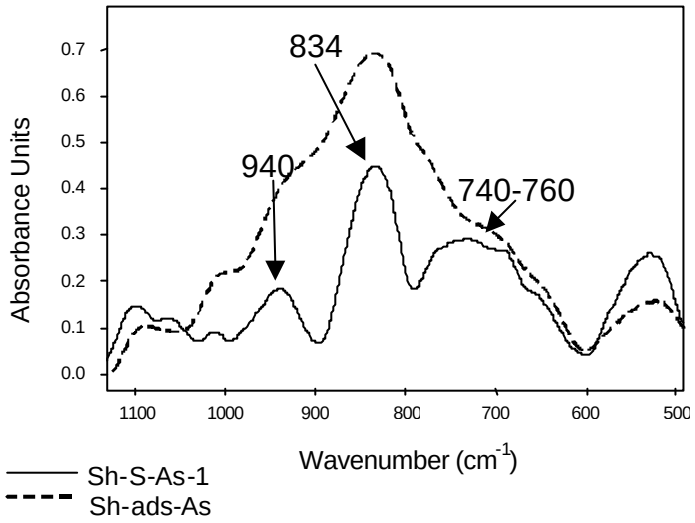

Fig. II.3-5 FTIR-difference spectra of arsenated schwertmannite (Sh-S-As-1) and arsenate adsorbed to schwertmannite after synthesis (Sh-As-ads).

The ν_4-vibration of arsenate could not be detected, although it should be located at ~ 400 cm^{-1} according to the values from dissolved arsenate (Tab.II.3-3). This region is close to the detection limit of the instrument and may therefore not be properly resolved. It was therefore not possible in this study to discriminate between specific arsenate bonding types in schwertmannite.

There is some evidence from the spectra that arsenate is bound in its protonated form to schwertmannite. According to Myneni et al. (1998), the positions of arsenate bands shift with increasing protonation to higher wave numbers from 720 cm^{-1} for AsO_4^{3-} to 790 cm^{-1} for H_3AsO_4. In this study, this arsenate band was detected at 760 cm^{-1} and corresponds to a $H_2AsO_4^-$ species.

Tab.II.3-3 IR-absorption band position of sulfate, arsenate and chromate in different phases. Measured data compared to literature data and interpretation from literature.

The Protonation degree of oxyanions in experiments of this study correspond to a pH of 4.

	Oxyanion absorption band position (cm^{-1})	**Vibration mode**	**reference**
SO_4^{2-} in solution	1105, 611	ν_3, ν_4	Farmer, 1974
SO_4^{2-} adsorbed to goethite; pH 3.5	1254, 1141, 1040, 965	ν_1, ν_2, ν_3, ν_4	Parfitt & Smart, 1978
SO_4^{2-} adsorbed to goethite	1170, 1133, 1051, 977	ν_3, ν_4	Peak et al., 1999
SO_4^{2-} adsorbed to goethite	1200, 1120, 1060, 970	ν_1, ν_2, ν_3, ν_4	Parfitt & Smart, 1978
SO_4^{2-} adsorbed to goethite	1208, 1129, 1051, 980	ν_3, ν_4	this study
SO_4^{2-} in schwertmannite	1186, 1124, 1038, 976, 608		Bigham et al., 1990
AsO_4^{3-} in solution	878 (810), 463 (398)	ν_3, ν_4	Farmer, 1974
AsO_4^{3-} adsorbed Fe(III) hydroxide	700 (As-OH), 805 (As-OFe) 875 (As-O/ As-OFe)		Harrison & Berkheiser, 1982
AsO_4^{3-} adsorbed to goethite; pH 6	719 (As-OH) 810 (As-OFe), 834, 938 (As-OFe/H)		Lumsdon et al., 1984
AsO_4^{3-} adsorbed to goethite	713, 819, 839		this study
AsO_4^{3-} adsorbed to schwertmannite	834		this study
AsO_4^{3-} in schwertmannite	760, 834, 940		this study
CrO_4^{2-} in solution	884, 368	ν_3, ν_4	Farmer, 1974
CrO_4^{2-} adsorbed to goethite	843, 819,		this study
CrO_4^{2-} in jarosite	851, 921		Baron & Palmer, 1996
CrO_4^{2-} in schwertmannite	781, 926		Barham, 1997
CrO_4^{2-} in schwertmannite	761, 833, 946		this study
CrO_4^{2-} adsorbed to schwertmannite	777, 828, 933		this study

3.5. Conclusions

FTIR spectra of chromated and arsenated samples recorded in this study confirmed data obtained from X-ray diffraction: While a complete substitution of sulfate by chromate in the schwertmannite structure is possible, sulfate only partly can be exchanged by arsenate. Increasing amounts of arsenate added into the schwertmannite-synthesis solution, effect in the resulting precipitate decreasing schwertmannite features according to both, XRD and FTIR spectroscopy.

The method of FTIR spectroscopy was used to explain bonding structures of the oxyanions in schwertmannite. The comparison of measured FTIR data with data from literature demonstrates that both, arsenate and chromate, are mostly specifically sorbed to schwertmannite. This could comprise adsorption to the surface, substitution in the mineral and/or coprecipitation as new phases. A differentiation between these processes was not attained.

4. INCORPORATION OF AS(III) IN SCHWERTMANNITE

4.1. Introduction: Significance of Arsenite

In the hydrochemical environment of waters affected by AMD (acid mine drainage), arsenate (AsO_4^{3-}) and arsenite (AsO_3^{3-}) are, beside sulfate (SO_4^{2-}), the most frequent and, due to their high toxicity, the most important oxyanions (Bigham & Nordstrom, 2000). The mobility of arsenic in the environment is generally controlled by sorption to Fe(III) hydroxides (Pichler et al., 1999). For example, Savage et al. (1999), detected goethite (α-FeOOH) with arsenic contents of about 1260 ppm in AMD precipitates. The release of mineral-bound or surface-adsorbed arsenic usually follows a change of redox conditions. Due to its low oxidation rate, the trigonally coordinated form of arsenic (arsenite) is frequently associated with the tetrahedrally coordinated form (arsenate) in natural waters (Seith & Jekel, 1998). Fig. II.4 1 shows a redox stability diagram for possible arsenic species. At pH values < 2 and very high arsenic concentrations, arsenic precipitates as scorodite ($FeAsO_4 \cdot 2H_2O$) (Cullen & Reimer, 1989). At lower As concentrations and higher pH values adsorption and coprecipitation with Fe(III) hydroxides are the dominant fixation processes.

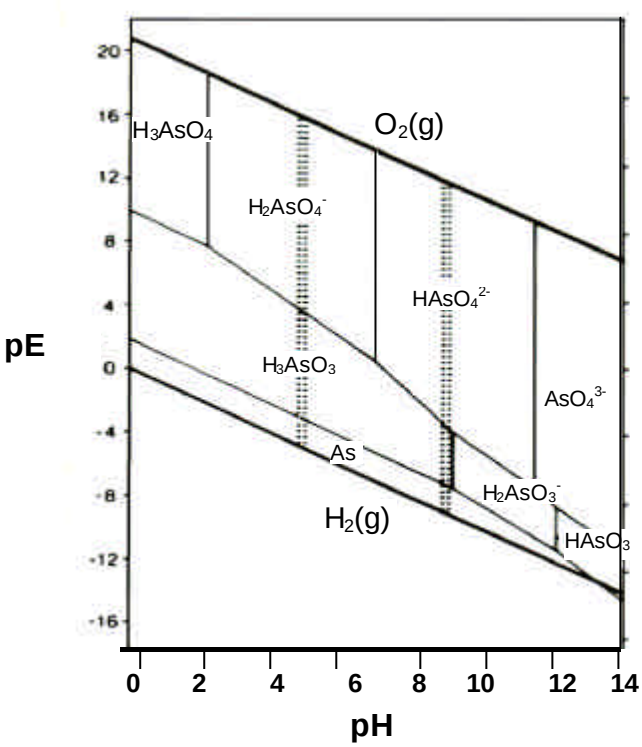

Fig. II.4-1 Redox-stability diagram and arsenic speciation (Cullen & Reimer, 1989).

At the chemical conditions of potential schwertmannite formation (acidic and oxic) protonated arsenate should be expected. However, due to the slow oxidation kinetics of

As(III) to As(V), arsenite can also (temporarily) exist in the presence of schwertmannite. As(III) is about 10 times more toxic than As (V) (Pontius et al., 1994) and is therefore of major ecological interest.

This part of my study deals with the question if arsenite can be enriched in a similar way to arsenate in schwertmannite. However, results should be considered as preliminary investigations, because only few experiments were performed to differentiate the oxidation state of As.

4.2. Materials and Methods

Sampling

Five water samples were taken from the AMD system of the former ore mine "Saalfelder Feengrotten" in Thuringia (chapter II.2.2.5) and examined with respect to their As(V) and As(III) content. The samples were chosen for analysis if schwertmannite was identified in corresponding precipitates containing more than 100 ppm As (appendix B). During field trips, samples were filtrated (0.2 µm) and frozen in the lab until analysis could take place.

As measurement

Quantitative analysis of As(tot) and As(III) was performed in the central analytic labs at the Bayreuth institute for terrestrial ecological system research (BITOEK) with a coupled HPLC ICP-MS system (Dionex). Nitric acid and benzene-disulfon acid served as eluents at a flow of 1 $mL \cdot min^{-1}$. The detection limit for As(III) was 2 $\mu g \cdot L^{-1}$ and for As(tot) 3 $\mu g \cdot L^{-1}$.

Synthesis of solids

The sample "Sh-AsO_3" was produced following the dialysis method for schwertmannite (chapter II.2.2.1., Bigham et al., 1990) with added arsenite (as $Na_2HAsO_3 \cdot 7\ H_2O$). Thus the synthesis suspension contained 40 $mmol \cdot L^{-1}$ Fe^{3+}, 10 $mmol \cdot L^{-1}$ SO_4^{2-} and 0.819 $mmol \cdot L^{-1}$ AsO_3^{3-}. After 30 days of dialysis, the sample was filtered (blue ribbon) and the filter residue freeze-dried. Evidence for schwertmannite formation was obtained by powder X-ray diffraction. A part of the solid had completely dissolved in 1 M HCl (1 $g \cdot L^{-1}$) and in the extract the total concentration of iron (flame AAS), sulfur (ICP-MS) and arsenic (graphite-tube AAS) was determined (methods are described in II.2.2.2).

The sample "Sh-ads-AsO_3" was produced by suspension of pure schwertmannite (1 $g \cdot L^{-1}$), after its synthesis (method: synthesis in Fe(III)-solutions) into an arsenite solution (c = 1 $mmol \cdot L^{-1}$) which was gazed with N_2 in three parallels. After a reaction time of 24 h, shaken at

constant temperature (20 °C), the suspension was filtered (blue ribbon filter) and As(tot) and As(III) were determined in the filtrate. The amount of arsenic adsorbed to schwertmannite was calculated on the basis of the difference between the total- and the measured As concentration.

FTIR spectroscopy

The solid samples were measured as KBr pellets (3mg sample/300 mg KBr) in transmission between wavenumber of 370 to 4500 cm^{-1} (analytics are described in chapter II.3.2.). Subtraction spectra were obtained as a result of differentiation of the spectra of As-containing samples with an As-free spectrum of schwertmannite.

4.3. Results and Discussion

4.3.1. Arsenite in the AMD water of the Saalfelder-Feengrotten

The total arsenic concentrations of the examined acid mine drainage waters of the "Saalfelder-Feengrotten" where As-enriched schwertmannite was formed, were usually below the detection limit (Tab. II.4-1). Solely in two samples As(III) was observed.

Tab.II.4-1. Arsenite and arsenate concentrations in the AMD water of the Saalfelder-Feengrotten.

sample	AsO_3^{3-} (ppb)	AsO_4^{3-} (ppb)
1	< d.l..	9
2	< d.l.	< d.l.
3	8	83
4	6	52
5	< d.l.	< d.l.

d.l. detection limit: for As(III) < 2, for As(V) < 3 ppb

Since the As(tot) content in the schwertmannite precipitates was relatively high (> to 100 ppm, appendix B), this result indicates that either schwertmannite filters As(III) similarly to As(V) from water or that, due to the oxic conditions in the examined waters, As(III) does not exist in this environment. The oxidation state of arsenic bound to these schwertmannite precipitates was not examined.

4.3.2. Arsenite associated with schwertmannite: coprecipitation and adsorption

The sample "Sh-AsO_3" (arsenite coprecipitated with schwertmannite) was composed of 45.1 wt.- % iron, 3.97 wt.-% sulfur and 5.72 wt.- % arsenic. If arsenic in this schwertmannite sample would be present as arsenite, the chemical formula can be given as $Fe_8O_8(OH)_{3.3}(SO_4)_{1.22}(AsO_3)_{0.75}$. Compared to arsenate incorporation in schwertmannite a similarly high incorporation-capacity and a similar formula can be obtained ($Fe_8O_8(OH)_{3.9}(SO_4)_{0.9}(AsO_4)_{0.75}$; chapter II.2.3).

Arsenite uptake by schwertmannite after mineral synthesis (sample "Sh-ads-AsO_3") from an arsenite solution (c = 1 mmol·L^{-1}) resulted in 0.88 mmol·g^{-1}. Analyses of the oxidation state of arsenic remaining in solution indicated no oxidation to arsenate.

4.3.3. Distinction of the oxidation state of arsenic by FTIR spectroscopy

In this FTIR study it was to be examined whether the oxidation states of arsenic bound to schwertmannite can be distinguished, or whether the binding of arsenic to schwertmannite involves oxidation to arsenate. The FTIR spectra of the samples Sh-ads-AsO_3 (arsenic uptake after schwertmannite synthesis) and of Sh-AsO_3 (arsenic uptake during schwertmannite synthesis) are presented in Fig. II.4-2. Both spectra show 4 to 5 absorption bands, of which the maxima are not located in the range of schwertmannite bands as described by Bigham et al. (1990). Therefore, it was assumed that they correspond to the arsenic. In both spectra these bands are located at the same wavenumbers (734, 808, 840, 870, 904 cm^{-1}). They differ from the bands identified in arsenate containing schwertmannite (760, 834 and 938, chapter II.3.3).

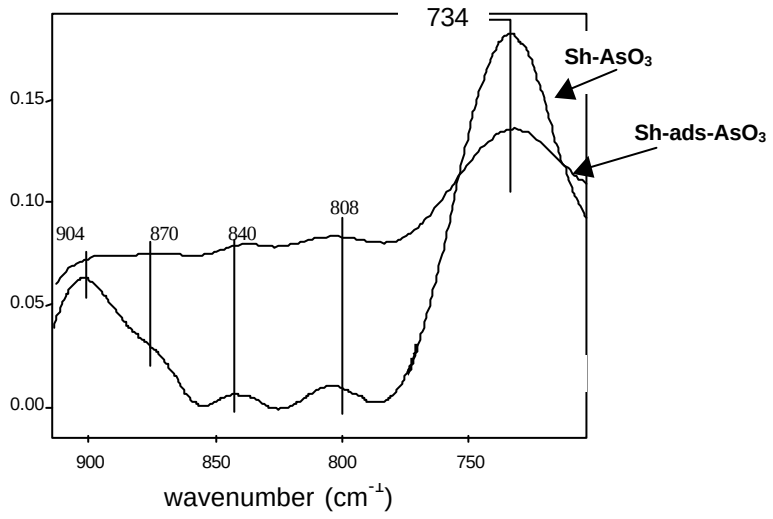

Fig. II.4-2 FTIR subtraction-spectra of arsenite bound to schwertmannite. (Sh-AsO_3: Arsenite uptake during schwertmannite synthesis Sh-ads-AsO_3: Arsenite uptake after schwertmannite synthesis)

The biggest difference, compared to the arsenate spectra, is the high intensity of the absorption band located at 734 cm^{-1}. It was identified in arsenate spectra with weaker intensity and located at a higher wavenumber (760 cm^{-1}) and probably correlates to an As-OH vibration (Lumsdon et al., 1984).

The description and differentiation of possible binding-modes of arsenite and arsenate to goethite by FTIR spectroscopy were examined by Sun & Doner (1996). Their study is based on investigations of changes in the band location of the surface OH groups of the iron hydroxides depending on bound arsenate and arsenite concentrations. They demonstrated that As(III) and As(V) exchange partly differently coordinated OH groups during their sorption to the iron hydroxide. Thus evidence was found for different sorption modes and an oxidation of arsenite during the adsorption could be excluded. In my investigations only the IR-active bands which can be directly assigned to the arsenic, were interpreted. Since these bands differ in both spectra of arsenite containing samples from the spectra of arsenate containing samples, it was assumed that arsenite directly binds to schwertmannite without oxidation to arsenate. Investigations of Manning et al. (1998) which described the binding of arsenite at goethite by XAS (X-ray absorption spectroscopy) and EXAFS (extended X-ray absorption fine structure) measurements, confirm this thesis. They stated that arsenite forms very strong, bidentate-binuclear complexes (Fig. II.6-3) at the surface of goethite. These surface complexes resist an oxidation to arsenate.

Results of this study suggest that schwertmannite can take up high concentrations of arsenite during and after its formation. Further investigations concerning the bonding strength of arsenite to schwertmannite and the possible mobilisation of this toxic compound seem promising.

5. MOBILISATION OF ARSENATE AND CHROMATE DURING MICROBIAL REDUCTION OF SCHWERTMANNITE

5.1. Introduction

The Fe(III)-mineral schwertmannite [$Fe_8O_8(OH)_x(SO_4)_y$ with $1 \leq y \leq 1.75$ and $2y = 8-x$] can be frequently found as a product of pyrite oxidation in areas exposed to acid mine drainage (Bigham et al., 1990, 1994). Its formation requires oxic, acidic (pH 2.5 - 4), and sulfate-rich (> 10 mmol L^{-1}) conditions. Schwertmannite is a mineral of poor crystallinity and high instability. Changing of the chemical or physical conditions in the system lead to its dissolution or transformation to more stable minerals such as goethite (Bigham et al., 1996). Schwertmannite contains between 12 and 15 wt.-% of sulfate, part of which is structurally bound to the mineral. Because of the large surface area of schwertmannite (~200 m^2 g^{-1}), about 30 % of the total sulfate can be also adsorbed to the surface (Bigham et al., 1990). The mineral can take up large amounts of the oxyanions arsenate (Carlson et al., 2001) and chromate (Barham, 1997). Up to 11 weight % of arsenate and 15 % of chromate can be bound either structurally or adsorbed to schwertmannite (Regenspurg and Peiffer, 2000). Thus, schwertmannite might act as a sink for these toxic elements in contaminated waters.

In general, the solubility of chromium and arsenic in the environment is controlled by the presence of iron oxides and parameters like pH or redox potential. Dissimilatory Fe(III)-reducing bacteria can promote the mobilisation of arsenate by the reductive dissolution of iron-arsenate minerals (Cummings et al., 1999). Direct reduction of arsenate by arsenic-reducing bacteria may also play a significant role in mobilising arsenic from those minerals (Ahmann et al., 1997). The microbial reduction of chromate (VI) to a less toxic insoluble chromium (III) precipitate is a detoxification mechanism of some bacteria (Lovley, 1993; McLean and Beveridge, 2001). In acidic mining-impacted habitats, the reductive dissolution of Fe(III) is a dominant electron-accepting process for the oxidation of organic carbon and reduced sulfur mediated by the activity of acidophilic bacteria (Fortin et al., 1996; Peine et al., 2000; Küsel and Dorsch, 2000; Küsel *et al*., 2001). *Acidiphilium cryptum* JF-5, a facultative anaerobic, non-fermentative Fe(III) reducer, has been isolated from an acidic coal mining lake sediment containing schwertmannite (Küsel et al., 1999). Thus, the objectives of this study were to evaluate the effect of reductive dissolution of arsenated and chromated schwertmannite on the mobilisation and potential reduction of arsenate and chromate by *A. cryptum* JF-5, and to study the effect of schwertmannite transformations on these processes.

5.2. Materials and Methods

5.2.1 Preparation of Schwertmannite Specimens

Three different specimens were synthesised using a modified method described by Cornell and Schwertmann (1996). Suspensions of 1 $g \cdot L^{-1}$ Fe(III) (provided as $FeCl_3 \cdot 6\ H_2O$) and 1 $g \cdot L^{-1}$ sulfate (provided as Na_2SO_4) were dialysed for 30 days against demonised water using dialysis bags of cellulose membranes. Sulfate was partially substituted by addition of arsenate or chromate (Tab.II.5-1). After synthesis of the different schwertmannite samples, total Fe(III), sulfate, arsenate, and chromate were determined in freeze dried minerals by flame AAS (Fe), ICP-AES (S), and graphite-tube AAS (As, Cr). (Tab.II.5-I). The identification of schwertmannite was performed by X-ray diffraction (Siemens D5000 goniometer with a Co-$K\alpha_{1,2}$-anode), and samples were examined by FTIR (Fourier-Transformed Infrared) spectroscopy (Vektor 22 FTIR–MIR, Bruker, spectral resolution of 1 cm^{-1}) in transmission mode as KBr pellets between 370 and 4500 cm^{-1}.

Tab.II.5-1 Composition of the synthesis solution and of the solid schwertmannite specimens.

	Synthesis solution			Schwertmannite specimens					
	Sh	Sh-As	Sh-Cr	Sh		Sh-As		Sh-Cr	
Components		(mM)		(wt.-%)	(mM)	(wt.- %)	(mM)	(wt.- %)	(mM)
Fe^{3+}	40	40	40	44.5	40	43.3	40	32.9	40
SO_4^{2-a}	10.6	10.6	10.6	12.3	6.4	8,3	4.4	7.3	5.1
AsO_4^{3-a}	0	0.72	0	0	0	10.3	3.8	0	0
CrO_4^{2-a}	0	0	0.86	0	0	0	0	1.8	0.6

[a] addition as Na-salt

5.2.2 Microbial Reduction of Schwertmannite Samples

Cells of *A. cryptum* JF-5 were grown both aerobically and anaerobically in a tryptic soy broth medium (TSB, 0.025%). Anoxic medium was boiled and cooled, and 15 ml were dispensed under flowing N_2. Oxic medium contained air in the headspace. The pH approximated 2.7 after autoclaving. Approximately, 5.2 to 5.4 g schwertmannite samples were added to 1 l medium either before or after autoclaving (121°C for 20 min) to reach a final concentration of 40 mM Fe(III). Glucose was added from a sterile, anoxic stock solution to reach a final concentration of 3 mM. For inoculation, approximately 4 x 10^9 cells of aerobically grown cells of *A. cryptum* JF-5 were transferred to anoxic medium containing schwertmannite samples in 3 replicates.

Uninoculated tubes containing schwertmannite samples served as controls. In order to determine whether *A. cryptum* JF-5 can enzymatically reduce arsenate or chromate, aerobically grown cells of *A. cryptum* JF-5 were transferred to anoxic TSB medium containing arsenate (5 mM) or chromate (2 mM) as the sole electron acceptor and glucose as electron donor. Controls received no glucose. The incubation temperature was 30 °C.
The microbiological investigations were performed by Kirsten Kuesel at the department of microbial ecosystem research, BITOEK.

5.2.3 Analytical Techniques

Reduction of Fe(III) was estimated by measuring the amount of Fe(II) formed. Aliquots (0.2 mL) of the media were taken by sterile syringes, transferred to 9.8 mL of 0.5 M HCl, and incubated for 1 h at RT (Lovley and Philipps, 1986). Fe(II) was measured after the addition of acetate by the phenanthroline method (Tamura et al., 1974). Glucose was determined with Hewlett-Packard 1090 series II high-performance liquid chromatographs (Palo Alto, Calif.) as previously described (Küsel et al., 1995). Sulfate was measured by ion chromatography with a Metrohm IC, Separation Center 733 (Suppressor module 753; Metrosep Anion Dual 1 column) with an eluent mixture of $NaHCO_3$ and Na_2CO_3 in a concentration of 2.4 mM and 2.5 mM, respectively, and a flow of 0.5 mL min^{-1}. As(III) and As(tot) were measured by HPLC-ICPMS (detection limit: 0.03 µM), an eluent of $NH_4H_2PO_4$ (flow rate: 1 mL min^{-1}). Cr(tot) was measured with a graphite-tube AAS (Varian/Spectr-AA-30, GTA-96

5.3. Results

5.3.1. Characterisation of Uninoculated Schwertmannite Samples

The synthesised specimens Sh, Sh-As and Sh-Cr were identified as schwertmannite by XRD analysis of freeze-dried samples (Fig.II.5-1).

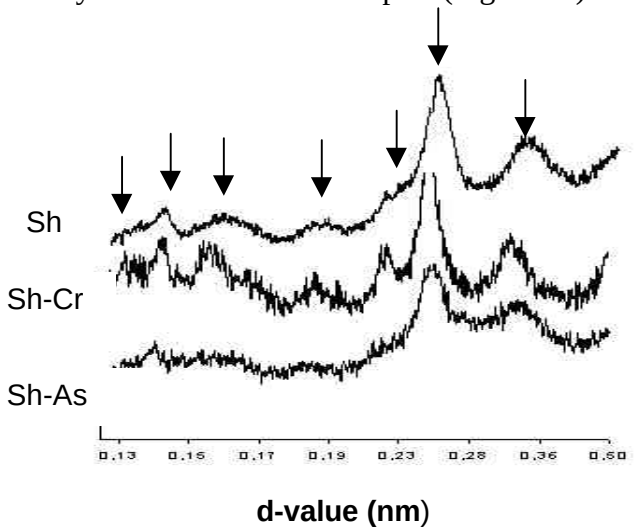

Fig. II.5-1 XRD patterns of the three synthesised freeze-dried samples: schwertmannite (Sh), chromated schwertmannite (Sh-Cr) and arsenated schwertmannite (Sh-Cr). Arrows mark the positions of the characteristic broad peaks of schwertmannite (Bigham et al., 1994).

All samples seem to have the same crystal structure as schwertmannite described in literature (Bigham et al., 1994) and were, therefore, defined as schwertmannite. In TSB medium, pure schwertmannite (Sh) released about 30 % of bound sulfate probably due to a desorption process of surface sorbed oxyanions (Fig.II.5-2). Chromated schwertmannite (Sh-Cr) released approximately 20 % of the chromate into solution, and arsenated schwertmannite (Sh-As) released only negligible amounts of As(V) (0.3 to 0.4 µM). Autoclaving of schwertmannite samples caused a complete release of sulfate bound to pure schwertmannite (Fig. II.5-2).

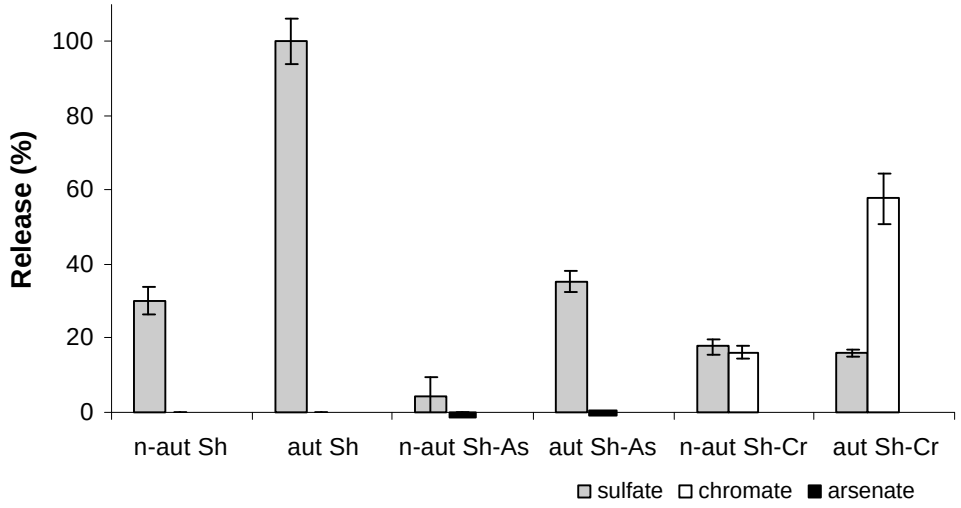

Fig. II.5-2 Release of sulfate, chromate and arsenate (% of total) from autoclaved and non-autoclaved samples of pure (Sh), chromated (Sh-Cr) and arsenated (Sh-As) schwertmannite, respectively, in uninoculated media. Abbreviations: n-aut, non-autoclaved samples; aut, autoclaved samples. The results are given in % of the total anion content of the sample. The release of arsenate from arsenated schwertmannite (Sh-As) was smaller than 0.01 % of the total arsenate content in autoclaved and non-autoclaved samples. Presented data are the averages of triplicates (± standard deviation).

The IR spectrum of autoclaved pure schwertmannite differed from that of non-autoclaved pure schwertmannite (Fig.II.5-3) due to the disappearance of the schwertmannite-typical FeO absorption-band at 704 cm^{-1} and of the peak at 610 cm^{-1} that is characteristic for structural sulfate in schwertmannite.

In contrast, the presence of absorption bands of OH and O vibrations at 892, 795, 630, 495, 449 and 397 cm^{-1} are typical for synthetic goethite (Cornell & Schwertmann, 1996). This indicates a structural change (transformation) of schwertmannite to goethite, which occurs during heating a solution of schwertmannite.

The four absorption bands between 990 cm^{-1} and 1300 cm^{-1} can be attributed both to sulfate bound to schwertmannite (Bigham et al., 1990) and sulfate adsorbed to the surface of goethite (Peak et al., 1999). IR spectra of Sh-As and Sh-Cr revealed no differences between the autoclaved and non autoclaved samples (data not shown) and were similar to the spectrum of pure schwertmannite.

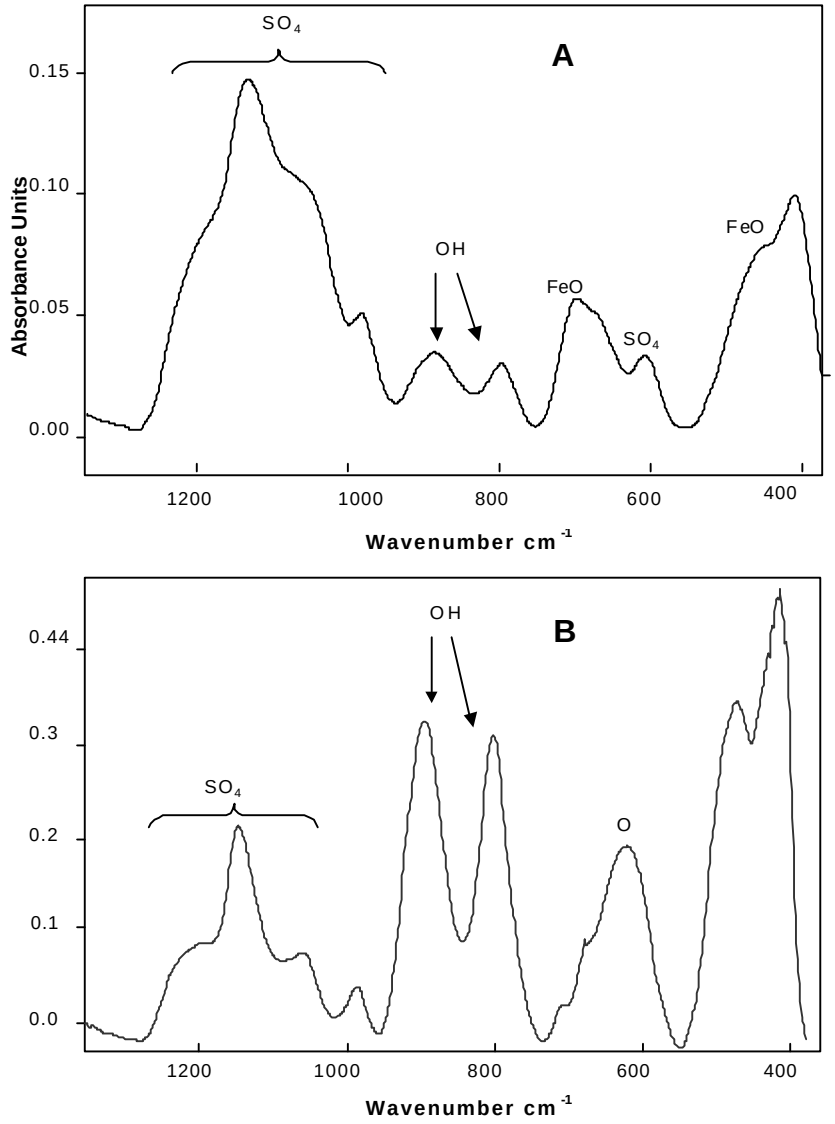

Fig. II.5-3 Effect of heat on the FTIR-spectra obtained from non-autoclaved (A) and autoclaved (B) pure schwertmannite (Sh) in uninoculated media.

5.3.2. Microbial Reduction of Schwertmannite Samples

Pure non-autoclaved schwertmannite was reduced by *A. cryptum* JF-5, and approximately 3.5 mM Fe(II) were formed during an incubation of 14 days (Fig.II.5-4A). Similar amounts of Fe(II) were formed by *A.cryptum* JF-5 from autoclaved pure schwertmannite (Fig.II.5-4B) indicating that alterations of schwertmannite apparently to goethite did not affect the microbial reducibility. No Fe(II) was formed in controls containing no cells.

Differences in the lag phases prior to the formation of Fe(II) in autoclaved and non-autoclaved samples might be due to different activities of aerobically grown *A. cryptum* cells, because cells were harvested either from the exponential or from the stationary growth phase to inoculate tubes of non-autoclaved and autoclaved samples, respectively.

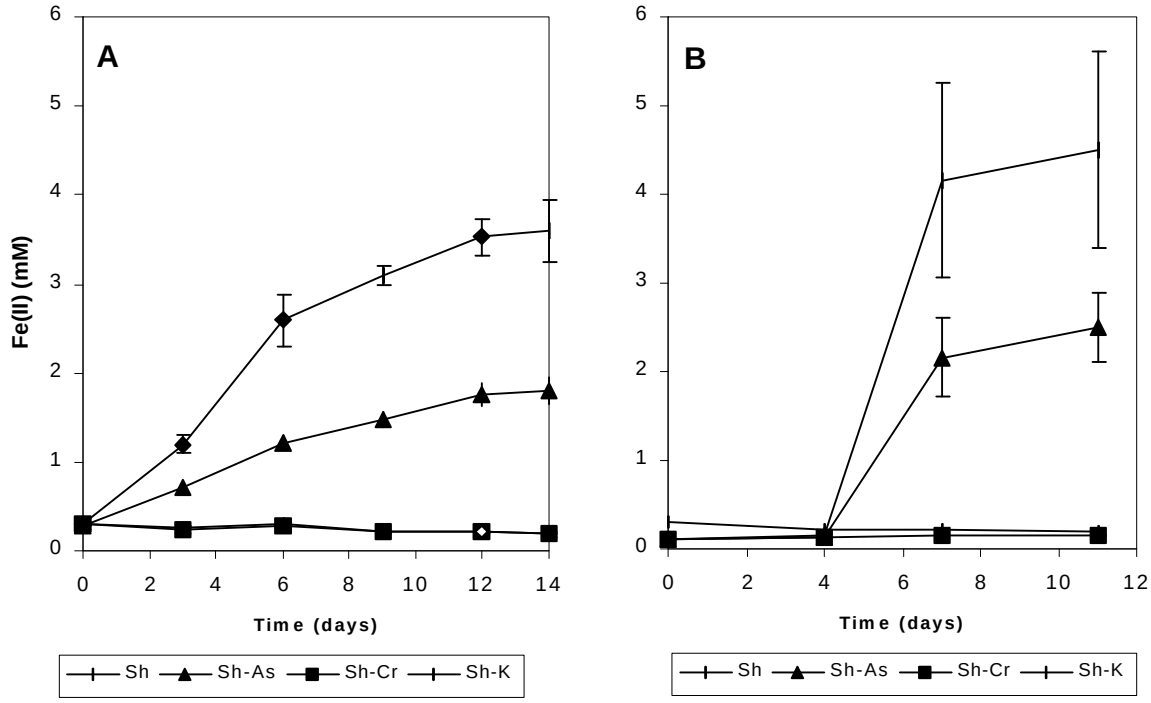

Fig. II.5-4 Formation of Fe(II) from non-autoclaved (A) and autoclaved (B) pure schwertmannite (Sh), arsenated schwertmannite (Sh-As), and chromated schwertmannite (Sh-Cr) by *A. cryptum* JF-5 incubated in anoxic, acidic TSB-medium supplemented with glucose at 30 °C. No Fe(II) was formed in uninoculated controls (Sh-K) containing Sh, Sh-As, or Sh-Cr. Presented are the averages of triplicates (± standard deviation).

Compared to the formation of Fe(II) from pure schwertmannite, lower amounts of Fe(II) were formed from arsenated schwertmannite (Fig.II.5-4). Whereas 10 % of the Fe(III) present in pure schwertmannite were reduced by *A. cryptum* JF-5, only 5% of the Fe(III) present in arsenated schwertmannite could be reduced.

In addition, no As(III) could be detected in solution at the end of incubation. In medium containing chromated schwertmannite, neither Fe(II) was formed, nor glucose was consumed indicating that chromate abiotically released at the beginning of incubation in a concentration of 0.2 mM was toxic to cells of *A. cryptum* JF-5. FTIR analysis of the specimens at the end of incubation did not show any structural change compared to the spectra of uninoculated schwertmannite samples (data not shown)

When aerobically grown cells of *A. cryptum* JF-5 were transferred to an anoxic medium containing arsenate or chromate as the sole electron acceptor, no growth occurred, no reduction of As(V) or Cr(VI) could be detected and no glucose was consumed.

5.3.3 Effect of Microbial Fe(III) Reduction on the Release of Sulfate, Arsenate, and Chromate

During the microbial reduction of Fe(III) of non-autoclaved pure schwertmannite (Sh), higher amounts of sulfate were released (2.75 mM) compared to the amount of sulfate released in uninoculated controls (1.4 mM). In medium, pure schwertmannite contained 6.4 mM sulfate (12.3 wt.-% sulfate; Tab.II.5-1). Thus, 40 % of the total amount of sulfate bound to Sh were released during the reductive dissolution of pure schwertmannite compared to 20 % in the uninoculated controls. During the reduction of arsenated schwertmannite, lower additional amounts of sulfate (0.54 mM) were released compared to the release from pure schwertmannite. Compared to the uninoculated controls, no additional amounts of arsenate were released during the microbial reduction of Fe(III) of arsenated schwertmannite. The presence of cells did not affect the amount of sulfate or chromate released from chromated schwertmannite.

5.4. Discussion

Although the general capacity to reduce Fe(III) is widespread among heterotrophic acidophiles inhabiting Fe(III)-rich habitats, rates and the extent of Fe(III) reduction vary greatly between the isolates examined (Johnson and McGinness, 1991). Sorption of Fe(II) by cell and oxide surfaces can limit the extent of Fe(III) reduction (Urrutia et al., 1998). In batch cultures, Fe(III) oxide reduction typically ceased after 15 to 30 days of incubation due to a decline in cell viability (Urrutia et al., 1998). Thus, under *in situ* conditions more than 10% of Fe(III) present in schwertmannite might be available for reductive dissolution.

At low pH, Fe(III)-reducing bacteria like *Acidiphilium* species likely do not have to attach to the surface of iron minerals to transfer electrons to Fe(III); probably they can utilise the small pool of dissolved Fe(III) for reduction (Bridge and Johnson, 2000). Consequently, the reducibility of Fe(III) depends on the solubility of the iron oxide and the chemical speciation of Fe(III) in solution. Substitutions in iron oxides change their solubility (Schwertmann et al., 1991). Arsenated schwertmannite seemed to be less available for microbial Fe(III) reduction than pure schwertmannite. Since all dissolution processes are surface reactions, surface complexation also influences the dissolution.

The dissolution of Fe(III)oxides can particularly be inhibited by binuclear surface complexes formed by oxyanions such as sulfate and arsenate (Biber et al., 1994). In acidic environments, these oxyanions are protonated, and the reaction, for example for surface complexation of arsenate on hydrous ferric oxide, equals: $\equiv FeOH + H_2AsO_4^- + = \equiv FeHAsO_4^- + H_2O$ (Dzombak & Morel, 1990). Complexation constants in the pH-range of 2 to 4 increase in the sequence sulfate (log K = 7.8), chromate (log K = 10.8), and arsenate (log K = 23.5) (Dzombak and Morel, 1990). Differences in the equilibrium constants of soluble Fe(III) to solid Fe(III) in arsenated schwertmannite compared to pure schwertmannite might have caused the reduced bioavailability of Fe(III) by lowering the pool of soluble Fe(III). Since no arsenate was released during the reductive dissolution of arsenated schwertmannite, only Fe(III) not bound to arsenate seemed to be available for microbial reduction. Due to the release of sulfate during the microbial reduction of arsenated schwertmannite, the remaining arsenated schwertmannite should be enriched with arsenate. Differences in the surface complexation constants might also explain the negligible and low release of arsenate and chromate from arsenated and chromated schwertmannite, respectively, compared to the high release of sulfate from pure schwertmannite in uninoculated controls.

No Fe(III) was reduced from chromated schwertmannite. The low amount of released chromate present at the beginning of incubation might have been toxic to cells of *A. cryptum* JF-5. In some neutrophilic bacteria, chromate is intracellularly reduced to Cr^{3+} after active transport *via* the sulfate active transport system (Snow, 1991). The trivalent form of chromium tends to form relatively insoluble compounds and is less harmful than the hexavalent chromate (Nieboer and Jusys, 1988). Since Fe(III)-reducing *Acidiphilium* species do not seem to have detoxification mechanisms, chromated schwertmannite might be not dissolvable in acidic habitats.

In natural systems, goethite is often associated with schwertmannite, because it is thermodynamically more stable than schwertmannite (Schwertmann, 1995; Yu et al., 1999).

In situ transformation of schwertmannite into goethite in deeper sediment layers of an acidic lignite mining lake has been demonstrated by Peine et al. (2000). In contrast to pure schwertmannite, autoclaving seemed to have no effect on the structure of arsenated and chromated schwertmannite. Thus, these oxyanions seemed to stabilise the structure of schwertmannite or to block the nucleation of goethite during autoclaving and prevent or decelerate its transformation to goethite.

Differential thermal analysis experiments demonstrated that an increase in temperature up to 100 to 200°C causes a weight loss of schwertmannite indicating a structural transformation process (Bigham et al., 1990). In this study, the complete release of sulfate from hydrous schwertmannite during autoclaving demonstrated that the structure of schwertmannite, characterised by structural bound sulfate, seemed to be changed or even destroyed. Therefore, the results of the microbial reduction of autoclaved and non-autoclaved schwertmannite have to be interpreted in terms of two different Fe(III) minerals. Nevertheless, similar amounts of Fe(II) were formed during 14 days of incubation by *A. cryptum* JF-5 from non-autoclaved and autoclaved schwertmannite. In general, the reactivity of Fe(III) minerals decreases as crystallinity increases (Munch and Ottow, 1980). Since rates and extent of microbial Fe(III) reduction are controlled by surface areas, which can vary between 9 $m^2\ g^{-1}$ and 153 $m^2\ g^{-1}$ for goethite (Schwertmann et al., 1985), goethite formed by autoclaving schwertmannite seemed to be of low crystallinity.

5.5. Conclusions

In sediments of acidic lignite mining lakes, freshly precipitated schwertmannite is dissolved by the activity of Fe(III)-reducing acidophilic bacteria or transformed into goethite. Thus, incorporated toxic oxyanions like arsenate or chromate bound to schwertmannite might be remobilize during reductive dissolution. However, the microbial dissolution of arsenated schwertmannite mediated by the Fe(III)-reducer *A. cryptum* JF-5 isolated from those sediments will be not associated with a release of arsenate into the pore water. The abiotic release of chromate from chromated schwertmannite to the pore water seems to be toxic for those bacteria. Transformation of schwertmannite to goethite might not enhance the mobility of arsenate or chromate. Thus, arsenate and chromate, once bound to schwertmannite, will be retained in the solid phase, and schwertmannite will act as an effective scavenger for these elements in acidic habitats.

6. SURFACE CHARACTERISTICS OF SCHWERTMANNITE

6.1. Surface- Size, -Morphology and -Charge

6.1.1. Introduction: Surfaces of Fe(III)-hydroxides

The relevance of ferric oxides and hydroxides in natural systems lies particularly in their capability to bind anions and heavy metals on their surface and thus inhibiting the mobility of these ions in the environment (Scheffer & Schachtschabel, 1998). Their high uptake-capacities can be explained by their large surface areas at which the Fe atoms react as Lewis acid (electron acceptor) resulting in a high chemical reactivity (Cornell & Schwertmann, 1996). The large ratio of surface to volume in weakly crystalline iron minerals results in their high solubility and good microbial availability (micro-organism can use Fe(III) as energy source). Fe(III) hydroxides prefer to the binding of anions at their surface (OH^- ions in aqueous systems), due to their usually positive surface charge. Non-specific (or outer-sphere) adsorption exists, if the binding is a result of electrostatic attraction with a hydrate layer between the adsorbed ion and the surface. In contrast, the exchange of the surface-OH groups with other anions to form a covalent binding is known as specific (or inner-sphere) adsorption (Cornell & Schwertmann, 1996). The surface charge of an iron hydroxide follows from the dissociation of the surface hydroxyl group if no other ions are specifically adsorbed (Cornell & Schwertmann, 1996; equation 6-1 and 6-2).

$$\equiv FeOH_2^+ \leftrightarrow FeOH + H^+ \qquad K_{a1} = \frac{\{\equiv FeOH\}\cdot a(H^+)}{\{\equiv FeOH_2^+\}} \quad (mol\cdot L^{-1}) \qquad [6\text{-}1]$$

$$\equiv FeOH \leftrightarrow FeO^- + H^+ \qquad K_{a2} = \frac{\{\equiv FeO^-\}\cdot a(H^+)}{\{\equiv FeOH\}} \quad (mol\cdot L^{-1}) \qquad [6\text{-}2]$$

{ºX}: surface concentration

Figure II.6-1 illustrates the popular model of charge distribution on a mineral surface.

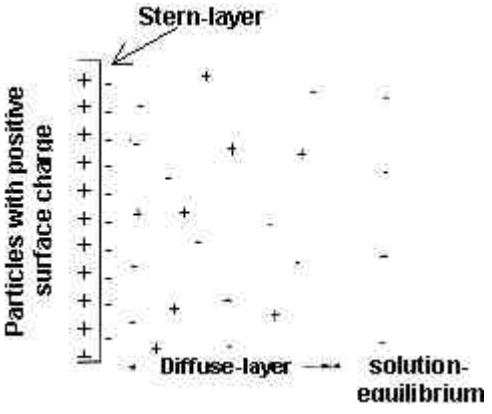

Fig. II.6-1 Distribution of ions within the electric double layer (model of Stern-Graham, Cornell & Schwertmann, 1996).

According to this "Stern-Graham" model, the counter ion layer is divided into two planes, each with its own energy of adsorption. In the relatively fixed “Stern-layer” the ions are specifically adsorbed. In the “Diffuse-layer” the non-specifically adsorbing ions are located. With increasing distance from the surface the electric potential decreases within the Diffuse-layer (Cornell & Schwertmann, 1996). The surface charge density is balanced by the charges in the Stern- and Diffuse-layer ("electric double layer").

Due to the indefinite charge in the diffuse layer it cannot be directly determined. The measurable potential is designated as ζ-potential and is located in an indefinite distance to the mineral surface within the diffuse layer. Exclusively at the “point of zero charge”, at which the sum of all positive and negative charges is equal, the ζ-potential corresponds to the surface potential (Cornell & Schwertmann, 1996). The pH complying with this uncharged surface is named "pH point of zero charge" (pH_{pzc}) and is a material characteristic value. It can be determined either by acid-base titration or by electrophoresis (= isoleletric point, pH_{iep}).

The object of this section of the study is the surface characterisation of schwertmannite by investigations of its particle morphology, surface area and charge.

6.1.2. Materials and Methods

Schwertmannite containing different amounts of sulfate, arsenate and chromate was synthesised by the dialysis method (Bigham et al., 1990). The preparation and composition of the used samples of goethite and schwertmannite is described in chapter II.2.2. and in Tab. II.2-4.

Additionally, a few samples of natural schwertmannite from the sediment of a mining lake (Sh-ML 77, chapter III-2) and from the ore mine “Saalfelder Feengrotten” (Sh-FG, chapter II.2-2.5.) were investigated .

Particle morphology: Scanning electron microscopy

Scanning electron micrographs (SEM) were obtained with a Leo 1530 field emission and scanning electron microscope, equipped with a zircon oxide cathode on wolfram wire as radiation source. This instrument optically resolves structures down to a few nm. The freeze-dried samples were covered for 30 minutes with a platinum layer (~1 nm) in a vacuum to reach diversion of electron radiation from the sample surface during the subsequent measurement. The normally used coating with carbon was not suitable for the investigated fine-crystalline samples. Thereby, the tiny thin schwertmannite crystals stuck together so that the morphology of the particles could not be identified.

Surface area: method of BET

The surface area was determined by the BET (Brunauer, Emmett, Teller) method (Brunauer et al., 1938). Thereto the adsorption capacity of the material for N_2 was investigated as a function of the relative pressure. The surface is proportional to the adsorbable quantity of N_2.

Therefore, a linear relationship exists between the surface area and the relative vapour pressure p/p_0 (Cornell & Schwertmann, 1996). The used instrument, a Gemini 2370 V1.02 provided by the institute of material sciences (IMA) of Bayreuth, supplies a multipoint BET report (compiling an adsorption isotherm in dependence on the pressure). Just before the measurement, the samples were heated for 30 min. at 110 °C in glass tubes in order to completely eliminate any moisture. After determination of the dry weight, samples were gazed with N_2 under increasing pressure with an evacuation speed of 300 mm $Hg \cdot min^{-1}$. Usually, two or three BET reports were created per sample.

Surface potential: electrophoretic measurement

Determination of the isoelectrical point (pH_{iep}) was obtained by electrophoretic measurements of the ζ-potential (potential within the diffuse layer) using a Zetasizer (Malvern, Zetasizer 3000). Firstly, the samples (about 1 $g \cdot L^{-1}$ of synthetic schwertmannite or goethite) were suspended in an inert electrolyte ($NaNO_3$ solution; $c=1 \cdot 10^{-3}$ M) and different quantities of HNO_3 or NaOH (1 to 10 ‰ from a master solution with each $c=1 \cdot 10^{-3}$ M) were added. After 1 h of equilibration, the pH-values in the suspensions were determined and afterwards the ζ-potentials were immediately measured in three replicates. The mean values were plotted into a diagram (ζ-potential vs. pH) from which the pH_{iep} could be perceived as the intersection of the constructed curve with the pH axis (at a surface charge of zero).

In suspensions containing schwertmannite, the ionic strength varied (between $3.5 \cdot 10^{-3}$ M and $5 \cdot 10^{-3}$ M) depending on the sulfate release. Though ionic strength affects the slope of the curve, it has no influence on the point of zero charge (Cornell & Schwertmann, 1996). Consequently, a complete constancy of ionic strength is not necessary. The equilibration time of 1 h was not sufficient for the adjustment of the equilibrium. However, due to the metastable characteristic of schwertmannite which causes its transformation or dissolution, the adjustment of an equilibrium is never possible. The maximum error of the measurements was ± 0.5 pH units. The instrument accuracy was determined by measuring a synthetic standard (DTS5050) with the known ζ-potential of 50 mV (the error was < 3 %).

In order to change the charge of the mineral surface, samples of schwertmannite (1 $g \cdot L^{-1}$) were suspended either for 2 min in 0.1 M HCl (sample Sh-HCl) or for 24 h in 0.1 M $BaCl_2$-solution (sample Sh-Ba). To change the surface charge of goethite, 1 $g \cdot L^{-1}$ of this mineral was suspended at pH 4 (sample Gt-SO_4) for 24 h in a sulfate-solution (c= 10 $mmol \cdot L^{-1}$). Afterwards the three suspensions were filtrated, the filter residues washed with deionised water and finally re-suspended in an inert electrolyte to determine the pH_{iep} as described above.

6.1.3. Results and Interpretation

Particle Morphology and Surface Size

The external shape of a crystal (habit or morphology) reflects its preferential growth direction and is therefore a typical characteristic for many minerals. It depends on many factors, such as the symmetry of the unit cell, the chemical potential-difference in the crystallisation process (= the supersaturation of the system) and the growth environment (Cornell & Schwertmann, 1996). Goethite crystallises in a relatively wide range of environmental conditions and thus it occurs in several shapes (star shaped, hexagonal, bipyramidal or cubic). In contrast, schwertmannite only forms in a small window of chemical conditions and solely one habit of its particles is known. In the literature it is called as "hedgehog-like" (Bigham et al., 1990) due to its long, star-likely arranged crystal needles. This was also observed in the synthetic samples of the present study.

Due to the small particle size of weakly crystalline materials, a direct view on their habits is only possible by the use of transmission- or scanning electron microscopes. The thin crystals of schwertmannite (few nm) were frequently at the resolution limit of the used instrument and consequently the micrographs became diffuse. In samples with an incorporated arsenate and chromate content no visible influences on the habit were monitored (appendix D).

The acanthoid shape of schwertmannite particles results in its high specific surface area. For synthetic schwertmannite an area between 150 and 330 $m^2 \cdot g^{-1}$ was determined (see Tab. II.6-1). This is about 10-fold larger, than that of goethite.

Tab. II.6-1 Specific surface area of schwertmannite (Sh) in dependence on the oxyanion content and of goethite (Gt) (mean value and standard deviation s).

sample	oxyanion content (wt.-%)	spec. surface area ($m^2 \cdot g^{-1}$)	± s	sample	oxyanion content (wt.-%)	spec. surface area ($m^2 \cdot g^{-1}$)	± s
Sh	sulfate: 14.87	193	16	**Sh-S-As-1**	sulfate: 8.3 arsenate: 10.3	217	29
Sh-S-Cr-1	sulfate: 7.3 chromate: 1.97	224	8	**Sh-S-P-1**	sulfate: 4.5 phosphate: 11.3	263	15
Sh-S-Cr-2.5	sulfate: 5.58 chromate: 2.4	328	-	**Sh-FG**[1]	sulfate: 8.2	162	-
Sh-S-Cr-5	sulfate: 6.27 chromate: 5.6	181	17	**Sh-ML 77**[2]	sulfate: 16.2	72	-
Sh-Cr-10	chromate: 15.94	299	9	**Gt**	-	19.6	4

[1] natural precipitated schwertmannite of an ore mine or [2] from the sediment of an acidic mining lake

Natural schwertmannite ("Sh-ML 77 "and" Sh-FG") showed lower surface areas (72 - 162 $m^2 \cdot g^{-1}$) which are still similar to data in literature of schwertmannite (100 to 200 $m^2 \cdot g^{-1}$, Bigham et al., 1994). The incorporation of different oxyanions in schwertmannite affected the surface areas of the precipitates in dependence on their quantity. A varying content of chromate and sulfate in the samples mostly changed the specific surface area. However, this dependency was not linear (Tab. II.6-1).

Surface Charge and Point of Zero Charge

Electrophoresis involves measurements of particle movements affected by an electric field. This ζ-potential is measured in different suspensions in dependence on the pH. The pH-value at which the measured potential is zero (no particle movement because the strength of positive and neagtive charges are equal) is denoted as the isoelectric point (pH_{iep}; Cornell & Schwertmann, 1996). The pH_{iep} corresponds to the pH_{pzc} received by acid-base titration.

In this study the material characteristic pH_{iep} was determined for schwertmannite containing different oxyanions.

Fig. II.6-2 shows the results of ζ-potential measurements of schwertmannite. The presented data obtained from three experimental series were measured under similar conditions at different days. The different slopes of the curves probably arose from fluctuations in the ionic strength ($3.5 \cdot 10^{-3}$ to $5 \cdot 10^{-3}$ M). However, the pH_{iep} is independent of the ionic strength and of the slope of the potential curve, respectively (Cornell & Schwertmann, 1996). The intersection with the pH-axis was between 6.3 and 7. Iron minerals typically show neutral pH-points of zero charge (e.g. haematite: 7.0 - 9.5, akaganéite: 6.4 - 7.3 or goethite: 7.4 - 9.5). This explains their amphotere characteristic to adsorb both, cations and anions (Cornell Schwertmann, 1996).

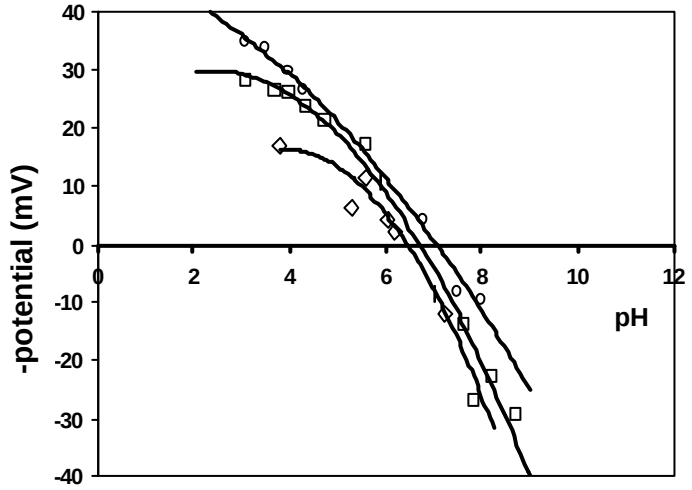

Fig. II.6-2 ζ-potential-curves of schwertmannite to determine the pH_{iep}.

Influence of the oxyanion composition in schwertmannite on the point of zero charge

Deviations of the point of zero charge of a mineral up to three pH units can be achieved by changes in the number of surface hydroxyl groups. Impurities due to specific adsorption, coatings (cover of one mineral with another) or changes of the suspension temperature or of the water content of the solid (Cornell & Schwertmann, 1996, Lyklema, 1987; Bum & Koopal, 1986) might be a reason for these variations.

Thus, in the present study the question should be answered to what extent the incorporation of oxyanions affects the pH_{iep} of schwertmannite. Therefore, electrophoretic measurements of schwertmannite with different chemical compositions and of goethite were accomplished. The results are summarised in Table II.6-2. The pH_{iep} values of schwertmannite range between 5.4 and 7.4. For the pH_{iep} of goethite a value of 7.4 was received which is similar to data from literature (e.g. 7.4; Tipping & Cooke, 1982). Adsorption of sulfate to goethite caused a small degradation of this value to 7.2 (Tab. II.6-2). According to Stumm (1992), a decrease of the positive surface charge caused by specific anion adsorption results in the degradation of the point of zero charge. Parfitt & Smart (1978) described a similar decrease of the pH_{iep} due to the sorption of phosphate on goethite and the associated formation of negatively charged surface complexes.

As a result of the present investigations, the assumption was made that sulfate which is normally adsorbed to the schwertmannite surface, probably debases the "true" pH_{iep}. In this context the "true" pH_{iep} denotes a sulfate-free schwertmannite surface. The removal of this adsorbed sulfate should therefore result in an increasing pH_{iep} compared to the determined pH_{iep} of the “normal” (sulfate-rich) surface of schwertmannite (6.6 ± 0.3). In order to eliminate or form complexes with surface-sulfate, schwertmannite was shaken in HCl- and Ba-solutions, respectively. Afterwards the filter residues were re-suspended and therein the pH_{iep} determined. Within both procedures the pH_{iep} rose to values of 6.9 or 7.1, respectively (Tab. II.6-2). This neutralisation of the schwertmannite surface confirmed the assumption of sulfate elimination and complexation, respectively.

According to the results of this study, no direct dependency of the pH_{iep} on the oxyanion content of schwertmannite was observed. Phosphate and arsenate incorporation in schwertmannite hardly caused changes in the pH_{iep}. In contrast, considerable fluctuations (5.4 to 7.1) were observed as a consequence of incorporated chromate, but no correlation could be found. The inaccuracy of the present findings (± 0.5 pH units) is a result of the metastability of schwertmannite which prevents the adjustment of pH-values outside its stability range (pH 2.5 to 4.5). According to Bigham et al. (1996) high pH values (> 4) accelerate the

transformation of schwertmannite and low ones result in its dissolution. However, after the equilibration time of 1 h, the pH measured further in the suspensions changed very slowly.

Tab. II.6-2 pH_{iep} of schwertmannite (Sh) and goethite (Gt) in dependence on the oxyanion content. (The maximum deviation of the values amounts ± 0.5 pH-units.)

sample	pH_{iep}	sample	pH_{iep}	sample	pH_{iep}	sample	pH_{iep}
Sh	6.6	**Sh-S-Cr-1**	7.1	**Sh-S-As-1**	6.4	**Gt**	7.4
Sh-Ba[1]	7.1	**Sh-S-Cr-2.5**	7.1	**S-As-2.5**	5.8	**Gt-SO_4**[3]	7.2
Sh-HCl[2]	6.9	**Sh-S-Cr-5**	5.4	**Sh-S-P-1**	6.4		
		Sh-S-Cr-10	6.4				
		Sh-Cr-10	6.3				

1 schwertmannite, with Ba^{2+} adsorbed to its surface (as $BaSO_4$-complexes).
2 schwertmannite, shaken for 2 min. in 0.1 M HCl (to eliminate the adsorbed sulfate)
3 goethite, with adsorbed sulfate ($1 g \cdot L^{-1}$ was suspended for 24 h in a 10 $mmol \cdot L^{-1}$ sulfate-solution)

6.2. Acid-Base Titration

6.2.1. Introduction

The surface of schwertmannite is, as shown in the previous chapter, very large (100 to 300 $m^2 \cdot g^{-1}$) and positively charged within its pH-range of stability. The amount of sulfate adsorbed on its surface is approximately 0.4 $mmol \cdot g^{-1}$ or 5.5 wt.-% (Bigham et al., 1990). Due to this high sulfate adsorption capacity, it was assumed that high concentrations of arsenate and chromate would also be adsorbed.

Using acid-base titration, Sigg & Stumm (1981) analysed processes occurring on the surface of goethite during adsorption. They showed that sulfate and phosphate adsorb to goethite specifically through the formation of a direct (covalent) binding. According to their study, the OH-groups of the iron hydroxide surface were exchanged by the oxyanions. Similarly to the schwertmannite experiments, an exchange of both hydroxides and surface-sulfate as well as by the adsorbates should be expected.

Surface charge determination by acid-base titration

In the previous chapter (II.6.1) the electrophoretic determination of the point of zero charge was described.

Due to different chemical conditions in this experiment, the point of zero charge (pH_{pzc}) was determined by titration curves (surface-charge vs. pH) obtained by acid-base titration.

Thereby the surface charge σ_0 was calculated from the chemical parameters in the solution according to equation 6-3 (Sigg & Stumm, 1981).

$$\sigma_0 = (C_A - C_B - C_{H^+} + C_{OH^-}) \cdot \frac{F}{m \cdot S} \qquad [6\text{-}3]$$

s_0	*surface charge ($C \cdot m^{-2}$)*	m	*mass of the mineral ($g \cdot L^{-1}$)*
C_A	*concentration of acid (M)*	F	*Faraday constant: 96485.3 ($C \cdot mol^{-1}$)*
C_B	*concentration of base (M)*	S	*surface area of the mineral ($m^2 \cdot g^{-1}$)*

The value of the point of zero charge determined by titration (pH_{pzc}) should correspond to the value of the isoelectric point (pH_{iep}) determined by electrophoresis (described in II.6-1). For iron oxides and -hydroxides the pH_{pzc} is defined as the pH, at which the total surface charge of the oxide is zero and no specific adsorption of the investigated ion takes place (Cornell & Schwertmann, 1996). Anion adsorption can affect the surface charge and thus shift the titration curve. Specific adsorption can result, on the one hand, in increased values of the pH_{pzc} due to the release of OH^- ions (Stumm, 1992) and on the other hand, as explained in the previous chapter (II.6.1.), negatively charged surface complexes can lower the positive charge and thus decrease the pH_{pzc}. This was observed for phosphate adsorption to goethite (Parfitt & Smart, 1978).

Adsorption of arsenate and chromate to iron hydroxides

Trivalent oxyanions, such as PO_4^{3-} or AsO_4^{3-} form stronger complexes with iron hydroxides compared to divalent anions, such as SO_4^{2-} and CrO_4^{2-} (Bigham & Nordstrom, 2000). Due to this intensive and normally irreversible binding of arsenate, the mobility of arsenic in the (oxic) environment is clearly lower than that of chromium (Fendorf et al., 1997).

In previous studies, the sorption of sulfate, phosphate, arsenate and chromate to goethite was described as specific, bidentate and binuclear (one ligand is bound to the surface of the adsorbent via 2 oxygen atoms to 2 iron atoms) (e.g. Parfitt et al., 1977; Torrent et al., 1990; Waychunas et al., 1993; Hayes et al., 1988). However, recent studies indicate that the possible bindings of oxyanions are more complex. Based on EXAFS measurements, Fendorf et al. (1997) described three surface complexes for arsenate and chromate bound to goethite. Depending on their sorption density on the surface, they can form monodentate-, bidentate-binuclear and bidentate-mononuclear complexes (Fig. II.6-3). Minor covering of the surface results in monodentate complexes and with increasing sorption bidentate-mononuclear and finally bidentat-binucleare complexes are formed. The different complexes imply different bonding strengths and consequently the adsorption of an adsorbate to an adsorbent is described with up to 3 constants. Similar complexes can be assumed for the binding of these

ions to schwertmannite. However, based on acid-base titration, no distinction between these complexes is possible.

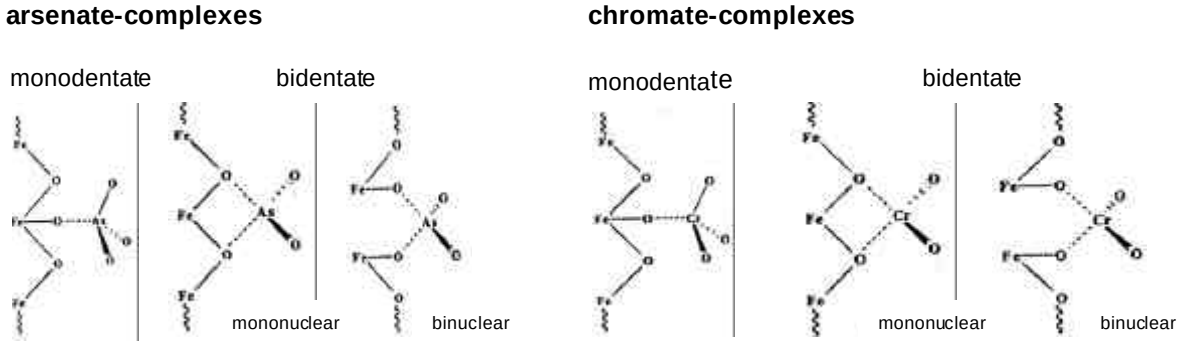

Fig. II.6-3 Schematic illustration of the surface structure of As(V) and Cr(VI) on goethite (Fendorf et al., 1997).

The object in this section of the study was to characterise the adsorption of arsenate and chromate on schwertmannite by acid-base titration. For this purpose, titration curves (plot of pH against vs. charge) and adsorption isotherms (plot of pH vs. adsorbate concentration) serve as tools and goethite as reference for comparisons.

6.2.2. Method: Batch Experiment

Electrolyte solutions of KNO_3 (c =0.1 M) were gazed with N_2 while 1 $g \cdot L^{-1}$ or 4 $g \cdot L^{-1}$ freeze-dried schwertmannite (synthesised by the dialysis method) or goethite (the mineral synthesis of both minerals is explained in chapter II.2.2.) were simultaneously added. Either chromate or arsenate (as Na-salts) were added to the suspensions to obtain oxyanion concentrations of c=10^{-3} M, 10^{-4} M or 0 M. Subsequently the suspensions were titrated with HCl or NaOH (in each case with a maximum of c=0.1 M). The resulting 400 aliquots (appendix E), each with a volume of 25 mL were shaken at 20 °C over 24 or 48 h. After filtration (0.45 µm), the pH and the concentrations of oxyanions were measured in the filtrate (sulfate by ionic chromatography, As and Cr by graphite-tube AAS and iron by flame AAS (description of the analytic in II.2.2.).

Construction of the titration curves: The calculation of the surface charge of schwertmannite is based on eq. 6-3. Additionally, depending on the pH, schwertmannite releases sulfuric acid and (at pH < 2.5) iron. Therefore, the equation (6-3) was extended to include the appropriate concentrations (eq. 6-4 and 6-5). The concentrations of SO_4^{2-} and HSO_4^- were calculated using the protolysis coefficient of sulfuric acid in dependence of the

pH. In the case of arsenate or chromate additions eq. 6-4 and 6-5 were further extended to include their (protonated) concentrations.

$$\sigma_0 = (C_A - C_B - C_{H+} + C_{OH-} + 2 \cdot C_{SO_4^{2-}} + C_{HSO_4^-}) \cdot \frac{F}{m \cdot S} \qquad pH > 2.5 \qquad [6\text{-}4]$$

$$\sigma_0 = (C_A - C_B - C_{H+} + C_{OH-} + 2 \cdot C_{SO_4^{2-}} + C_{HSO_4^-} + 3 \cdot C_{Fe^{3+}}) \cdot \frac{F}{m \cdot S} \qquad pH < 2.5 \qquad [6\text{-}5]$$

(legend according to eq. 6-3)

6.2.3. Results and Discussion

Titration curves

Fig. II.6-4 and Fig. II.6-5 show the titration curves for goethite and schwertmannite, respectively based on the concentration of solid (1 $g \cdot L^{-1}$ and 4 $g \cdot L^{-1}$). The composition of the suspensions (concentrations of the added acid, base and oxyanion) as well as the measured pH value are presented in appendix E.

The pH_{pzc} of **goethite** was 9.2 ± 0.3 (Fig. II.6-4). This is higher than the value of 7.2 obtained by Sigg & Stumm (1981) in a similar experiment. However, it falls within the range cited in literature (7.2 - 9.5) (Cornell & Schwertmann, 1996). Different synthesis conditions of goethite and the subsequent washing of the synthesis product with deionised water, are responsible for the large range of its pH_{pzc}-values. Additionally, the equilibration time during which the dry goethite-samples were suspended in solutions (hydroxilation of the surface) affects the quantity of OH groups released from the surface. In this study, the high measured pH_{pzc} can probably be attributed to inadequate washing of the filter residue subsequent to the goethite synthesis which took place in caustic potash.

Hence it can be assumed that the surface of goethite was enriched with hydroxides which were partly released during the re-suspension of the mineral. This results in a shift of the titration curve to the right, compared to that obtained by Sigg & Stumm (1981). Similarly, the pH_{pzc} is clearly higher compared with results obtained by electrophoretis (pH_{iep} = 7.4; chapter II.6.1.), despite the use of the same goethite material.

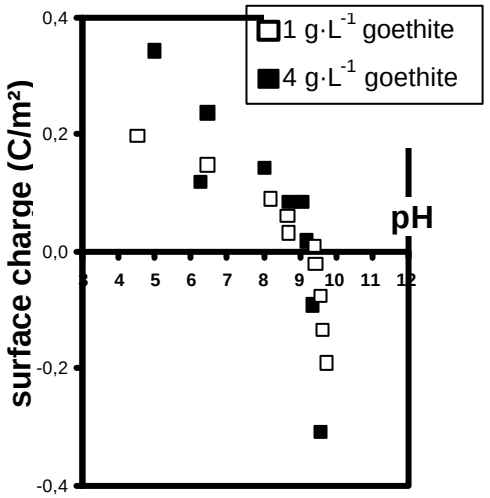

Fig. II.6-4 Titration curve of goethite to determine the pH_{pzc} (measurement after 24 h).

It was therefore assumed that the equilibration time which amounted in the acid-base titration to 24 h and in the ζ-potential measurements to only 1 h was responsible for the observed differences. A longer time interval would result in an increased release of OH ions.
Nevertheless, the pH_{pzc} value of goethite determined in this titration experiment was proven to be relatively stable (± 0.3 pH units) and independent to the reaction time (24 or 48 h) as well as to the quantity of the adsorbent (1 $g \cdot L^{-1}$ or 4 $g \cdot L^{-1}$). It was hence concluded that the experimental procedure could be used for schwertmannite in the same way.

Although the same concentrations of acid and base were added to the aliquots of goethite, the titration curve of **schwertmannite** exhibits a clearly different gradient. In contrast to the relatively constant ionic strength adjusted to the suspensions of goethite titration (0.1 M), in schwertmannite suspensions, the ionic strength amounted up to 0.6 M due to its pH-dependent sulfate release. However, the value of the pH_{pzc} is generally independent to the ionic strength (Cornell & Schwertmann, 1996).

As demonstrated in Fig. II.6-5, the surface of schwertmannite was always positively charged up to a pH-value of approximately 4.5 (at a NaOH addition of $c = 8.2 \cdot 10^{-4}$ M). Negative surface charges were determined at pH > 9 (at a NaOH addition of $c=2.5 \cdot 10^{-3}$ M).

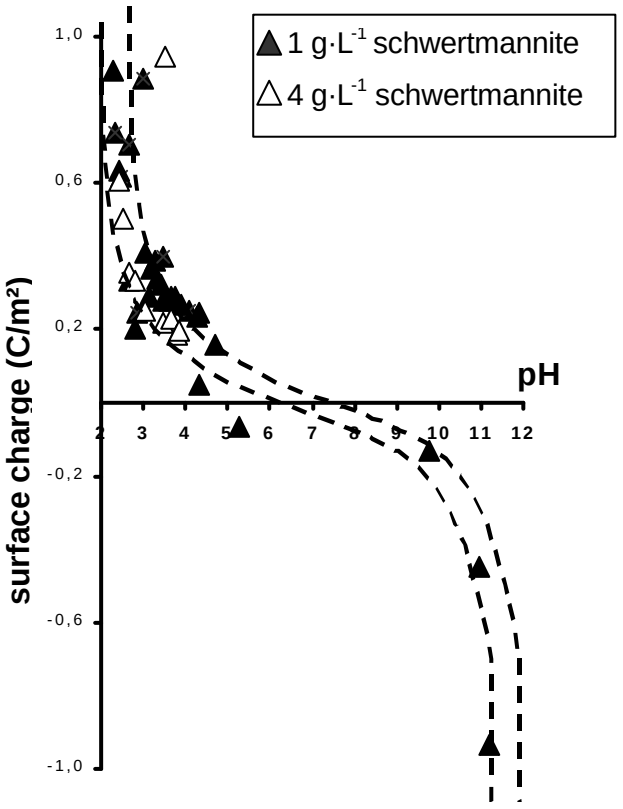

Dashed lines mark the estimated run of the titration curve.

The pH_{pzc} ranges between 6 and 8.

Fig. II.6-5 Titration curve of schwertmannite to determine the pH_{pzc} (measurement after 24 h).

Intermediate pH-values which should mark the pH_{pzc} were not measurable, since small variations of the titrated base causes high pH fluctuations within this pH-range. Therefore, equilibrium cannot be reached. It was therefore assumed that the point of zero charge fell into the range between 6 and 8.

The results obtained in this acid-base titration experiment, although more uncertain, were similar to those obtained by electrophoretic measurements which resulted in a pH_{iep} of 6.6 ± 0.3. An increased concentration of the adsorbent (4 $g \cdot L^{-1}$) caused an increased release of sulfuric acid and thus a small shift in the titration curve to lower pH values.

The titration curves of both, schwertmannite and goethite, were not influenced by the duration of the experiment (24 or 48 h) (data are shown in appendix E). Consequently, experiments with added arsenate- and chromate-solutions (represented in the following) were only run for 24 hours.

Influence of arsenate and chromate on the titration curve

In order to investigate the interactions between the schwertmannite surface and the added anions it was assumed that no oxyanions can be incorporated into the structure (the tunnel cavities) of crystalline schwertmannite. This means that only adsorption processes take place. Eick et al. (1999) observed that the negative surface charge increased due to the adsorption of arsenate and chromate to goethite. The addition of these anions to suspensions of goethite and schwertmannite should therefore cause a similar shift of the titration curves.

Table II.6-3 shows the results of pH_{pzc}-determinations obtained from titration curves of **goethite** suspended in arsenate- and chromate-solutions (titration curves of the experimental series are presented in appendix E). The values indicate that the added oxyanions only slightly affected the titration curves. The pH_{pzc} reached maximum values of 9.6 during the titration of goethite with arsenate ($c=10^{-3}$ M). The lowest pH value of 8.8 was observed in the reaction of 1 $g \cdot L^{-1}$ goethite with chromate ($c=10^{-3}$ M). A general decrease in the pH_{pzc} was observed in small quantities of suspended goethite (1$g \cdot L^{-1}$) and low adsorbate concentrations ($c = 10^{-4}$ M) as a result of anion addition.

High concentrations of adsorbent (4 $g \cdot L^{-1}$) and adsorbate ($c = 10^{-3}$ M) prevented a monitoring of surface effects, due to the strong increase of OH^- concentration in the solution.

Tab. II.6-3 pH_{pzc} of goethite determined from curves of acid-base titration (appendix E) in dependence on adsorbate- and adsorbent-concentration.

	1g·L^{-1} goethite					4 g·L^{-1} goethite				
adsorbate	**0**	**10^{-4} M AsO_4**	**10^{-3} M AsO_4**	**10^{-4} M CrO_4**	**10^{-3} M CrO_4**	**0**	**10^{-4} M CrO_4**	**10^{-3} M AsO_4**	**10^{-4} M CrO_4**	**10^{-3} M CrO_4**
pH_{pzc}	9.2	9.0	9.6	8.9	8.8	9.45	9.55	9.6	9.55	9.55

By the method of acid-base titration, no pH_{pzc} was received **for schwertmannite**. However, the anion sorption influenced its surface charge and caused shifts of the titration curves.

Fig. II.6-6 shows the obtained curves in comparison with Cr- and As-free (dots) titration-solutions of schwertmannite. In suspensions containing 4 g·L^{-1} adsorbent, lower surface-charges and pH-values were generally determined. I.e. these curves debase compared to the curves of suspensions containing 1 g·L^{-1} schwertmannite. Therefore, a decrease of the pH_{pzc} could be supposed. The high concentration of sulfuric acid released of schwertmannite during its suspension, explains this acidification which increases with the increased suspended mass. In suspensions containing 1 g·L^{-1}, the characteristics of the anion solution strongly affected the run of the titration curves. Highly concentrated adsorbates (c=10^{-3} M) caused an increase of the pH, because in these electrolytes the pH are in neutral range.

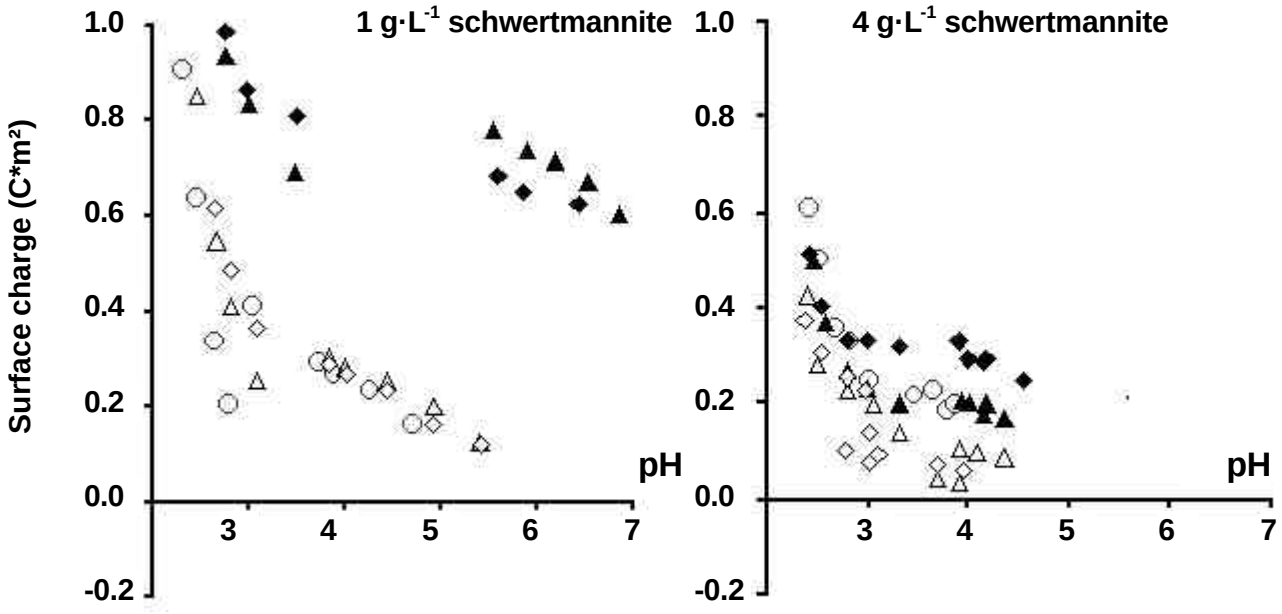

Fig. II.6-6 Titration curve of schwertmannite in arsenate- (triangles) and chromate- (rhombs) solutions. 10^{-3} M solutions are presented by empty symbols; 10^{-4} M solutions by filled symbols. Circles stand for schwertmannite suspensions containing no adsorbate. (measurement after 24 h).

The titration curve resulting after the addition of low adsorbate concentrations ($c=10^{-4}$ M) was nearly identical to the curve of schwertmannite without adsorbate addition. However, the (slight) shift to the left of the titration curves in the 10^{-4} M solutions can be considered as a consequence to the formation of negatively charged surface complexes. This was already described for goethite (see above) and confirmed by Parfitt & Smart (1978) who observed a debasement of the pH_{pzc} due to phosphate adsorption on goethite.

The results suggest only little influence of chromate and arsenate adsorption on the surface charge of schwertmannite. Therefore, it was supposed that the oxyanions predominantly exchange the surface-sulfate of schwertmannite. Thus no substantial change of the surface charge was observed.

Adsorption Isotherms

The adsorption of anions to iron hydroxides in a solution generally increases with decreasing pH (Cornell & Schwertmann, 1996). Adsorption isotherms describe this dependency. In this study, the adsorption of arsenate and chromate to schwertmannite and goethite was examined as a function of the added amount of adsorbate ($1\cdot10^{-3}$ M or $1\cdot10^{-4}$ M), the quantity of the adsorbent (1 or 4 $g\cdot L^{-1}$) and that of the pH. In schwertmannite containing suspensions the release of sulfate (desorption) was simultaneously measured. Fig. II.6-7 shows the resulting adsorption- and desorption-isotherms within the pH stability-range of schwertmannite.

Adsorption of arsenate and chromate: The adsorption of chromate and arsenate to **goethite** is generally high within the examined pH range (> 60 % in all experimental series, Fig. II.6-7) and decreases only slightly with increasing pH. Eick et al. (1999) showed in their investigations of arsenate and chromate adsorption to goethite between pH of 2 and 12 a strong difference in the adsorption isotherms slope in dependence of these anions. This was explained by different complexes of arsenate and chromate formed on goethite surfaces: The triple negatively charged arsenate predominantly forms strong, bidentate-binuclear complexes, whereas the twice negatively charged chromate forms to a major part weaker, monodentate complexes (Eick et al., 1999).

The adsorption on **schwertmannite** was proven to be completely independent to the pH within the pH range examined in this study (Fig. II.6-7). In nearly all experimental series more than 80 % of both adsorbates were adsorbed to schwertmannite (results to the adsorption capacity of schwertmannite are shown in chapter II.2.3).

Sulfate desorption: Suspending schwertmannite normally results in a release of sulfate ions from the solid phase into the solution. Provided that the released amount is exclusively surface bound, it was quantified as described in the following: According to Bigham et al. (1990) the ratio of Fe:S in schwertmannite is 8, if the tunnel cavities of the crystal lattice are exclusively occupied by sulfate. Additionally adsorbed sulfate reduces this value and its release by suspending the mineral causes its re-increase. Eq. 6-6 illustrates the assumption that schwertmannite with a Fe:S stoichiometry of 6.27 (averaged measured data of synthetic schwertmannite samples) converts into schwertmannite with the "ideal" Fe:S ratio of 8. Thus only adsorbed sulfate would be released into solution.

$$Fe_{16}O_{16}(OH)_{10.9}(SO_4)_{2.55} + 1.1\ H_2O \rightarrow Fe_{16}O_{16}(OH)_{12}(SO_4)_2 + 1.1\ H^+ + 0.55\ SO_4^{2-} \qquad [6\text{-}6]$$

A complete release of the surface sulfate due to suspending of 1 $g \cdot L^{-1}$ schwertmannite (1 g = $7.2 \cdot 10^{-4}$ M) corresponds therefore to a sulfate concentration of $c=0.39 \cdot 10^{-3}$ M. The measured sulfate concentration after suspending of 1 $g \cdot L^{-1}$ schwertmannite in deionised water amounted $0.38 \cdot 10^{-3}$ M to $0.43 \cdot 10^{-3}$ M and confirmed the concentration calculated by equation 6-6.

Adsorption reactions on the surface of schwertmannite imply interactions with the surface sulfate, since this competes with the added adsorbates for surface places. The crucial factor to determine the surface adsorption is the binding intensity of the competitive ions to the iron-hydroxide surface (Fendorf et al., 1997). Surface complex constants describe binding affinity and stability of the surface complexes at a mineral surface. Arsenate and chromate form stronger complexes than sulfate at the surfaces of Fe(III) hydroxides (Dzombak & Morel, 1990). Therefore, in schwertmannite suspensions containing arsenate and chromate, a displacement of surface sulfate by an exchange with arsenate and chromate was expected.
The sulfate desorption of the respective experimental series represented in Fig. II.6-7 indicates that with increasing adsorbate concentration the release of sulfate increases, too. That refers to a "sulfate displacment" due to stronger binding intensities of chromate and arsenate. This effect seems more obvious for arsenate compared to chromate. With increasing pH (2.5 to 4.5) the sulfate desorption generally increased. However, the release of sulfate never extended a third of the total schwertmannite-sulfate ($4 \cdot 10^{-4}$ M to $5 \cdot 10^{-4}$ M g^{-1}) which corresponds to the adsorbed quantity of sulfate (Bigham et al., 1990). Rose & Ghazi (1997) confirmed this pH-dependency in an analysis of the sulfate release from AMD iron-hydroxides. In their experiments, the sulfate desorption proportionally increased with increasing pH (the examined range of pH was between 2 and 12). The highest sulfate release ($4 \cdot 10^{-4}$ $M \cdot g^{-1}$ to $6 \cdot 10^{-4}$ $M \cdot g^{-1}$) was measured in suspensions which did not contain any

adsorbate. This can be explained by the formation of strong surface complexes of arsenate and chromate preventing a further sulfate release.

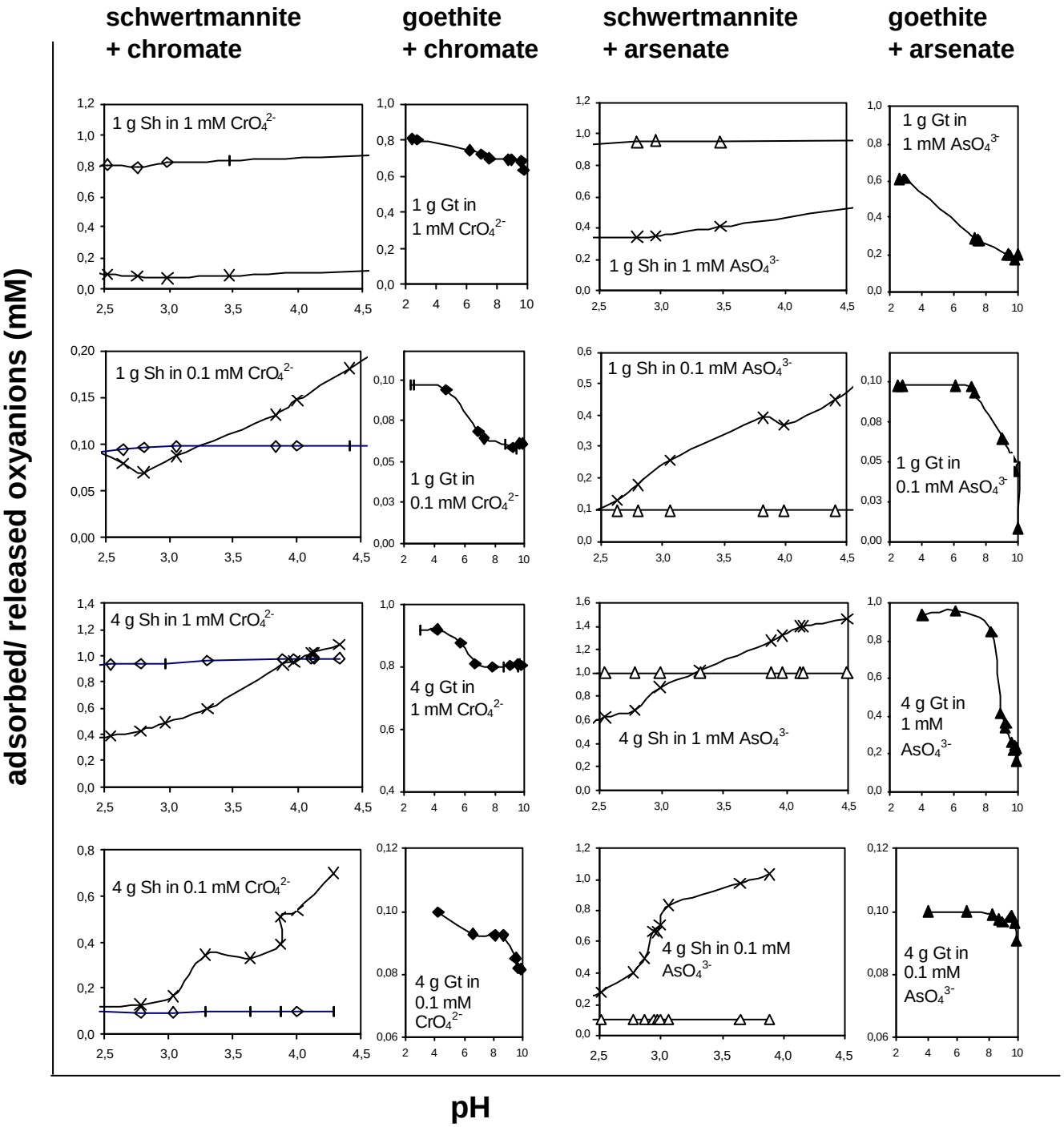

Fig. II.6-7 Adsorption of chromate (rhombs) and arsenate (triangles) to schwertmannite (Sh, white symbols) and goethite (Gt., black symbols) and desorption of sulfate (crosses) from schwertmannite, in dependence on the pH (the demonstrated pH range shows the stability range of the respective mineral.

6.4. Summary and Conclusions

In this study investigations to characterise size, morphology and charge of the schwertmannite surface were accomplished. It was demonstrated that the surface of schwertmannite is with up to 300 $m^2 \cdot g^{-1}$ particularly large, and within the considered pH stability range (~ 2.5 to 4.5), positively charged. Therefore, the criteria for schwertmannite to adsorb high concentrations of oxyanions (e.g. arsenate and chromate) either additionally to or in exchange with its generally adsorbed sulfate are fulfilled.

Bigham et al. (1990) determined the adsorbed amount of sulfate on schwertmannite by complexation of its surface sulfate with Ba^{2+} cations. This value normally ranges between $4 \cdot 10^{-4}$ and $5 \cdot 10^{-4}$ $mol \cdot g^{-1}$ and is similar to the sulfate concentration which was released in to suspending schwertmannite in deionised water ($c=3.9 \cdot 10^{-4}$ $mol \cdot g^{-1} \cdot L^{-1}$). The good desorbability of sulfate indicates a weak binding of these anions. In literature, the adsorption of sulfate to Fe(III) hydroxides is predominantly described as an outer-sphere or intermediate (combined outer- and inner-sphere) adsorption form (Cornell & Schwertmann, 1996).

A comparison between the isotherms of schwertmannite and goethite for arsenate and chromate adsorption shows hardly any differences between the minerals in the considered pH-range (Fig. II.6-7). Thus, the presented results give no clear evidence for an elevated adsorption capacity of schwertmannite compared to goethite. In chapter II.2. of this thesis the adsorption capacity of schwertmannite is discussed in more detail.

Fendorf et al. (1997) determined the adsorption of arsenate and chromate to goethite as a consequence of the formation of monodentate as well as bidentate complexes with different binding intensities (Fig. II.6-3).

Adsorption isotherms constructed in this and other studies (Eick et al., 1999; Fendorf et al., 1997) indicate that adsorption of arsenate on Fe(III) hydroxides is stronger compared to chromate (Fig. II.6-7). Although Fendorf et al. (1997) stated that the type of the formed surface complex of arsenate and chromate strongly depends on the surface coverage of an adsorbent, in numerous studies the binding of arsenate to Fe(III) hydroxides was described as specifically bidentate-binuclear (e.g. Waychunas et al., 1992; Sun & Doner, 1996). In contrast, chromate adsorption is defined by some authors as specifically binuclear (Hsia et al., 1993) and by others as outer-sphere (Hayes et al., 1988).

However, it is generally accepted that the strength of surface complexes at low pH increase from $\equiv FeSO_4^-$ to $\equiv FeCrO_4^-$ to $\equiv FeH_2AsO_4$ (surface complexation-constants of the complexes

were calculated by Dzombak & Morel, 1990; Tab. II.2-8). Observations obtained in this study confirm this order of complexation strength.

Surface complexation model of schwertmannite

In literature the oxyanion binding to iron hydroxides is normally described by detailed surface complex models (e.g. Sigg & Stumm, 1981; Fendorf et al., 1997, 2001; Fuller et al., 1989; Dzombak & Morel, 1991). These models give information about strength and types of surface complexes.

I suppose that a similar modelling for schwertmannite can not be performed due to the metastability of this mineral which results in its dissolution or transformation during suspension (Bigham et al., 1996). The associated released amount of sulfate differs in dependence to both, pH and adsorbate and it prevents the adjustment of a stable equilibrium in schwertmannite suspensions. Moreover, the total surface-sulfate (released and adsorbed amount) is in competition with possible adsorbates for surface places and influences the obtained adsorption isotherms.

Investigations of Gao & Mucci (2001), who characterised the simultaneous adsorption of phosphate and arsenate on the surface of goethite, confirm this assumption. They stated that in the presence of several oxyanions in a solution the description of their adsorption by a universal model is not possible. Though the 2-layered model of Stern (Fig. II. 6-1) is conditionally suitable to characterise such systems, in conclusion, the different processes of competition- and exchange reactions of inner- and outer-sphere adsorption are too complex and not yet completely comprehended.

Similarly, the results of this adsorption study suggest that during anion adsorption on schwertmannite competition reactions with the surface sulfate are always implied. The obtained results partly permit a determination of the surface processes, but the complex interactions of several oxyanions on the schwertmannite surface prevent an exact modelling with the available data.

Future investigations of adsorption processes on schwertmannite should involve the use of higher concentrated adsorbates to detect the limit of schwertmannite adsorption-capacity. Furthermore the use of spectroscopic measurement techniques as EXAFS can be recommended to determine the types of formed complexes.

III. FORMATION AND TRANSFORMATION OF SCHWERTMANNITE IN SEDIMENTS OF ACID LIGNITE OPENCAST LAKES

1. INTRODUCTION

In Germany, lignite mining in opencast was of major importance to the industry since the middle of the 20th century (Asche et al., 1999). For several years it has not been profitable anymore and as a consequence many mines were closed. A resulting rise in the groundwater level leads to the formation of lakes in the former pits. Characteristics of these lakes are their hostile conditions to the environment due to high concentrations of sulfate, iron (both are frequently present of about 10 mM) and acid (pH 3 to 4) in most of the surface waters (Herzsprung et al., 1998; Peine et al., 1998). In Germany many acidic lignite mining lakes exist, most of them located in "Mitteldeutschland" and in "Lausitz". Consequently it is the objective of governments and water management offices to neutralise them to reach an integration in recreation and conservation areas (Landesumweltamt Brandenburg, 1995). Therefore, it is of great importance to understand the processes occurring in these acid lakes to prevent further acidification and to make way for renaturation projects.

Groundwater flowing through dumps surrounding the opencast lake oxidises the pyrites included in the lignite. Pyrite oxidation is a complex process consisting of numerous chemical reactions which were extensively investigated during the last years (Nordstrom et al., 1982; Evangelou & Zang, 1995; Nordstrom & Alpers, 1998):

The initial process (occurring in the lignite dumps) is the oxidation of the pyrite sulfide to sulfate by groundwater oxygen (Nordstrom & Alpers, 1998):

$$FeS_2 + 7/2O_2 + H_2O \rightarrow Fe^{2+} + 2\ SO_4^{2-} + 2H^+ \quad [1]$$

This anoxic, weakly acid (pH 5-6), Fe^{2+} and sulfate-rich water oxidises when it enters into the lake (Nordstrom & Alpers, 1998):

$$Fe^{2+} + 1/4O_2 + H^+ \rightarrow Fe^{3+} + 1/2\ H_2O \quad [2]$$

Finally, the Fe^{3+} precipitates as hydroxide by the release of acid. A summary of all reactions involved is given in the following equation (Nordstrom & Alpers, 1998):

$$FeS_2 + 3.75\ O_2 + 3.5\ H_2O \rightarrow Fe(OH)_3 + 2\ SO_4^{2-} + 4\ H^+ \quad [3]$$

In this reaction the product "$Fe(OH)_3$" represents a group of different secondary minerals including jarosite, goethite and ferrihydrite as the most common minerals. But the Fe(III) oxyhydroxysulfate schwertmannite has also been identified in the sediment of an acidic mining lake (Peine & Peiffer, 1998).

Schwertmannite is, due to its weak crystallinity, metastability, variable composition and similarity to other minerals (Bigham et al., 1990, 1996) difficult to identify and therefore few investigations about its importance for the environment were carried out.

For a better understanding of its characteristics mentioned above, it is necessary to consider the crystal structure of schwertmannite which is isostructural to the well described akaganéite ($FeO(OH)_{1-x}Cl_x$) (Bigham et al., 1990). The crystals of this mineral are composed of double chains of $FeO_3(OH)_3$ octahedra that share corners to yield square tunnels extending parallel to the c-axis. Each tunnel is composed of adjoining cavities formed by eight OH groups, with one cavity per unit cell (Murad, 1979). In akaganéite, chloride is normally enclosed in the cavities and bonded by electrostatic interactions, whereas in schwertmannite sulfate is directly incorporated by sharing its oxygen atoms with the iron-hydroxide octahedra. The resulting complexes are linked by Fe-O-SO_2-O-Fe complexes which distort the akaganéite structure. This can be explained by the size of the sulfate ion which is, compared to chloride, too large for an undisturbed storage in the tunnel cavities of the structure. This distortion results in a reduced crystal growth which is consistent for the poor crystallinity of the mineral. Therefore, schwertmannite consists only of small particles (< 200 nm in diameter) with a large surface area (around 200 m^2 per gram) on which a large amount of sulfate is normally adsorbed. Due to this adsorbance, the composition of schwertmannite varies, resulting in a variable formula of the unit cell which is expressed as $Fe_{16}O_{16}(OH)_y(SO_4)_z$, where 16-y=2z (Bigham et al., 1994). Other consequences of the poor crystallinity are a high solubility and low stability which suggest that schwertmannite is only stable in the pH-range between 2.5 and 4.5 (Bigham et al., 1996).

Most waters of lignite mining lakes are characterised by this pH-range (Landesumweltamt Brandenburg, 1995) and therefore schwertmannite can be expected in this environment. The purposes of this study are (1) to examine the frequency of schwertmannite in the sediments of acid lignite opencast lakes (AML) and to predict which mineral is the predominantly formed iron(III) hydroxide in these environments; (2) to investigate if schwertmannite buffers the pH of the surface waters due to formation and dissolution of schwertmannite and prevents further acidification; (3) to elucidate the cycle of formation, dissolution and transformation of schwertmannite in the lakes.

2. MATERIALS AND METHODS

2.1. Study sites

The 18 investigated acidic mining lakes (AML) are located in three different lignite mining areas in Germany (Fig. III-1). In the region of the Lausitz, twelve lakes were examined. Geology is marked by Quaternary glacier-sediments mostly sands and till-marls which cover Tertiary sediments (Nowel et al., 1995). Pyrite content in the excavation amounts 0.014 % (Landesumweltamt Brandenburg, 1995) and the sulphur content in the lignite is 0.3 to 1.5 % (Nowel et al., 1995).

In the mining area Oberpfalz, where four lakes were investigated, Tertiary and Cretaceous sediments of sand and clay form secondary-rocks. Lignites, inter-bedded in these high permeable, miocene sands (Meyer & Mielke, 1993), contain 1.8 to 2.6 % pyrite (Meyer & Poschlod, 1993). Just as lignites from Lausitz and Oberpfalz, the lignites in the area of Mitteldeutschland, where two lakes were investigated, pertain to the Tertiary Eozene to Oligozene (Henningsen & Katzung, 1998). The dumps contain up to 4 % pyrite, further minerals are mostly quartz 50-90 %), feldspar (5-20 %) and kaolinite (0-10 %) (Krüger & Reinhäckel, 2001).

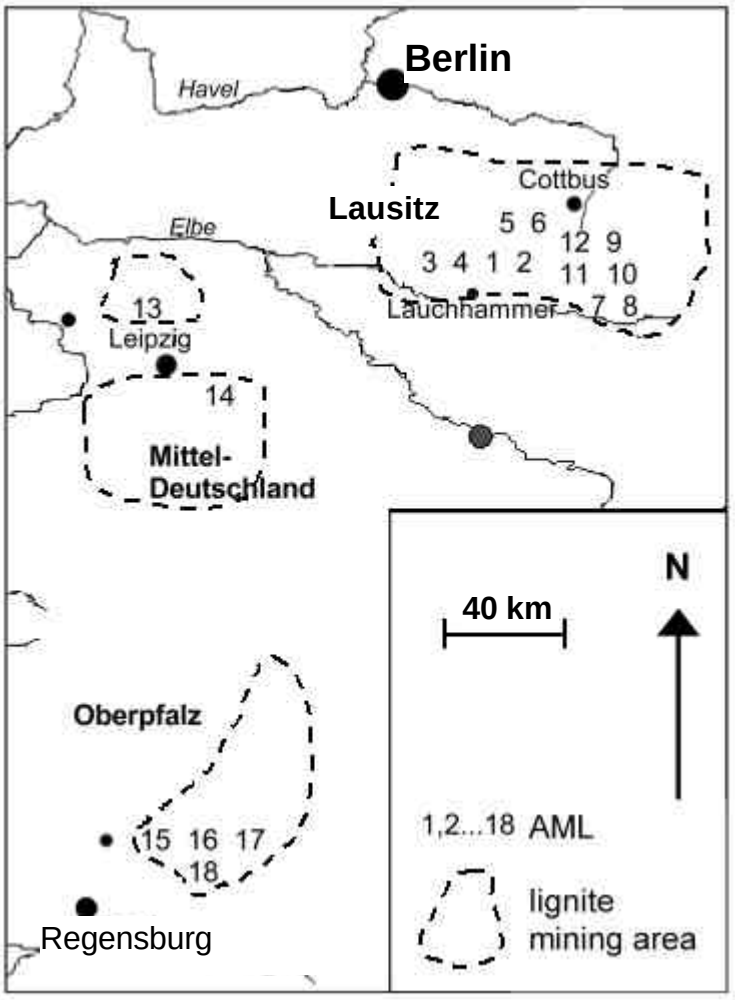

Fig. III-1 Study sites in the eastern Germany: 18 acidic mining lakes (AML).

All investigated lakes are located near the excavation dumps of the lignite. Due to the groundwater inflow which infiltrated the dumps before, the surface water of the lakes is affected by acid mine drainage and thus characterised by low pH-values. An overview about names, location and volume of the lakes is given in Table III-1.

Table III-1 Site description of 18 acidic mining lakes investigated (Peine, 1998; LMBV, 1997, Brand, 2001).

No	Lake name	region	Flooding period/ lake age (years)	Surface (ha)	Lake volume or max. depth
1	ML 77	Lausitz	~ 40	24	depth: 7 m
2	ML 117		~ 40	~ 60	depth: 13 m
3	ML 107		~ 40	-	-
4	ML 111		~ 40	~ 100	-
5	ML 13		end: 2013	38	volume: 5 Mio m³
6	ML F		1999 - 2005	234	volume: 25 Mio m³
7	Spreetal NO		1998-2003	314	volume: 97 Mio m³
8	Kortitzmühle		~ 30	-	-
9	Koschen		1999 - 2001	620	volume: 39 Mio m³
10	Bluno		1999 - 2006	1211	volume: 152 Mio m³
11	Skado		1999- 2007	980	volume: 130 Mio m³
12	Sedlitz		1999 - 2011	1311	volume: 141 Mio m³
14	Borna Ost	Mittel-Deutschland	not finished	-	-
13	Niemegk		flooding start: 1999	-	-
15	Murnersee	Oberpfalz	flooding start: 1979	145	depth: 45 m
16	Brückelsee		(No 15), followed	24	depth: 40 m
17	Ausee		by No 16, 17 and 18	90	depth: 30 m
18	Lindensee		(not yet finished).	121	depth: 12 m

2.2. Sampling

Sampling of lake sediment and water was carried out between August and October 2000, during the stagnation period of the lakes. In ML 77 samples were already taken in summer 1997.

Depth profiles of pH, oxygen, temperature and electrical conductivity were measured with a multi-parameter probe. Water samples were taken 1 m below the surface and 1 m above the ground with a water trowel. A sub-sample was acidified with 1 $^{0}/_{00}$ concentrated HNO_3 already in the field and the Fe^{2+} concentration was determined at the same day photometrically in laboratory. The remaining sample was filtrated (0.2 µm) in the field, cooled during transport and stored deep frozen in laboratory before further investigations.

Sediment sample cores were taken with a gravity corer (∅ 6 cm) in plexi-glass tubes from the deepest (if known) part of each lake. Visually, an upper reddish to yellow layer between 1 to 5 cm could be distinguished from the deeper layers. We attributed this layer to freshly deposited iron(III)minerals, their occurrence being directly linked to the geochemical processes within the lakes, and separated only this layer for sediment analysis. The sediment samples were flushed with N_2 immediately after arrival and deep-frozen. Before further analysis the samples were defrosted, filtrated (blue-ribbon) and the residue was dry frozen.

In ML 77, freshly precipitated material was collected in sediment traps, installed 1 m above the lake ground. The traps consisted of cylindrical tubes constructed after Bloesch and Burns (1980). The sediment core taken in this lake reached a sediment depth of 37 cm, the upper 12 cm were separated into intervals of 1 cm thickness. These sub-samples were dry frozen.

In order to obtain colloidal particles, water samples of three mining lakes (ML 77, ML117 and Borna Ost) were first (pre-)filtered through a 0.2 µm cellulose acetate filter. The filter residues of this filtration were separated from the cellulose filter by dissolution in aqua bidest (10 mL) and simultaneous treatment by ultra sound (15 min.). Finally enrichment occurred by centrifugation (20 minutes and 20800 G; the supernatant was removed with a pipet) and the dried (60 °C) solids were analysed for mineralogical composition by FTIR spectroscopy (described below).

The remaining material in the filtrate was enriched by an ultra-filtration system (Amicon). Fractionation of particles was obtained by the use of different cellulose membranes (1 kDa, 10 kDa, 100 kDa). In the filtrate of each 50 mL fractionated sample the iron and sulfate content was determined in four replicates. High amounts of colloidal material of the four different fractions were produced by filtration of each 800 ml water sample. The filter residues of the three fractions were enriched by centrifugation (3 times for 20 min. and 20800 G) and finally dried (60 °C) and prepared for FTIR spectroscopic analysis (described below).

2.3. Analytical Methods

The redox voltage in the lake waters was determined using a platinum cell and converted in pe-values after calibration against chinhydron saturated pH- buffer solutions.

SO_4^{2-}, Cl^-, Ca^{2+}, Mg^{2+}, K^+, Na^+ and NH_4^+ were measured by ion chromatography, Fe(II) photometrically by the phenantroline method (Tamura et al., 1974) and Fe(tot) and Al(tot) by flame atomic absorption spectrometry. Fe(III) was determined as the difference between total and ferrous iron.

Water-free sediment-samples were partly extracted with acid ammonium-oxalate (pH 3) for 15 minutes in the absence of light to separate the weakly-crystalline and well soluble solid-phase from the better crystalline material. Weakly crystalline iron minerals as schwertmannite dissolve completely within this time and without the influence of the UV radiation (Carlson & Schwertmann, 1981, Bigham et al., 1990) contrary to well crystalline minerals as goethite and jarosite. In the oxalate extracts (1 $g \cdot L^{-1}$ solid phase reacted with the oxalate solution), total iron was determined by flame AAS and total sulphur by ICP-AES.

The mineral composition of the sediment material (without extraction) was determined after grinding the samples by powder X-ray diffraction (XRD) analysis using a Siemens D 5000 X-

ray diffractometer with Co-K$\alpha_{1,2}$ anode. The specimen were step-scanned from 10 to 80° 2θ in increments of 0.02 2θ with 2 s counting time (in few cases 0.01 2θ per 8 s).
Mineral identification occurred either by the library evaluation-program DiffracAT Vers. 3.3 or in the case of schwertmannite by comparison with a schwertmannite standard, synthesised in the laboratory (the diffraction pattern was identical to that of schwertmannite described by Bigham et al., 1990).

Fourier Transform Infrared (FTIR) spectra of the samples were generated using a Vektor 22 Bruker FTIR spectrometer with a KBr beamsplitter. The sample scans ranged between wavenumbers of 7500 and 370 cm^{-1} (the middle infrared) with 1 cm^{-1} resolution. 32 scans were collected for each measurement. The samples were measured in transmission as KBr-pellets which were produced as homogenous mixture of 3 mg sample and 300 mg KBr pressed with a hydraulic press at a load of ~eight tons. The peaks were identified with the evaluation programme OPUS-NT and compared to mineral-librarys of Farmer (1974), Van der Morel & Beutelspacher (1976) and the IR spectrum of schwertmannite described by Bigham et al. (1990). In order to eliminate interferences from kaolinite or other silicates frequently present in the natural samples, the spectra of the filter residue from the oxalate insoluble fraction were subtracted from those of the original sediment sample.

Additionally to qualitative identification of the minerals, the quantitative composition was determined with IR spectroscopy in the sample cores of ML 77. Generally, by IR spectroscopy only semi-quantitative analysis of natural samples can be obtained, because the IR-absorption intensity is influenced of the crystallinity and grain size of one mineral. Normally these characteristics differ between calibration minerals and natural samples resulting in a non-uniformly scattering of the infrared radiation at the crystals surfaces (Günzler & Heise, 1996). Moreover, large errors in weight are probable, due to the very low net weight (3 mg) which should be weighted as exact as possible (Russel & Fraser, 1994). Therefore, the standard deviation in quantitative IR measurements is about ± 10 % (Günzler & Heise, 1996). Yet, to quantify the mineral composition of the sample core, the spectrometer was calibrated with the synthetic produced minerals schwertmannite and goethite, the two minerals contained in the sample which were identified by XRD. In different ratios the two minerals were mixed (in intervals of 10 wt.-%), pressed to pellets and for each mixed ratio the spectrum was measured. The absorption intensities of four mineral-characteristic peaks (for goethite, the OH bands located at 891 cm^{-1} and 795 cm^{-1} and for schwertmannite, the ν_3-sulfate band at 1132 cm^{-1} and the FeO band at 702 cm^{-1}) were measured and the mixed

intensity for each ratio and peak was calculated. A mixture of a % goethite and b % schwertmannite features the mixed intensity (I_{mix}) in the IR spectrum at peak-location x :

$$I_{mix,\,x} = 0.a \cdot I_{Gt,x} + 0.b \cdot I_{Sh,x} \quad [4]$$

$I_{Gt,x}$, $I_{Sh,x}$: mean values of the intensities of three parallel measured goethite and schwertmannite standards, respectively at location x (wavenumber).

The error for the calculated mixtures at each wavenumber was evaluated after the law of error propagation for additions (Sachs, 1992):

$$s_{mix} = \sqrt{0,2(s_{Gt})^2 + 0,8(s_{Sh})^2} \quad [5]$$

The calibration line was created by plotting I_{mix} against the corresponding mineral composition. The intensities of the measured peaks of sediment-segment samples of the core taken in ML 77 were compared to this calibration line to predict the contents of schwertmannite and goethite in the sediment in dependence on sediment depth.

Particle morphology and surface area

Scanning electron microscopy (SEM) was used to determine the particle morphology of the solid samples (Leo 1530). Samples were covered with platinum layer before measurement.

The specific surface area was determined by N_2 adsorption using the BET method (Brunauer et al., 1938).

2.4. Geochemical Modeling

The geochemical modelling program PhreeqC (vers. 2.02) was used to calculate chemical equilibria between the solid and dissolved phase in the lakes and to predict the dominating species and ionic complexes in the water as well as the formation of minerals. Most stability constants were taken from the PhreeqC data file which based on Nordstrom et al (1990). Table III-2 lists the solubility functions of the four Fe-minerals considered in this study, i.e. goethite, jarosite, schwertmannite and ferrihydrite according to Bigham et al (1996) and Parkhurst (1995).

Eq. 6 gives the relative error (r) of ionic activities (determined after the Davis equation) as result of charge imbalances L which were determined with PhreeqC.

$$r(\log a(i)) = \frac{\left|\log a_L(i)\right| - \left|\log a_0(i)\right|}{\left|\log a_0(i)\right|} \quad [6]$$

were log a_L (i) is the logarithm activity of species i at charge imbalance L and log a_0 (i) is the logarithm activity of species i at L=0.

Table III-2 Equations (7-10) to determine the solubility-product and the Fe(III)-activity of schwertmannite (Sh), ferrihydrite (Fh), K-jarosite (Jt)and goethite (Gt).

mineral	dissolution reaction	Log K	Fe(III) activity	
Sh[1]	$Fe_8O_8(OH)_x(SO_4)_y + (24-2y)\,H^+ \Rightarrow 8\,Fe^{3+} + y\,SO_4^{2-} + (24-2y+x)/2\,H_2O$	18±2.5	$\log a(Fe^{3+}) = \frac{\log K_{sh} - y\log a(SO_4^{2-}) - (24-2y)pH}{8}$	[7]
Fh[2]	$Fe(OH)_3 + 3H^+ \Rightarrow Fe^{3+} + 3\,H_2O$	4.81	$\log a(Fe^{3+}) = \log K_{Fh} - 3 \cdot pH$	[8]
Jt[2]	$KFe_3(SO_4)_2(OH)_6 + 6H^+ \Rightarrow 3\,Fe^{3+} + 6\,H_2O + K^+ + 2\,SO_4^{2-}$	-9.21	$\log a(Fe^{3+}) = \frac{\log K_{Jt} - 2\log a(SO_4^{2-}) - \log a(K^+) - 6pH}{3}$	[9]
Gt[1]	$FeOOH + 3H^+ \Rightarrow Fe^{3+} + 2H_2O$	1.4	$\log a(Fe^{3+}) = \log K_{Gt} - 3pH$	[10]

[1] Bigham et al. (1996) [2] Parkhurst (1995)

2.5. Synthetic Samples

Synthetic schwertmannite was produced by two different methods: (1) The long-term synthesis takes approximately 30 days and was described by Bigham et al. (1990): 1 $g \cdot L^{-1}$ Fe(III) (as $FeCl_3 \cdot 6\,H_2O$) and 1 $g \cdot L^{-1}$ sulfate (as Na_2SO_4) were added into heated (60°C) deionised water. The resulting suspension was dialysed for several weeks against 4 L deionised water with a daily exchange of water using cellulose membranes with an average pore radius permeability of 2.4 nm. After this period the electric conductivity in the water (outside the dialysis bag) was < 5 µS and the precipitate was finally filtrated and freeze-dried. The short time synthesis takes several hours and was performed by oxidation of a $FeSO_4$-solution with H_2O_2 (Pentinghaus, pers. comu.). The orange-coloured precipitates obtained from both methods were analysed by FTIR spectroscopy, XRD, BET and SEM.

Synthetic goethite was produced by the reaction of KOH with $Fe(NO_3)_3$ according to the recipe described by Cornell & Schwertmann (1996).

2.6. Stability experiment

The synthetic schwertmannite samples produced by the long-term method (Bigham et al., 1990) were transferred in suspension directly from the dialysis bags into six different glass-vessels of 1 L each. The pH in the vessels was adjusted to values of 2, 3, 4, 5, and 7 by continuously adding HNO_3 or NaOH. The experiments were performed in a dark room at constant temperature (25°C ± 1°C). From time to time aliquots of the continuously stirred

suspension were sampled from each vessel and filtrated through a blue ribbon filter. Sulfate and Fe(tot) were measured in the filtrate and the filter residue was investigated by FTIR spectroscopy. Finally (after 362 days) the remaining solid was analysed by XRD.

3. RESULTS

3.1. Hydrochemistry of Acidic Mining Lakes (AML)

Measured data: All investigated mining lake surface waters had a similar hydrochemical composition with low pH-values (2.3 to 4.7) and high sulfate concentrations (3-19 mmol·L^{-1}). The predominant cations were calcium (> 1.4 mmol·L^{-1}), magnesium (> 0.2 mmol·L^{-1}) and iron (up to 11 mmol·L^{-1}), both in the ferric and ferrous form. Fe(III) concentrations generally exceeded that of Fe(II) and O_2-saturation was between 35 and 97 %. The results of the most important hydrochemical parameters, used in calculations of solubility in the modelling are shown in Table III-3. The completely measured data are presented in appendix F.

Table III-3 Hydrochemical parameter of ML surface water samples, taken 1 m below surface. Sampling time was in summer 2000 (Brand, 2001) and in summer 1997 (ML 77, Peine, 1998).

ML	pH	pe	SO_4^{2-} (mM)	O_2 (mM)	Fe(III) (mM)	Fe(II) (mM)	ML	pH	pe	SO_4^{2-} (mM)	O_2 (mM)	Fe(III) (mM)	Fe(II) (mM)
ML 77	2.9	n.m.	8.5	0.34	1.5	0.03	Bluno	2.9	13.2	13.7	0.27	0.9	0.015
ML 107	2.3	13.8	65	n.m.	11.1	0.04	Skado	2.8	13.4	18	0.28	1.5	0.017
ML 117	3.0	13.4	9.3	0.30	0.3	0.004	Sedlitz	3.0	13.2	18.6	0.28	0.4	0.010
ML 111	2.7	13.3	14.9	0.26	2.6	0.055	Borna Ost	2.9	13.7	19.4	0.27	1.2	0.021
ML 13	2.9	12.8	7.5	0.29	0.23	0.028	Niemegck	4.7	4.5	3.4	0.28	n.d.	n.d.
ML F	2.8	12.9	17	n.m.	0.5	n.d.	Murner See	3.3	13.3	3.2	0.25	0.025	0.028
Spreetal NO	3.6	10.8	10.4	0.24	0.01	0.001	Ausee	3.0	n.m.	4.6	0.25	0.183	0.033
Kortitzmühle	4.7	7.8	12.4	0.27	0.004	n.d.	Lindensee	2.8	n.m.	6.6	0.24	0.27	0.078
Koschen	3.1	12.4	7.6	0.26	0.22	0.001	Brückelsee	3.1	n.m.	3.4	0.27	0.54	0.024

n.d. not detected (< 0.1 µmol·L^{-1}), n.m. not measuered

Calculated data (PhreeqC): Calculation of the chemical speciation indicated that in all lakes with pH-values < 3.5, iron(III) was predominantly (~75 % of total ferric iron) complexed as sulfate ($Fe(SO_4)^+$ and $Fe(SO_4)_2^-$). Other complexation forms as $Fe(OH)^{2+}$, $Fe(OH)_2^+$, $Fe(OH)_3$ or free Fe^{3+} play a minor role. Ferrous iron was for ~50 % uncomplexed as Fe^{2+}, ~30 % as $FeSO_4$ and ~20 % as $FeHSO_4^+$ (quantitative distribution of the speciation of ferric and ferrous iron is presented in appendix G).

Saturation indices (SI) were > 0 (oversaturated) for goethite and jarosite in 17 of all lakes studied and equalled 0 in case to schwertmannite in 15 of the lakes.

Charge imbalances (eq. 5) which can affect the relative error r for SO_4^{2-}- and Fe^{3+}-activities (eq. 6) were negative (between -10 and -30 %,) for most AML. In one lake even – 50 % (ML 107) were detrmined. The maximum error (r) due to this highest charge imbalance would result in an overestimate of the sulfate activity of 14 % and in an underestimate of 11 % for Fe^{3+} activity relative to the activity determined by calculations of PhreeqC.

Fig. III-2 shows a plot of calculated activities of Fe^{3+} as a function of pH. Included in this diagram are the solubility lines of goethite, jarosite, ferrihydrite and schwertmannite (eq. 7-10). The solubility windows of schwertmannite and jarosite (marked by dashed lines in Fig. III-2) result from variable SO_4^{2-}- and K^+-concentrations of these minerals. Nearly all samples are located in the solubility-window of schwertmannite indicating that schwertmannite controls the solubility of Fe(III) in most of the lakes.

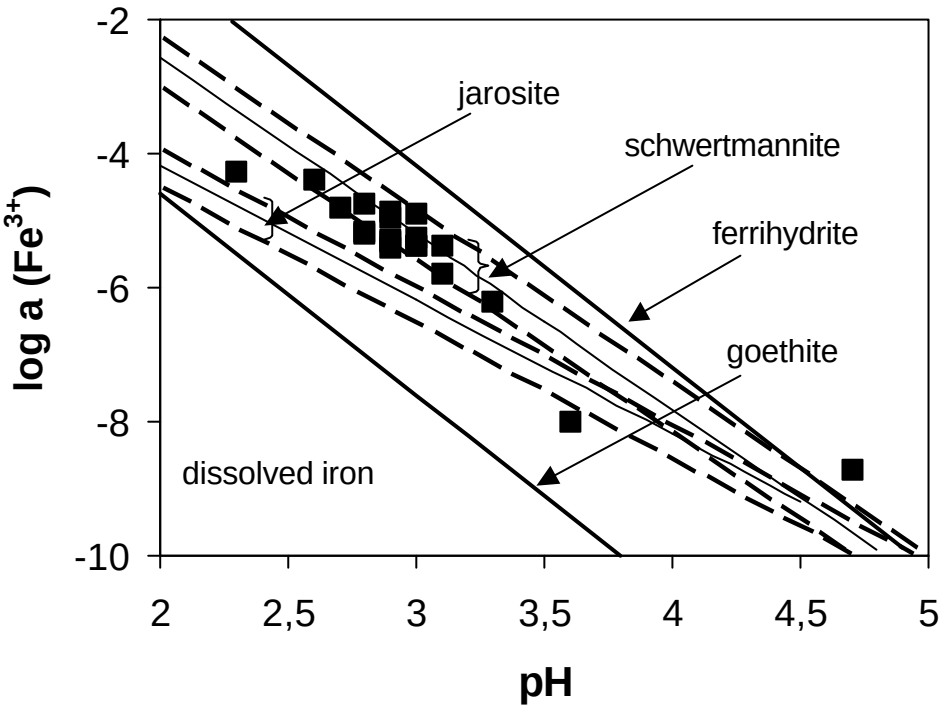

Fig III-2 Plot of the logarithm of Fe^{3+} activity against pH for surface-waters of 18 acidic mining lakes with solubility lines for goethite (log a(Fe^{3+}) = 1.4 - 3pH), ferrihydrite (log a(Fe^{3+}) = 4.83 - 3pH), K-jarosite (mid-line: log a(Fe^{3+}) =-0.19-2 pH) and schwertmannite (mid-line: log a(Fe^{3+}) = 2.7 - 2.63 pH). Maxima- and minima (dashed lines) for solubility windows of schwertmannite were given using log a (SO_4^{2-}) = -1 to -1.5 and of jarosite using log a (SO_4^{2-}) = -1.85 to –2.5 and Log a (K^+) = -3.5 to - 4.07.

Measuered pe-values in the lakes were compared to the ratio of the redox couple Fe^{2+}/ Fe^{3+} ($Fe^{2+} \rightarrow Fe^{3+} + e^-$) according to equation 11.

$$p\varepsilon = -\log k_{Fe(II)/Fe(III)} + \log a(Fe^{3+})/ \log a(Fe^{2+}) \quad [11]$$

$$\log K_{Fe(II)/Fe(III)} = -13$$

It was shown for most of the surface waters (except ML Niemegk and ML Kortitzmühle) that pε ≈ pe and therefore the ratio Fe^{2+}/Fe^{3+} controls the pe and the use of a pε-pH-diagram (Fig. III-3) can give information about redox-equilibria and stabilities of iron minerals in the lakes.

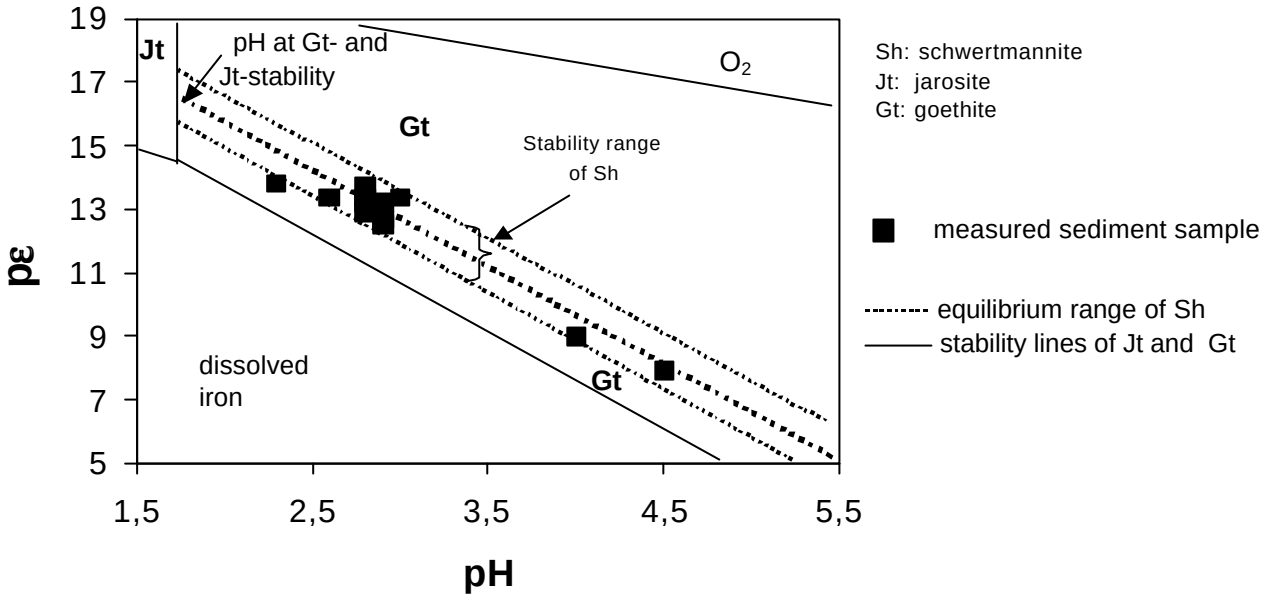

Fig. III-3 pε-pH-diagram for the system K-Fe-SO_4^2. Equilibration lines were calculated using formula in Table 3. The stability line between Jt and Gt was calculated using $KFe_3(SO_4)_2(OH)_6 \leftrightarrow 3\ FeOOH + 3\ H^+ + K^+ + 2\ SO_4^{2-}$ (log K = -13.4) and between H_2O and O_2 using $2\ H_2O \leftrightarrow O_2 + 4\ H^+ + 4\ e^-$ (log K= 86.08). Datapoints represent measured values of pe and pH. Goethite and jarosite are the thermodynamic stable minerals.

3.2. Composition of the Upper Sediment Layers

Due to the uncertainty in determination of weakly crystalline iron minerals, three independent methods were applied to identify the mineral composition of the sediments of mining lakes.

Powder X-ray diffraction (XRD) proved the occurrence of schwertmannite in four lakes and suggested it to be probable in two lakes. The XRD pattern of schwertmannite consists of eight broad and "noisy" peaks with maxims at d values (in nm) of 0.486, 0.339, 0.255, 0.288, 0.195, 0.166, 0.151, 0.146 (Bigham et al., 1990).

Fig. III-4 shows the XRD pattern of two sediment samples (ML Skado and Murnersee) compared to synthetic schwertmannite. While the broad peaks of schwertmannite were identified in the XRD pattern of sample "ML Skado", they were not detected in the sample "Murnersee". Instead of, the clearly visible peaks in this sample correspond to the minerals quartz and kaolinite which are also present in this sample.

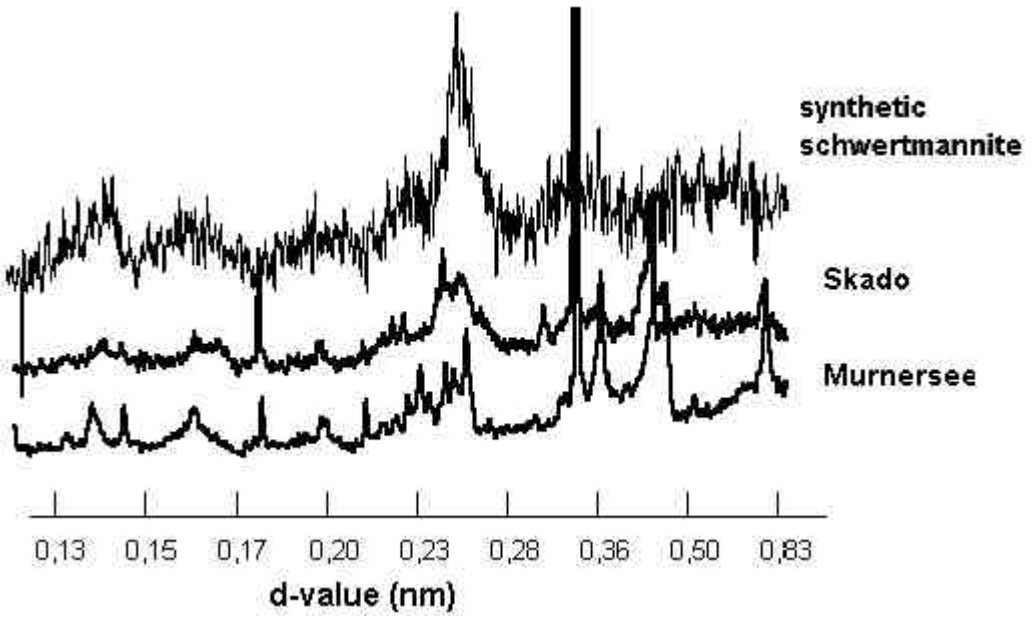

Fig. III-4 X-ray diffraction pattern of synthetic schwertmannite and of sediment samples taken from ML "Skado" and "Murnersee". While "Skado" shows the features of schwertmannite, the clear peaks in Murnersee" mostly correlate with kaolinite.

The occurrence of jarosite was proven in two lakes and that of goethite in four lakes (Tab. III-4). Identification of schwertmannite in sediments of other lakes was not be possible by XRD. Its presence, however could not be ruled out due to the high background of minerals of higher crystallinity (for example quartz and kaolinite).

In contrast to the minerals goethite and jarosite or to silicates, weakly crystalline minerals as schwertmannite and ferrihydrite are well soluble in acid ammonium oxalate. Therein the Fe:S ratio was used as indicator for the occurrence of schwertmannite. It typically ranges between 5 to 8, if schwertmannite is the predominant iron (III)mineral phase and exceeds eight in the presence of ferrihydrite to which sulfate can only be adsorbed. A low ratio should indicate the presence of jarosite (normally 1.5) but this mineral is similar to goethite not extractable in the oxalate solution. The soluble part in most of sediment samples of the mining lakes was larger than 50 %. Therein the determined Fe:S ratio indicated in eight lakes the occurrence of schwertmannite (Table III-4). Ratios lower than 5 were determined in six lakes. Therein schwertmannite potentially occurs in combination with other, not identified (X-ray amorphous) sulfates.

Fig. III-5 shows the IR spectrum of the sample "ML Skado", with bands of kaolinite and goethite (OH vibrations) and the spectrum of the same sample after subtraction of the oxalate-insoluble fraction from the sediment spectrum. This difference spectrum contains the same bands as synthetic schwertmannite. Therefore, it can be assumed that the oxalate-extractable fraction of the sediment consists of schwertmannite. Evidence for the occurrence of

schwertmannite by this method was obtained in eleven lakes, in five lakes goethite and in three lakes jarosite were identified (Table III-4).

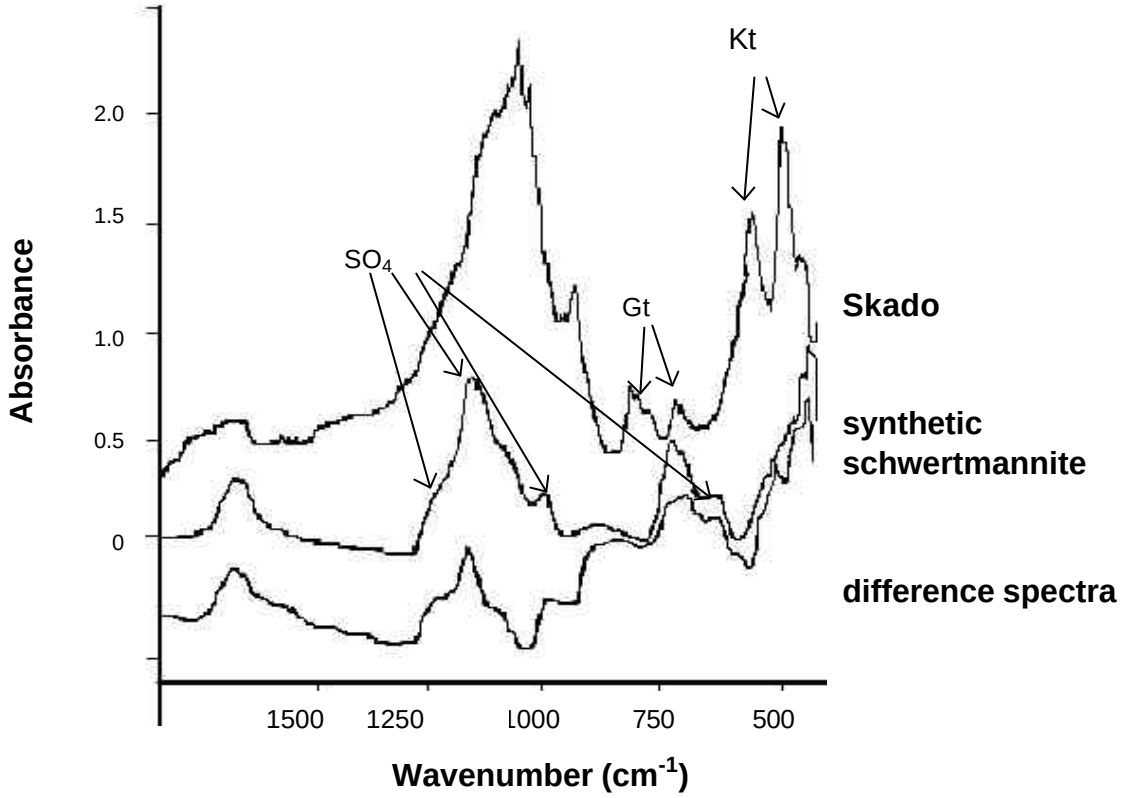

Fig. III-5 FTIR-spectrum of the sediment sample "Skado" with marked bands of kaolinite (Kt) and goethite (Gt) and the difference spectrum of "Skado" (result of the untreated sample minus the filter residue from the NH_4-oxalate extraction) compared to the spectrum of synthetic schwertmannite (middle) with marked sulfate bands (at 610, 976, and 1000 to 1200 cm^{-1}).

Table III-4 Identification of iron minerals in the upper sediment layer of AML by XRD, FTIR spectroscopy and Fe:S ratio in the oxalate-extractable fraction.

The "total result" gives a mean value of the three analytical methods for predication.

ML sample	XRD	Ratio of Fe/S	FTIR	total result	ML sample	XRD	Ratio of Fe/S	FTIR	total result
ML 77	Sh	5.9 Sh	Sh	Sh	**Bluno**	i.n.p.	3.7 (Sh)	Sh, Jt	(Sh, Jt)
ML 107	(Sh),Gt	2.9 (Sh)	Sh, Gt	Sh, Gt	**Skado**	Sh, Gt	4.9 Sh	Sh, Gt	Sh,Gt
ML 117	(Sh), Jt	1.4	Sh, Jt	Sh, Jt	**Sedlitz**	Sh, Gt	5.1 Sh	Sh, Gt	Sh,Gt
ML 111	Jt	2.6 (Sh)	Jt	Jt	**Borna Ost**	i.n.p.	3.1 (Sh)	i.n.p	(Sh)
ML 13	i.n.p.	4.3 Sh	i.n.p.	(Sh)	**Niemegck**	Gt	7.9 Sh	Sh, Gt	(Sh, Gt)
ML F	i.n.p.	5.1 Sh	Sh	(Sh)	**Murner See**	i.n.p.	1.3	i.n.p.	i.n.p.
Spreetal NO	i.n.p.	5.5. Sh	Sh	(Sh)	**Ausee**	i.n.p.	3.3 (Sh)	i.n.p.	(Sh)
Kortitzmühle	i.n.p.	16	Sh, Gt, Jt	(Sh)	**Lindensee**	i.n.p.	1.5	i.n.p.	i.n.p.
Koschen	Sh	4.7 Sh	Sh	Sh	**Brückelsee**	i.n.p.	3.5 (Sh)	i.n.p.	(Sh)

Sh: schwertmannite, Gt: goethite, Jt: jarosite; minerals in brackets stand for „probably formed minerals"
i.n.p. identification not possible

To summarise, schwertmannite was unambiguously identified by all three methods in six samples, whereas its presence can be clearly excluded in one samples (Murnersee). In the other lakes identification using XRD failed, however, the other methods indicate the occurrence of schwertmannite.

3.3. Colloid Analysis of Surface Waters

Colloid analysis of surface waters in three different lakes (Borna Ost, ML 117, ML 77) by mass-balance approach showed that most of the colloids containing iron and sulfate (~ 93 -97 %) were found in the smallest filter-size in the range of 10-1 kDa (appendix H). This colloidal fraction was identified in the three lakes as schwertmannite using FTIR spectroscopy.

3.4. Depth-dependent Alteration of the Sediment Composition (ML 77)

The variation of Fe(III) mineralogy in the sediment and in sediment traps as well as the pH-value in the pore water depending on depth (0 to 11 cm) was examined. By X-ray diffraction, the Fe(III) mineralogy in the top layer and in the sediment trap (installed 1 m about ground level) was determined as pure schwertmannite and in the deepest layer (11 cm depth) of the investigated sediment as pure goethite.

FTIR spectroscopic measurements were used to describe the change in mineralogy by depth. The spectrum of each sample was analysed for the intensity of each two characteristic peaks of schwertmannite (at 1124 and at 704 cm^{-1}) and goethite (at 892 and at 795 cm^{-1}). These intensities were compared to the calibration lines which were obtained by intensity measurements of the same peaks of known mixtures of synthetic schwertmannite and goethite. Therefrom the schwertmannite-goethite ratio in the natural samples were estimated. The result for each sample is presented in Fig. III-6.

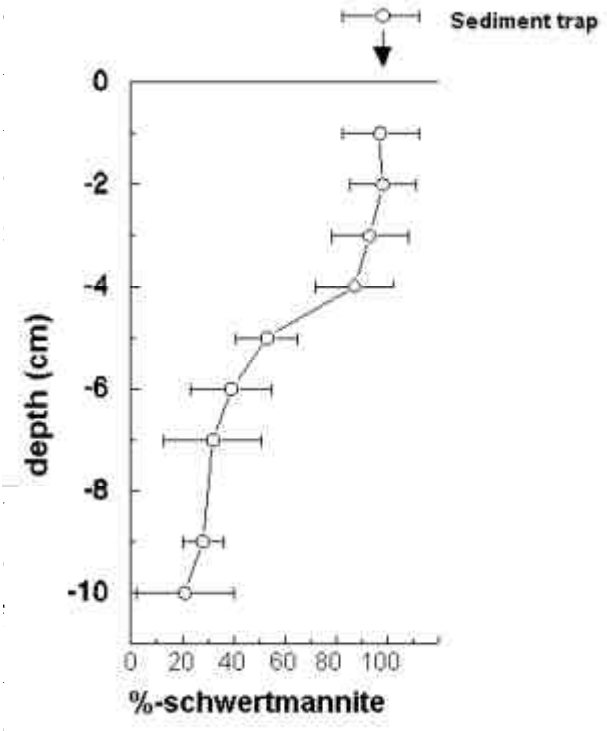

Fig. III-6 Ratio of schwertmannite to goethite in the sediment of ML 77 (Tritschler, 1997). With increasing depth the schwertmannite-content decreases and the amount of goethite simultainously increases.

3.5. Synthetic Schwertmannite

Both synthesised specimen were, independent on their synthesis method identified as schwertmannite by analysis of X-ray diffraction and FTIR spectroscopy. The differences between both precipitates were found mostly with respect to their surface by measurements of SEM and BET.

The surface area of quickly crystallised schwertmannite (Sh-H_2O_2) was much smaller (~ 10 $m^2 \cdot g^{-1}$) compared to the surface of the long-time synthesized schwertmannite (Sh, ~ 200 $m^2 \cdot g^{-1}$). Correspondingly the particles which were formed by quick synthesis are large spheroidal aggergates with a diameter of ~ 600 nm (Fig. III-7). The slow synthesis method resulted in crystalls, grown as long needles which form the characteristic "hedge-hog" habit of schwertmannite. Figure III-7 shows scanning electron micrographs of these synthesized particles and of a natural schwertmannite taken from ML 77. The natural sample had a surface area of 72 $m^2 \cdot g^{-1}$ and its morphology was better comparable to the long time synthesized schwertmannite.

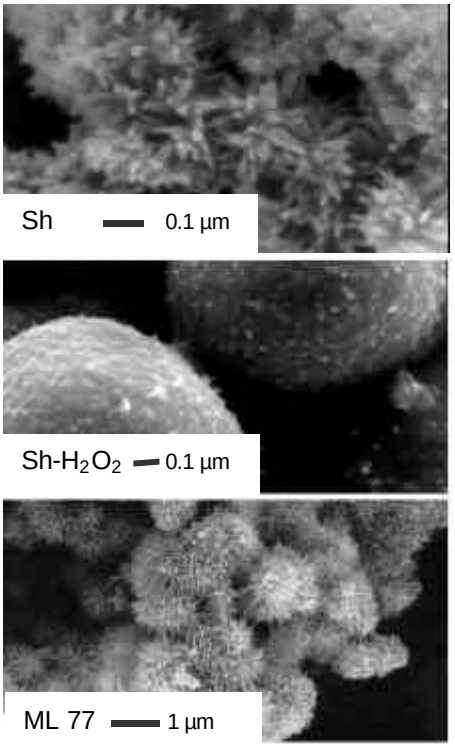

Fig. III-7 Scanning electron micrographs of schwertmannite-samples produced by slow formation in dialysis bags (Sh) and by quick formation by oxidation of $FeSO_4$ (Sh-H_2O_2) compared to a natural sample (ML 77).

3.6. Stability of Schwertmannite in Dependence on Time (362 days)

The long-term stability experiment with synthetic schwertmannite-samples which were each kept at different constant pH-values, showed that the release of sulfate over time was strongly depending on the pH. In the suspension of pH 2 equilibrium between the pH and solid solutions was reached after about 75 days. Compared to the other suspensions, the release of sulfate was highest (70 % of total or 740 µM sulfate, Fig. III-8). The simultaneous high release of iron (40 % of total iron) indicates a mineral dissolution.

In samples with the adjusted pH-values of 3, 4, 5 and 7, respectively the equilibrium was already reached after about 20 days. Compared to the suspension, kept at pH 2, no iron and clearly less sulfate was detected in the suspensions. The sulfate concentration was lowest at pH 4, followed by pH 3, 5 and 7 (Fig. III-8).

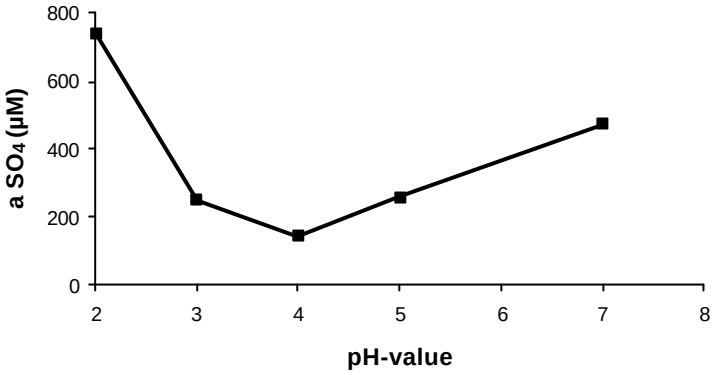

Fig. III-8 Sulfate activity in 5 schwertmannite suspensions after 362 days at constant pH.

In the end of the experiment the crystal- and molecule structures of the filtrated solids were analysed by XRD and FTIR. Fig. III-9 shows the powder X-ray diffraction pattern of the final precipitates kept at a pH four and seven. Traces of goethite (marked peaks) were monitored in all diffractograms. Moreover, it was observed that with increasing pH-value the intensity of the goethite peaks also increased. Additionally, the broad peaks of schwertmannite are still present in all samples. FTIR spectra of samples taken during and after the stability experiment from the suspensions confirm this observation. The intensity of the goethite-characteristic absorption bands increased with increasing time and pH, in the schwertmannite suspensions (appendix C).

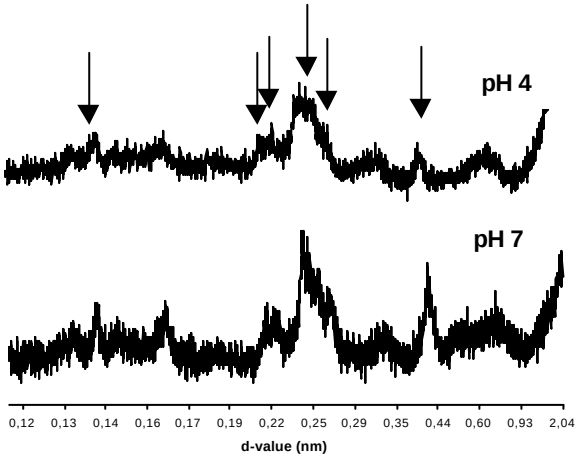

Fig. III-9 X-ray diffraction patterns of the solids taken from schwertmannite-containing solutions after 362 days at constant pH of 4 and 7. Both samples show the peaks of schwertmannite and goethite. However, the goethite features (arrows) are clearer in the sample from pH 7.

4. DISCUSSION

4.1. Occurrence of schwertmannite in acidic mining lakes (AML)

All examined lakes show a similar hydro-geochemical pattern favourable to the occurrence of schwertmannite which implies that this mineral is the predominant solid Fe(III)-phase occurring in these environments. This hypothesis is based on three observations:

(1) A plot of the activity of ferric iron versus pH (Fig. III-2) shows that almost all lake water samples fall on a straight line which reflects the solubility of schwertmannite and which indicates equilibrium between these two species. Most of the solutions are oversaturated with respect to the minerals jarosite and goethite.

(2) The colloidal matter in the investigated lakes which was supposed to be exclusively autochthone formed, is composed mainly of schwertmannite which suggests schwertmannite to be the primary oxidation product of iron(II) in the lake water. Neither goethite nor jarosite could be detected in this fraction.

(3) Schwertmannite appears to occur in almost all sediments studied. It was unequivocally identified using X-ray diffraction in 6 and more or less clear evidence for its occurrence exists in 16 of the 18 sediment samples studied (Table III-4). The occurrence of goethite which was definitively found in four of the upper sediment layers, is probably related to the transformation of metastable schwertmannite (Bigham, et al., 1996, cf. below). Similarly, also jarosite which was identified in three of the samples, may be a transformation product. Its origin can be also allochtonous in that this mineral is eroded into the lakes from the surrounding dumps, a process assumed to occur in lake 111 (Göttlicher & Gasharova; 2000) which is one of the lakes considered also in this study.

The observed formation of schwertmannite in acidic mining lakes is in accordance to the conclusion by Bigham & Nordstrom (2000) that reddish precipitates found in acidic (pH 2.7 – 4) waters influenced by acid mine drainage (AMD) mainly consist of schwertmannite.

There is one principal question arising from these observations: Which processes do control the composition of the lake waters and are responsible for both, the formation of the characteristic product schwertmannite, and the remarkably constant pH of 3.2 ± 0.7 in the lake water?

4.2. Processes regulating the mineralogy of iron in AML

It can be assumed that the formation of iron minerals in the acidic mining lakes is strongly related to the input of ferrous iron from the adjacent ground and dump pore water and to the composition of the solution at which oxidation and subsequent precipitation takes place.

Oxidation kinetics of Fe(II): Beside the solubility equilibrium between ferric iron, protons, and schwertmannite (Fig. III-2) the lake water appears also to be at a redox equilibrium. Fig. III-3 shows a pε-pH diagram for the redox equilibrium between ferrous iron and the stable ferric iron minerals jarosite and goethite. The construction of this diagram is based on the equilibria given in Table III-2. The K^+ and SO_4^{2-} concentrations were set to the mean value found in the lakes. Into this diagram were plotted the measured pe-and pH-values of the lake samples. Additionally, Fig. III-3 contains lines which correspond to the redox equilibrium between Fe^{2+} and the minerals goethite, jarosite and schwertmannite. For the metastable schwertmannite this can be expressed by:

$$8\ Fe^{2+} + y\ SO_4^{2-} + (24\text{-}2y + x)/\ 2\ H_2O \rightarrow Fe_8O_8(OH)_x(SO_4)_y + (24 - 2y)\cdot H^+$$

which writes as:

$$pe = \frac{(\log K^* - y \log a(SO_4^{2-}) - 8 \log a(Fe^{2+})}{8 - \frac{24 - 2y}{8\,pH}} \qquad [12]$$

where $$K^* = (K_{redox(Fe2+/Fe3+)})^8 \cdot IAP_{schwertmannite} \qquad [13]$$

$K_{redox(Fe2+/Fe3+)} = 10^{-13}$

$IAP_{schwertmannite} = 10^{18\pm2,5}$ $[mol^2 \cdot L^{-2}]$ *for y = 1.5*

Table III-5 shows the equilibrium formula between ferric iron and the other in this study considered Fe(III) minerals.

Table III-5 Calculation of pε-values of the minerals ferrihydrite (Fh), K-jarosite (Jt) and goethite (Gt). The formula were created by equating the mineral-dissolution formula (Table III-2) and the oxidation of Fe^{2+} ($Fe^{2+} \rightarrow Fe^{3+} + e^-$ log K = -13).

mineral	**equation**	
Jt	$p\varepsilon = (\log k_{redJt} - \log a(K^+) - 3\log a(Fe^{2+}) - 2\log a(SO_4^{2-}))/3 - 2pH$	[14]
Gt	$p\varepsilon = \log k_{redGt} - \log a(Fe^{2+}) - 3pH$	[15]
Fh	$p\varepsilon = \log k_{redFh} - \log a(Fe^{2+}) - 3pH$	[16]

It appears from Fig. III-3 that nearly all lake water samples are located in the equilibrium window of the redox-couple Fe^{2+}-schwertmannite. This implies that a steady state exists between these two species and moreover that the rate at which schwertmannite is formed, is controlled by the oxidation kinetics of Fe^{2+} being slow at the low pH values of the lakes.

Based on an annual budget of the Fe(II) flux into the sediments of ML 77, an oxidation rate for Fe(II) of 12.5 mol $m^{-2} \cdot a^{-1}$ was determined (Peine et al, 2000) which corresponds to an approximate half-life of Fe(II) of 0.9 years at the lake-water pH of 3. This was confirmed by Deng (1997) who demonstrated that the oxidation of Fe(II) in a solution which is similar to a natural aquatic system, is very slowly (a complete oxidation of 0.1 mM Fe^{2+} takes 8 days) and that the precipitated products (Fe(III)hydroxides) strongly depend on the solutes in the water.
Additionally, the hypothesis of schwertmannite being a kinetic product of Fe^{2+} oxidation is confirmed by the morphology of the schwertmannite particles found in the sediment of ML 77 (Fig. III-7). They show the same "hedgehog" like structure as those obtained from slow (30 days) schwertmannite synthesis (reaction of $FeCl_3$ with Na_2SO_4) using dialysis bags. In contrast, rapid (< 24 h) production of schwertmannite by oxidation of $FeSO_4$ using H_2O_2 as oxidant results in particles with only little structure (Fig. III-7).

It remains to be examined whether complexation of Fe(II) by sulfate is a further requirement for the preferential formation of schwertmannite. Due to the higher oxidation rate of $FeSO_4$ compared to that of Fe^{2+}, SO_4^{2-} would be already bound to the inner shell of Fe^{3+} during the oxidation process. Thus, OH^- needs to compete with sulfate for coordination sites which would eventually inhibit further polymerisation of a pure (hydr)oxide phase.

Complexation and coordination chemistry of iron: As suggested by the calculation of the chemical speciation of dissolved iron in the lake water, sulfate complexes of both, Fe(II) and Fe(III) make up a significant portion of the total concentration of the two components which we expect to be the main reason for the occurrence of schwertmannite.
In Fe(III)-containing solutions polynuclears of iron(III) oxides and hydroxides form and their structure and that of the crystallising mineral essentially depends on the pH-value and the composition of the solution (Cornell & Schwertmann, 1996; Schneider & Schwyn, 1987). The presence of chloride in acidic (pH 1-2) solutions leads to the formation of akaganéite (β-FeOOH, Aktinson, 1977, Music et al., 1981, Schneider, 1984), a mineral that is isostructural to schwertmannite with chloride incorporated into the structure instead of sulfate (Bigham et al., 1990). Initially formed polymers of Fe(III) oxide and hydroxide chains already contain some chloride ions instead of hydroxyl ions as demonstrated by Mössbauer spectroscopy (Music et al., 1981).
After the formation of oxybridges between these polymers and an incomplete elimination of chlorides in the course of precipitation, the β-FeOOH structure finally develops. In contrast to nitrate or chloride solutions, this initial exchange of OH^- in the polymers was also

demonstrated for SO_4^{2-} in sulfate containing solutions (Music et al., 1981). Formation of schwertmannite was not observed in the mentioned study, probably because some parameters in the laboratory experiments are completely different to the conditions in the acidic mining lakes or the solutions used for the synthesis of schwertmannite, such as the solution temperature of 90 °C and the pH-value which ranged between 1 and 2 in the experiments performed by Music et al. (1981). The difference in the polymerisation pattern was explained by an occupation of the first coordination shell of iron(III) by sulfate or chloride which does not occur with nitrate or perchlorate ions. Accordingly, the formation of $FeSO_4^+$ complexes would suppress further polymerisation of pure Fe-OH species and subsequent crystallisation as iron(hydr)oxides in favour to sulfate containing precipitates.

Scheider & Schwyn (1987) described a similar model according to which positively charged polynuclears in Fe(III)-salt solutions undergo specific interaction with the anions chloride or sulfate. By further steps of alteration which were described as aggregation and coagulation, chloride was eliminated for charge compensation and finally exclusively bound by electrostatic effects (outerspheric) at minimum energy position between the chains of Fe(III)-O-OH octahedra which enclose the chloride ion to form the structural "embryo" of akaganéite crystals. The favoured polymerisation of sulfate with iron can be explained chemically by the valence-sum-rule (Brown, 1981) which states that the bonding of tetrahedrally coordinated anions (sulfate) bound via an oxygen atom to an octahedrally coordinated cation (Fe^{3+}), have the ideal bond valence (Hawthorne et al. 2000).

To summarise, the iron(III)-sulfate complexes in solutions appear to prevent the formation of the goethite or hematite structures in a similar way as chloride (Aktinson, 1977). Due to the similar coordination of ferric iron with chloride and sulfate (Music et al., 1981) one can assume that the akaganéite (= schwertmannite) structure will be energetically preferred also in sulfate solutions.

Metastability of Schwertmannite: The redox equilibrium between Fe(II) and schwertmannite observed for most lakes (Fig. III-3) implies that this mineral is the kinetic product of Fe(II) oxidation, being metastable with respect to goethite (Bigham et al., 1996) and at very low pH to jarosite. It therefore transforms into this mineral in the lake sediments as observed in ML 77 (Fig. III-6). The depth profile along which the transformation occurs (upper 10 cm) is characterised by an increase of the pH from ≈ 3 to values between 3.5 and 6 due to the onset of alkalinity generation by sulfate. Fig. 10 plots the transformation rate of schwertmannite derived from Fig 7 and from sediment dating provided in Peine et al. (2000) together with the pore-water pH at various sampling periods.

The transformation rate has a maximum after 3 years with a value of 55 % per year. The mineral is more or less stable for the first two years as long as the pH remains constant. The onset of transformation is accompanied by an increase of the pH although the transformation reaction produces acidity (Bigham et al., 1996).

It appears that the transformation which can be explained by the combined dissolution of schwertmannite and subsequent re-precipitation of Fe^{3+} as goethite, is accelarated upon generation of alkalinity by sulfate reduction.

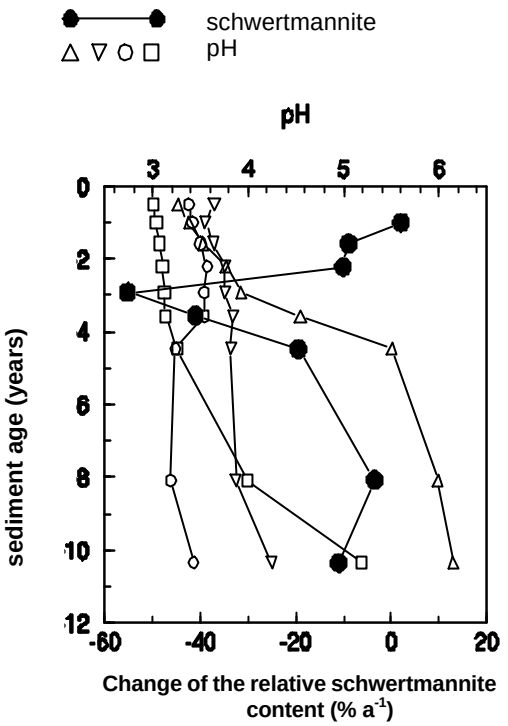

Fig. III-10 Correlation of the change of the relative schwertmannite content with the pH-value in the pore-water and the age of the sediment. Data from Peine et al. (2000).

Acceleration of the transformation reaction by an increasing pH was also displayed by the initial releasing rates of sulfate during the stability experiments (Fig. III-8). The overall release of sulfate during this transformation is low (11-37 % of total sulfate) and reaches an equilibrium already after about 15 days for the solutions at pH 3, 4 and 5 and after about 50 days for the solution at pH 7 (diagrams of the temporal release of Fe and sulfate are presented in appendix I). This indicates that either not all schwertmannite was transformed into goethite or that sulfate is adsorbed to goethite in high concentrations. X-ray diffractograms (Fig. III-9) and FTIR spectra (appendix C) demonstrated that the precipitates in all vessels in the pH-range of 3 to 7, consisted of both minerals in the end of the experiments (after 362 days). Hence, there is still some schwertmannite left at pH 7 which may be due to some unresolved passivation effect. However, the initial linear sulfate release clearly indicates a pH dependency of the transformation rate with a minimum between pH 3 and 5 and increasing values at higher pH (Fig. III-8). At pH 2 proton promoted dissolution of schwertmannite seems to be responsible for the release of sulfate as indicated by the high releasing rates of iron which may open pathway for the formation of jarosite (e.g. ML 111 and ML 117). Calculations of the saturation index for the waters of these lakes indicated indeed oversaturation with respect to this mineral.

4.3. The Regulation of the pH in AML

The observed pH range for the acidic mining lakes is in accordance to the survey of Cravotta et al. (1999) who could distinguish two groups out of 793 study sites influenced by AMD in the Eastern Coal province of the US, one of which with pH values between 2.5 and 4, the other with values > 6. A similar classification was derived by Kleeberg (1998) from the study of 25 mining lakes in the East-German lignite mining area.

So far, the discussion has demonstrated that the geochemical environment of acidic mining lakes provides suited conditions for the formation of the metastable mineral schwertmannite. It appears that the pH of the lake waters perfectly matches conditions where neither proton promoted dissolution of schwertmannite nor re-crystallisation to goethite occurs. This implies that the pH is directly linked to the mineral formation process. We therefore suggest that the pH of AML reflects a steady-state between several processes involved into the formation and consumption of schwertmannite, the mineral being the intermediate product: Preceding to the mineral formation is a steady supply of iron(II) into the lake with seepage waters from the adjacent dumps. These pore waters are anaerobic, weakly acidic and highly concentrated in Fe(II) and sulfate due to pyrite oxidation and subsequent weathering reactions in the dump. The Landesumweltamt Brandenburg (1995) surveyed such pore waters in tailings of two mine sites and found pH values between 4.3 and 7.2, rich in sulfate (15 to 25 mM) and iron (0.7 to 17.1 mM, mainly dissolved and in the ferrous form). Oxygen concentration was either not detectable or at the detection limit. Similar observations were made in sulphide bearing tailings from the exploitation of a sulphide ore body (Germain et al, 1994). Ferrous iron will enter a lake probably as a sulfate complex thereby being oxidised to a ferric sulfate complex. Subsequently precipitation of schwertmannite occurs via the intermediate product discussed above which is the principle acidifying process:

$$8\ Fe^{2+} + 2\ O_2 + 1.7\ SO_4^{2-} + 8.6\ H_2O \rightarrow Fe_8O_8(OH)_{4.6}(SO_4)_{1.7} + 12.6\ H^+ \qquad [17]$$

Peine et al. (2000) found an acidity production of 20 mol $m^{-2} \cdot a^{-1}$ based on this reaction for ML 77. In order to test this hypothesis we performed a scenario according to which a fictive pore water of the composition (sample “Meuro”, Table III-6) described by the Landesumweltamt Brandenburg (1995) is oxidised to find the pH at which equilibrium exists between the oxidised water and one of the three minerals schwertmannite, jarosite and goethite (Fig. III-11A). Even so schwertmannite had the highest supersaturation of all three minerals in the beginning of the oxidation, it readily achieved equilibrium with the solution (Fig. III-11A).

The pH value at which equilibrium establishes mainly depends on the initial Fe(II) concentration as it was calculated by oxidation of three fictive dump-solutions with different Fe(II)-concentrations (1-10 mM), as shown in Table III-6. The resulting pH (2.3 to 3.0) perfectly matches the pH-range observed in the lakes (Fig. III-11B).

Table III-6 Calculation of pH as result of an oxidation of a Fe(II) solution with the modelling program PhreeqC. As input (pH and water composition in mM) served the data of the dump water "Meuro" (Landesumweltamt Brandenburg, 1995) and of three fictive solutions (1, 2, 3).

	pH	iron(II)	sulfate	chloride	calcium	magnesium	sodium/ potassium	pH after oxidation	pH at SI=0
Meuro	6.14	4.6	21.5	2.4	14.8	4.1	1.3	3.51	2.67
1	6	1	10	-	2	2	1	3.71	3.01
2	6	5	10	-	2	2	1	3.38	2.53
3	6	10	10	-	2	2	1	3.24	2.32

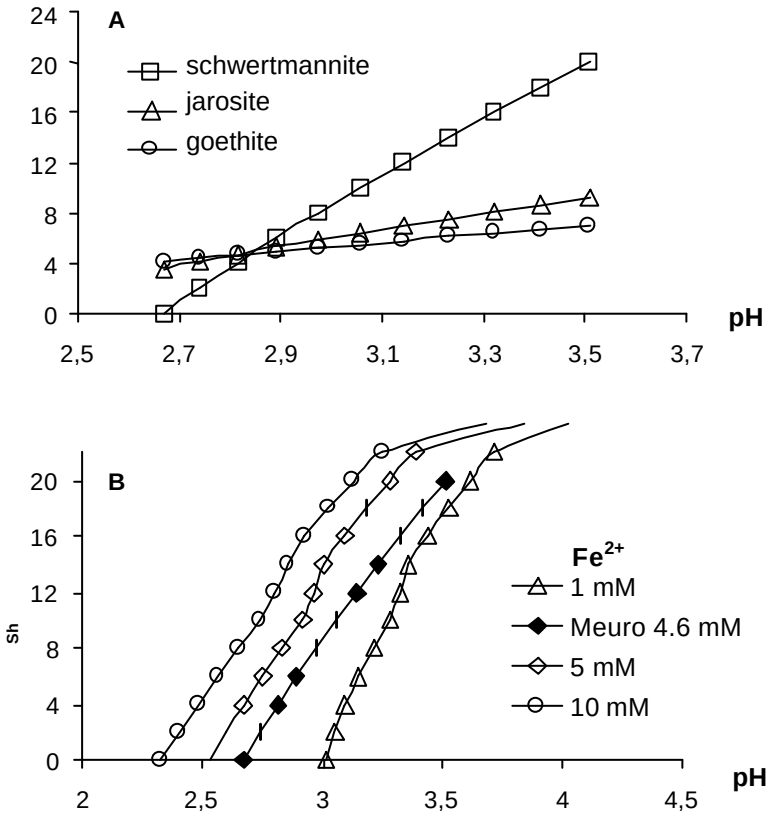

A)

Saturation index (SI) of schwertmannite, goethite and jarosite after oxidation of the dump-water "Meuro" (Landesumweltamt Brandenburg, 1995; Tab. III-6.).

B)

Saturation index (SI) of schwertmannite in dependence on Fe(II)-concentration: the fictive solutions contain 1, 5 and 10 mM Fe^{2+}, respectively compared to data from the dump-water "Meuro" (Landesumweltamt Brandenburg, 1995; Tab. III-6.).

Fig. III-11 Oxidation of Fe(II): Calculations of the SI and pH (PhreeqC).

Further acidification upon transformation to goethite seems to be balanced by alkalinity generating processes. Peine et al. (2000) observed that the rate of alkalinity formation from sulfate reduction (2.0 eq $m^{-2} \cdot a^{-1}$) was in the range of the acidity generation due to schwertmannite transformation (3.5 eq $m^{-2} \cdot a^{-1}$) in ML 77 and concluded that these two

processes balanced each other. We interpret this observation as a coupling of the both reactions, with sulfate reduction being rate limiting for the pH increase and thus driving the transformation reaction.

5. CONCLUSIONS

The oxidation of iron(II) in the presence of sulfate results in the crystallisation of the mineral schwertmannite. This can be expected due to geochemical calculations and observations in laboratory experiments (oxidation of $FeSO_4$ with H_2O_2). Evidence for this formation in the environment was found by sediment- and colloid-analysis of many acidic mining lakes. The groundwater entering into these lakes, has previously oxidised pyrite contained in the lake-surrounding lignite-dumps. This inflow is enriched in Fe(II) and sulfate and after contacting the oxygen-rich lake-water, the Fe(II) is oxidised to Fe(III) by a simultaneously release of acid. We hypothesised that schwertmannite forms due to structural and kinetic reasons as primary phase directly after Fe(II) oxidation. The resulting pH after that reaction corresponds to the stability window of schwertmannite (pH 2.5 to 4) and varies in this range in dependence on the Fe^{2+} concentration. Decreasing pH to a value < 2.5 would result in the dissolution of schwertmannite which is accompanied by a release of hydroxide, and a subsequent re-increase of the pH-value.

Compared to other Fe(III)-hydroxides and -hyrdoxysulfates as goethite and jarosite, respectively which are, according to geochemical calculations, also saturated in most of the AML waters the saturation index of schwertmannite is highest at the pH-value which adjusts after the total oxidation of Fe(II). However, schwertmannite is metastable with respect to these minerals, indicating that transformation occurs in the sediment by time. Formation and dissolution of schwertmannite effect that this mineral acts as a buffer in the range of its pH-stability window in postmining lakes. As long as the supply of iron(II) in the lakes and the subsequent oxidation is ensured, a change of the pH is not to expect.

In a broader sense this study suggests a general scheme which helps to understand the geochemistry of acid mine drainage systems in terms of a dynamic process.

Due to these observations it can be concluded that in-lake neutralisation of the acidic lakes by reduction of iron(III) and sulfate and fixing the weakly soluble products as Fe(II) sulphides in the sediment, as described by Peine et al. (1998) can only be obtained if the inflow of iron is prevented and further schwertmannite formation is stopped. It therefore should be considered that the groundwater inflow from the lignite dumps is the crucial factor for each kind of remediation of acidic mining lakes.

IV. SUMMARY AND CONCLUSIONS

This thesis shows the results of investigations concerning the formation and stability of schwertmannite as well as the interactions of this mineral with arsenate and chromate. Both, field investigations with naturally formed schwertmannite and laboratory experiments with synthetic schwertmannite, proved that this mineral cannot be defined clearly referring to its chemical and mineral composition. Its difficult classification can be explained by the characteristic of "weak crystallinity" which is a consequence of reduced crystal growth. This results in the formation of small sized particles with a high surface area which is responsible for the high reactivity and solubility of many weak-crystalline iron hydroxides. Schwertmannite features the crystal structure of akaganéite, is usually associated with goethite in natural systems and thermodynamically unstable referring to goethite and jarosite. Thus it represents a link between these minerals belonging to the group of iron(III) hydroxides and iron(III) hydroxysulfates. The “metastable” characteristic of schwertmannite which causes it to dissolve or to transform into more stable minerals by time (depending on the chemical environment) is the reason for its complicated verifiability in older precipitates (e.g. sediments with an age of some years).

However, results of this study have demonstrated that schwertmannite is the primary mineral phase which forms by the oxidation of iron(II) in sulfate containing solutions. This was proven by geochemical calculations and theoretical interpretations of the crystal structure and confirmed by analyses of natural samples from sediments of acid lignite mining lakes. In these acidic lakes the optimal conditions for schwertmannite formation exist. A steady supply of Fe(II)- and sulfate-rich seepage water from pyrite containing excavation dumps of lignite mining into the lake causes the crystallisation of schwertmannite. The associated hydrolysis of iron results in the decrease of pH in the surface water to ~ 3. An increased acidification (pH< 2.5) will dissolve the schwertmannite and result in the release of OH ions. Thus the water is buffered within the pH-stability range of schwertmannite (2.5 to 4.5). The permanent formation and/or dissolution of schwertmannite prevents both, the increased acidification and the (desired) neutralisation of surface waters in the lakes. Analyses of the top centimetres of a multitude of different lake sediments showed that schwertmannite is the mineral which forms in most of the lakes investigated in this study. Furthermore it was observed that with increasing sediment depth schwertmannite transforms to goethite. This “ageing” process of the sediment can be accelerated by rising pH values which are a consequence of bacterially induced sulfate reduction in the lakes. A permanent fixation of iron and sulphur can only be

reached by the reduction of iron(III) and sulfate in the deeper and oxygen-free sediment as assumed by Peine et al. (2000). However, a long-term neutralisation of surface water only seems possible if the supply of Fe(II)- and sulfate-rich groundwater from dumps will be prevented.

Apart from trying to comprehend the significance of schwertmannite and corresponding processes in acidic mining lakes, its characteristic to act as a sink for arsenate and chromate was examined in this study. Results obtained with synthetic schwertmannite showed that it cannot only store sulfate, but also chromate as a structural component into its crystal lattice. Both oxyanions can completely substitute themselves and the chromate content can amount up to 15 wt.- %. Similarly, arsenate can be enriched in high concentrations in schwertmannite (up to 10 wt.-%). However, arsenate incorporation into schwertmannite was only possible in combination with sulfate or chromate. Due to the mechanism of both, coprecipitation with- and adsorption onto schwertmannite, arsenate and chromate could be ex-filtrated from contaminated waters. Additionally to these ions, many other toxic compounds can probably be enriched in schwertmannite. This was shown by Webster at al. (1998) for heavy metals as well as in this study for arsenite (AsO_3^{3-}). However, only few experiments with As(III) were realised and further research in this section is required. Anyway, schwertmannite has great importance as a sink for poisonous materials. Therefore, a purposeful use as "cleaning agent" in contaminated water would be very useful. Future investigations should focus on the production of schwertmannite and its optimal dosage in drinking water processing plants.

Schwertmannite represents not only a sink, but also a potential source for previously enriched toxic compounds. As already explained, schwertmannite transforms or dissolves by time or due to changes of the chemical environment. This could possibly result in an additional release of toxic materials. The long-term investigation of arsenate- and chromate-containing schwertmannite showed that during schwertmannite dissolution the release of chromate is obviously higher than that of arsenate. The incorporation of arsenate even resulted in an increased mineral stability referring to dissolution caused by decreasing pH-values or microbiological iron(III) reduction. Further investigations on interactions between schwertmannite and micro-organisms which reduce not only Fe(III) but also sulfate, arsenate or chromate in schwertmannite, also seem to be of interest for a better understanding of the mobilisation processes of toxins.

Research on the extent of environmental risks by different contaminants which could be bound with different intensity to schwertmannite and potentially be released, seems recommendable.

V. REFERENCES

Aktinson R. J. (1977) Crystal nucleation and growth in hydrolysing iron(III)chloride solutions. *Clays and Clay Minerals* **25**, 49-56.

Asche H., Bork, H.-R., Heller, W. (1999) Entwicklung und Gestaltung von Erholungsgebieten in Bergbaufolgelandschaften der Niederlausitz. In *Potsdamer Geographische Forschungen, Institut für Geographie und Geoökologie der Universität Potsdam.* Vol. **17**, 137 p.

Barham J. R. (1997) Schwertmannite: A unique mineral contains a replaceable ligand, transforms to jarosites, hematites and/ or basic iron sulfate. *J. Mater. Res.* **12**, 2751-2758.

Baron D., Palmer C. D. (1995) Solubility of jarosite $KFe(SO_4)_2(OH)_6$ at 4 - 35 °C. *Geochim. Cosmochim. Acta* **60**, 185-195.

Baron D., Palmer C. D. (1996) Solubility of $KFe(CrO_4)_2(OH)_6$ at 4 to 35 °C *Geochim. Cosmochim. Acta* **60**, 3815-3824.

Berlepsch P., Armbruster Th, Brugger J., Bykover, E.Y., Kartashov P.M. (1999) The crystal structure of vergasovaite $Cu_3O[(Mo,S)O_4SO_4]$ and its relation to synthetic $Cu_3O[MoO_4]_2$. *Eur. J. Mineral* **11**, 101-110.

Biber M. V., dos Santos Afonso M., Stumm W. (1994) The Coordination Chemistry of Weathering IV. Inhibition of the Dissolution of Oxide Minerals. *Geochim. Cosmochim. Acta* **58**, 1999-2010.

Bigham J. M., Schwertmann U., Carlson L., Murad E. (1990) A poorly crystallized oxyhydoxysulfate of iron formed by bacterial oxidation of Fe(II) in acid mine waters. *Geochim. Cosmochim. Acta* **54**, 2743-2758.

Bigham J. M., Schwertmann U., Carlson L. (1992) Mineralogy of precipitates formed by the biogeochemical oxidation of Fe(II) in mine drainage. *Catena Supplement* **21**, 219-232.

Bigham J. M., Carlson L., Murad E. (1994) Schwertmannite a new iron oxyhydroxysulfate from Pyhäsalmi, Finland, and other localities. *Mineral. Mag.*, **58** (393), 641-648.

Bigham J. M., Schwertmann U., Traina S. J., Winland R. L., Wolf M. (1996) Schwertmannite and the chemical modelling of iron in acid sulfate waters. *Geochim. Cosmochim. Acta* **60**, 2111-2121.

Bigham J. M., Nordstrom D.K. (2000) Iron and aluminium hydroxysulfates from acid sulfate waters. In: Alpers C. N., Jambor J.L., Nordstrom D.K. *Reviews in Mineralogy and Geochemistry*, Mineralogical Society of America, 351-403.

Bishop J. L. (1996) Schwertmannite on Mars? Spectroscopic analysis of schwertmannite, its relationship to other ferric minerals and its possible presence in the surface material on mars. In: Dyar M.D., McCammon C., Schaefer M.W. (eds.) *Mineral Spectroscopy*: A Tribute to Roger G Burns Geochemical Society Spec. Publ. No 5, 337-358.

Bloesch J., Burns N.M. (1980) A critical review of sedimentation trap technique. *Schweiz. Z. Hydrol.* **42**, 15-55.

Brand A. (2001) Vorkommen, Bildung und Bedeutung von Schwertmannit in Sedimenten von Restseen des Braunkohletagebaus. *Unveröff. Diplomarbeit, Universität Bayreuth, Bayreuth.*

Bridge T.M., Johnson D.B. (2000) Reductive dissolution of ferric iron minerals by *Acidiphilium* SJH, *Geomicrob. J.* **17**, 193-206.

Brown I. D. (1981) The bond-valence method: an empirical approach to chemical structure and bonding. In *Structure and bonding in crystals* **29** (eds. M. O'Keeffe, Navrotsky A.), Acta Crystallogr.A., 266-282.

Brunauer S., Emmett P.H., Teller E. (1938) Adsorption of gases in multimolecular layers. *J. Am. Chem. Soc.* **60**, 309-319.

Carlson L., Schwertmann U. (1981) Natural ferrihydrites in surface deposits from Finland and their association with silica. *Geochim. Cosmochim. Acta* **45**, 421-429.

Carlson L., Bigham J.M. (2001) Retention of arsenic by precipitates from acid mine drainage. *Environ. Sci. Technol. (submitted to est).*

Chatterjee A., Das D. et al., (1995) Arsenic in groundwater in six districts of West Bengal, India: The biggest arsenic calamity in the world, Part 1. Arsenic species in drinking water and urine of the affected people. *Analyst* **120**, 643-656.

Chowdhury, U. K., Biswas, B.K., et al. (2000) Groundwater arsenic contamination in Bangladesh and West Bengal, India. *Environmental Health Perspectives* **108** (5), 393-397.

Cornell R. M. and Schwertmann U. (1996) *The Iron Oxides*. VCH Verlagsgesellschaft mbH, Weilheim, VCH Publishers, New York, 570 p.

Cravotta C. A. I., Brady K.B.C., Rose A.W., Douds J.B. (1999) Frequency distribution of the pH of coal-mine drainage in Pennsylvania DW. In: Morganwalp D.W. (ed.) *U.S. Geological Survey Toxic substances Hydrology Program-Proc. Technical Meeting*. US Geol. Surv. Water-Res. Invest Rep, 99- 4018A, 313-324.

Cullen W. R., Reimer K.J. (1989) Arsenic Speciation in the Environment. *Chem. Rev*. **89** No. 4, 713-764.

Deng Y. (1997) Formation of iron(III)-hydroxides from homogenous solutions. *Wat. Res.* **31** (6), 1347-1354.

Duesler E.N., Foord E.E. (1986) Crystal structure of hashemite, $BaCrO_4$, a barite structure type. *Am. Mineral.* **71**, 2117-1220.

Dzombak D.A. and Morel F.M.M. (1990) *Surface complexation modeling - hydrous ferric oxide*. Wiley-Interscience, New York, 393 p.

Eick M.J., Peak J.D., Brady W.D. (1999) The effect of Oxyanions on the oxalate-promoted dissolution of goethite. *Soil Sci. Soc. Am. J.* **63**, 1133-1141.

Evangelou V.P., Zhang Y.L. (1995) A review: pyrite oxidation mechanisms and acid mine drainage prevention. *Crit. Rev. Environ. Sci. Technol.*, **25** (2), 141-199.

Farmer V. C. (1974) *The infrared spectra of minerals*. Min. Soc., London, 539 p.

Fendorf S., Eick M.J., Grossl P., Sparks D.L. (1997) Arsenate and Chromate retention mechanisms on goethite. 1. Surface structure. *Environ. Sci. Technol.* **31**(2), 315-320.

Fitzpatrick R.W., Self P.G. (1997) Iron oxyhydroxides, sulfides and oxyhydroxysulfates as indicators of acid sulfate weathering environments. *Advances in GeoEcology* **30**, 227-240.

Fortin D., Davis B., Beveridge T.J. (1996) Role of *Thiobacillus* and sulfate-reducing bacteria on Fe biocycling in oxic and acidic mine tailings. FEMS *Microbiol. Ecol.*, **21**, 11-24.

Fuller C., Davis J.A., Waychunas G. A. (1992) Surface chemistry of ferrihydrite: Part 2. Kinetics of arsenate adsorption and coprecipitation. *Geochim. Cosmochim. Acta* **57**, 2271-2282.

Gao Y., Mucci A. (2001) Acid base reactions, phosphate and arsenate complexation, and their competitive adsorption at the surface of goethite in 0.7 M NaCl solution. *Geochim. Cosmochim. Acta* **65** (14), 2361-2378.

Glockner E. F. (1853) Über einen neuen Eisensinter von Obergrund bei Zuckmantel. Poggendorfs. *Ann. Phys. Chem*. **89**, 482-488.

Gmelin H. d. A. C. (1954) *Molybdat*. In: Handbuch der Aanorganischen Chemie, 8. Auflage, Springer, Berlin.

Goldberg S., Glaubig R.A. (1988) Anion Sorption on a calcareous, montmorillonitic soil-arsenic. *Soil Sci. Soc. Am. J.* **52**, 1297-1300.

Goldschmidt V.M. (1937) The principles of distribution of chemical elements in minerals and rocks. *J. Chem. Soc*. 665-673.

Göttlicher J., Gasharova B. (2000) Interactions of iron and sulfur bearing solid phases with water in surface coal mining pits and acidic mining lakes. In: Rammlmayr et al. (ed.) *Applied Mineralogy*, Balkema, Rotterdam, 1048 p.

Gottwald W., Wachter, G. (1997) *IR-Spektroskopie für Anwender*. Wiley-VCH, Weinheim, 294 p.

Günzler H., Heise, H.M. (1996) *IR-Spektroskopie*, Wiley-VCH-Weinheim, 397 p.

Harrison J.B., Berkheiser. V.E. (1982) Anion interactions with freshly prepared hydrous iron oxides. *Clays and Clay Minerals* **30** (2), 97-102.

Hawthorne F.C., Krivovichev S.V., Burns P.C. (2000) The crystal chemistry of sulfate minerals. In *Sulfate Minerals*, Vol. 40 (ed. C. N. Alpers, Jambor J.L., Nordstrom D.K.), The Mineralogical Society of America, 608. p.

Hayes K.F., Papelis C., Leckie J.O. (1988) Modeling ionic strength: Effects on anion adsorption at hydrous oxide/solution interfaces. *J. Colloid Interface Sci.* **78**, 717-726.

Henningsen D., Katzung G. (1998) *Einführung in die Geologie Deutschlands*. Enke, Stuttgart, 224 p.

Herzsprung P., Friese K., Packroff G., Schimmele M., Wendt-Potthoff K., Winkler M. (1998) Vertical and annual distribution of ferric and ferrous iron in acidic mining lakes. *Acta Hydrochim. Hydrobiol.* **26**, 253-262.

Hollandliste (1988) *Beurteilung von Konzentrationen verschiedener Stoffe im Boden und Grundwasser*. Aus: Hollandliste Interventiewaarden bodemsanering Staatscourant Nr. 9524.05.1994.

Holleman A.F., Wiberg E. (1985) *Lehrbuch der Anorganischen Chemie*, Walter de Gruyter, Berlin, New York, 1451 p.

Hsia T.H., Lo S.L., Lin C.F., Lee D.Y. (1993) Chemical and spectroscopic evidence for specific adsorption of chromate on hydrous iron oxide. *Chemosphere* **26**, 1897-1904.

Johnson D.B., McGinness S. (1991) Fe(III) reduction by acidophilic heterotrophic bacteria, *Appl. Environ. Microbiol.* **57**, 207-211.

Kato T. (1977) Further refinement of woodhouseite structure. *N. Jahrb. Mineral. Monatsh*., 54-58.

Kato T. Miura Y. (1977) The crystal structure of jarosite and svanbergite. *Mineral. J. (Japan)* **8** 419-430.

Kleeberg A. (1998) The quantification of sulfate reduction in sulfate-rich freshwater lakes-a means for predicting the eutrophication process of acidic mining lakes? *Water Air and Soil Pollution* **108**, 365-374.

Konnerts J.A., Evans H.T.Jr., McGee J.J., Erickson G.E. (1994) Mineralogical studies of nitrate deposits of Chile: VII. Two new saline minerals with the composition $K_6(Na,K)_4Na_6Mg_{10}(XO_4)_{12}(IO_3)_{12}*12H_2O$: fuenzaldaite (X=S) and carlosruizite (X=Se). *Am. Mineral* **79**, 1003-1008.

Küsel, K., Drake H.L. (1995) Effects of environmental parameters on the formation and turnover of acetate by forest soils. *Appl. Environ. Microbiol*. **61**, 3667-3675.

Küsel K., Dorsch T., Acker G., Stackebrandt E. (1999) Microbial reduction of Fe(III) in acidic sediments: Isolation of *Acidiphilium cryptum* JF-5 capable of coupling the reduction of Fe(III) to the oxidation of glucose, *Appl. Environ. Microbiol*. **65**, 3633-3640.

Küsel K., Dorsch T. (2000) Effect of supplemental electron donors on the microbial reduction of Fe(III) and sulfate in coal mining-impacted freshwater lake sediments, *Microb. Ecol*. **40**, 238-249.

Küsel K., Roth U., Dorsch T., Peiffer S. (2001) Effect of pH on the anaerobic microbial cycling of sulfur in freshwater mining-impacted lake sediments, in Ernst, W.H.O., Pezeshki, S.R. and Chabbi, A. (eds.), *Plants and organisms in wetland environments, Environ. Exper. Bot.* **46**, 213-224.

Landesumweltamt Brandenburg (1995) Wasserbeschaffenheit in Tagebaurestseen. In *Studien und Tagungsberichte*, Vol. 6, Potsdam, 86. p.

Lovley D.R. (1993) Dissimilatory metal reduction, *Annu. Rev. Microbiol*. **47**, 263-290.

Lovley D.R. and Phillips E.J.P. (1986) Availability of Fe(III) for microbial reduction in bottom sediments of the freshwater tidal Potomac River. *Appl. Environ. Microbiol*. **52**, 751-757.

Lu F. J. (1990) Review of fluorescent humic substances and blackfoot disease in Taiwan. *Applied Organometallic Chemistry* **4**, 191-195.

Lumsdon D.G., Fraser A.R., Russell J.D., Livesey N.T. (1984) New infrared band assignments for the arsenate ion adsorbed on synthetic goethite. *J.Soil Sci.* **35**, 381-386.

Lumsdon D.G., Evans L.J. (1994) Surface complexation model parameters for goethite (alpha-FeOOH). *Journal of Colloid and Interface Science* **164**, 119-125.

Lyklema J. (1987) Electrical double layers on oxides; disparate observations and unifying principles. *Chemistry and Industry*, 741-747.

Maly K. (1999) Jihlava ore region - geology and mineralogy. In Ekon (ed.) *Silver-mining and coinage of Jihlava (Iglau)*, Muzeum Vysociny, 110 p.

Mason B., Moore C. (1985) *Grundzüge der Geochemie*. Enke, Stuttgart, 340 p.

Matthes S. (1996) *Mineralogie.* VCH Springer, Berlin, 499 p.

McLean J., Beveridge T.J. (2001) Chromate reduction by a pseudomonad isolated from a site contaminated with chromated copper arsenate. *Appl. Environ. Microbiol.* **67**, 1076-84.

Mesuere K., Fish W. (1992) Chromate and oxalate adsorption on goethite. 1. Calibration of surface complexation models. *Environ. Sci.Technol.* 26(12), 2357-2370.

Munch J.C., Ottow J.C.G. (1980) Preferential reduction of amorphous to crystalline iron oxides by bacterial activity, *Soil Science* **129**, 15-21.

Murad E. (1979) Mössbauer and X-ray data on FeOOH (akaganéite). *Clay Min.* **14**, 273-283.

Music S., Vertes A., Simmons G.W., Dzako-Nagy I., Leidheiser, H.Jr. (1981) Mössbauer spectroscopic study of the formation of Fe(III) oxyhydroxides and oxides by hydrolysis of aqueous Fe(III) salt solutions. *Journal of Colloid and Interface Science* **85** (1), 256-265.

Myneni S.C.B., Traina S.J., Waychunas G.A., Logan T.J. (1998) Vibrational spectroscopy of functional group chemistry and arsenate coordination in ettringite. *Geochim. Cosmochim. Acta* **62** (21/22), 3499-3514.

Nakamoto K. (1986) *Infrared and raman spectra of inorganic and coordination compounds (3ed.).*Wiley, New York.

Nieboer E., Jusys A.A. (1988) *Chromium in the natural and human environments.* J.O. Nriagu, Nieboer E. (eds.), John Wiley, New York, pp.21-80.

Nordstrom D.K. (1982) Aqueous pyrite oxidation and the consequent formation of secondary iron minerals. In Kittrick J.A. et al. (eds.) *Acid sulfate weathering*. Soil Sci. Soc. Am., 37-56.

Nordstrom D.K., Alpers C.N. (1998) Geochemistry of acid mine waters. In Plumlee G.S., Logsdon M.J. (ed.) *The environmental geochemistry of mineral deposits. Reviews in Economic geology*. Society of ecologic geologists.

Nordstrom D.K., Munoz J.L. (1994) *Geochemical Thermodynamics*, 2nd edition. Blackwell Science, Boston.

Nordstrom D.K., Plummer L.N., Langmuir D., Busenberg E., May H.M., Jones B.E., Parkhurst D.L. (1990) Revised chemical equilibrium data for major water-mineral reactions and their limitations. *ACS Symp. Ser.* **416**, 398-413.

Nowel W., Bönisch R., Schneider W., Schulze H. (1995) *Geologie des Lausitzer Braunkohlereviers*. 2 ed. Lausitzer Braunkohle Aktiengesellschaft, Senftenberg, 104 p.

Parfitt R.L., Russell J.D. (1977) Adsorption on hydrous oxides IV. Mechanism of adsorption of various ions on goethite. *J. Soil Sci.* **28**, 297-305.

Parfitt R.L., Smart R.St.C. (1978) The mechanism of sulfate adsorption on iron oxides. *Soil Sci. Soc. Am. J.* **42**, 48-50.

Parkhurst D.L. (1997) Geochemical mole-balance modelling with uncertain data. *Water Resources Research* **33**(8), 1957-1970.

Peak D., Ford R.G., Sparks D.L. (1999) An in situ ATR-FTIR investigation of sulfate bonding mechansms on goethite. *J.Colloid Sci.,* **218**(1), 289-299.

Peine A. (1998a) *Saure Restseen des Braunkohletagebaus - Charakterisierung und Quantifizierung biogeochemischer Prozesse und Abschätzung ihrer Bedeutung für die seeinterne Neutralisierung.* Dissertation, Bayreuther Institut für Terrestrische Ökosystemforschung (Hrsg.) **62**, 131p.

Peine A., Peiffer S. (1998b) In-Lake Neutralization of acid mine lakes. In W. K. Geller, H. W. Salmons (ed.) *Acidic Mining Lakes*, Springer, Berlin.

Peine A., Trischler A., Küsel K., Peiffer S. (2000) Electron flow in an iron-rich acidic sediment - evidence for an acidity-driven iron cycle. *Limnology and Oceanography* **45(5)**, 1077-1087.

Penners N.H.G., Koopal L.K. (1986) Preparation and optical properties of homodisperse haematite hydrosols. *Colloids and Surfaces* **19**, 337-349.

Pichler T., Veizer J., Gwendy E., Hall M. (1999) Natural input of arsenic into a coral-reef ecosystem by hydrothermal fluids and its removal by Fe(III) Oxyhydroxides. *Environ. Sci.Technol.* **33**, 1373-1378.

Regenspurg S., Peiffer S. (2000) The mineral schwertmannite in sediments of acid lignite opencast lakes. In: Rammlmayr et al. (ed.) *Applied Mineralogy*, Balkema, Rotterdam, 1048 p.

Rose S., Ghazi A.M. (1997) Release of sorbed sulfate from iron oxyhydroxides precipitated from acid mine drainage associated with coal mining. *Environ. Sci.Technol.* **31**, 2136-2140.

Rüde T.R., Barth A., Pietsch R., Regenspurg S., Surwald F. (1999) Chemistry of the acidic waters of the Rötlbach, Zillertaler Alps, and the precipitation of iron oxides. In: Rammlmayr et al. (ed.) *Applied Mineralogy*, Balkema, Rotterdam, 1048 p.

Rüger F.R., Witzke T., Grunewald W., Langhammer D., Senf L. (1994) Die Saalfelder Feengrotten- eine mineralogische Kostbarkeit Deutschlands. Feuerpfeilverlag, 56 p.

Russel J.D., Fraser A.R. (1994) Infrared methods. In: Chapman M., Wilson H.J. (eds.) *Clay Mineralogy: Spectroscopic and chemical determinative methods.*

Sachs L. (1992) *Angewandte Statistik*. Springer, Berlin.

Savage K.S., Tingle T.N., O'Day P.A., Waychunas G.A., Bird D.K. (1999) Arsenic speciation in pyrite and secondary weathering phases, Mother Lode Gold District, Tuolumne County, California. *Applied Geochemistry* **15**, 1219-1244.

Scheffer P., Schachtschabel P., Blume H.-P., Brümmer G., Hartge K.H., Schwertmann U., Auerswald K., Beyer L., Fischer W.R., Kögel-Knaber I., Renger M. and Strebel O. (1998) *Lehrbuch der Bodenkunde* (14. edition). F. Enke Verlag, Stuttgart, 494 p.

Schneider W. (1984) Hydrolysis of iron(III)-chaotic olation versus nucleation. *Comments Inorg.Chem.* **3**, 205-223.

Schneider W., Schwyn B. (1987) The hydrolysis of iron in synthetic, biological and aquatic media. In: Stumm W. (ed.) *Aquatic surface chemistry.* Wiley Interscience, New York, 167-194.

Schwertmann U., Bigham J. M., Murad E. (1995) The first occurrence of schwertmannite in a natural stream environment. *Eur. J. Mineral.* **7**, 547-552.

Schwertmann U., Cambier P., Murad E. (1985) Properties of goethite of varying crystallinity. *Clays and Clay Minerals* **33**(5), 369-378.

Schwertmann U. (1991) Solubility and dissolution of iron oxides, *Plant and Soil* **130,** 1-25.

Schwertmann U., Fitzpatrick R.W. (1992) Iron minerals in surface environment. *Catena Supplement* **21**, 7-30.

Sigg L., Stumm W. (1981) The interaction of anions and weak acids with the hydrous goethite (a-FeOOH) surface. *Colloids and Surfaces* **2**, 101-117.

Smith D.K., Roberts A.C., Bayliss P., Liebau F. (1998) A systematic approach to general and structure type formulas for minerals and other inorganic phases. *Am. Mineral* **83**, 126-132.

Stumm W. (1992) *Chemistry of the solid-water interface.* Wiley, New York, 428 p.

Stumm W., Morgan, J. (1996) *Aquatic Chemistry*. Wiley, New York, 1022 p.

Stumm W., Furrer G., Wieland E., Zinder B. (1985) The effects of complex-forming ligands on the dissolution of oxides and aluminiumsilicates. In: Drever, J.I. (ed.) *The chemistry of weathering*, Dodrecht, R.,D., The Netherlands, 55-74

Sun X., Doner H.E. (1996) An investigation of arsenate and arsenite bonding structures on goethite by FTIR. *Soil Science* **161**(12), 865-872.

Szymanski J.T. (1988) The crystal structure of beudantite, $Pb(Fe, Al)_3((As,S)O_4)_2(OH)_6$. *Can. Mineral* **26**, 923-932.

Tamura H., Goto K., Yotsuyanagi T., Nagayam, M. (1974) Spectrophotometric determination of iron(II) with 1,10-Phenantroline in the presence of large amounts of iron (III). *Talanta* **21**, 314-318.

Tipping E., Cooke D. (1982) The effects of adsorbed humic substances on the surface charge of goethite in freshwaters. *Geochim. Cosmochim. Acta* **46**, 75-80.

Torrent J., Barron V., and Schwertmann U. (1990) Phosphate adsorption and desorption by goethites differing in crystal morphology. *Soil Society of America* **54**, 1007-1012.

Trinkwasserverordnung. (1990) *Trinkwasserverordnung vom 5.12.1990*. BMFJG, 1036 S.

Tritschler A. (1997) Quantifizierung und Charakterisierung von Eisenfestphasen im Sediment von sauren Restseen des Lausitzer Braunkohletagebaus. *unveröff. Diplomarbeit, Universität Bayreuth, Bayreuth.*

Urrutia M.M., Roden E.E., Fredrickson J.F. and Zachara J.M. (1998) Microbial and surface chemistry controls on reduction of synthetic Fe(III) oxide minerals by the dissimilatory iron-reducing bacterium *Shewanella alga*. *Geomicrobiol.* **15**, 269-291.

Van der Marel H.W., Beutelspacher H. (1976) *Atlas of infrared Spectroscopy of Clay Minerals and their Admixtures*. Elsevier Scientific Publishing Company, Amsterdam.

Walenta K., Zweiner M., Dunn P.J. (1982) Philipsbornite, a new mineral of the cranallite group from Dundas, Tasmania. *N. Jahrb. Mineral. Monatsheft* 1-5.

Waychunas G.A., Rea B.A., Fuller C.C., Davis J.A. (1992) Surface chemistry of ferrihydrite: Part 1. EXAFS studies on geometry of coprecipitated and adsorbed arsenate. *Geochim. Cosmochim. Acta* **57**, 2251-2269.

Waychunas G.A., Myneni S.C.B., Traina S.J., Bigham J.M., Fuller C.F., Davis, J.A. (2000) Reanalysis of the schwertmannite structure and the incorporation of SO_4-Groups: An IR, XAS, WAXS and simulation study. C*onference-abstract:* eleventh annual V.M. Goldschmidt Conference (2001).

Webster J.G., Swedlund P.J., Webster K.S. (1998) Trace metal adsorption onto acid mine drainage iron oxide. In Hulston A. (ed.) *Water-Rock interactions*, Balkema, Rotterdam, 951-954.

Wilkinson G., Gillard R.D., McCleverty J.A. (eds.) (1987) *Comprehensive coordination Chemistry*. Pergamon Print, Oxford.

WHO (2000) Environmental Health Criteria, Chromium. World Health Organisation, Genf.

Yu J.-Y., Heo B., Choi I.-K., Cho J.-P, Chang H.-W. (1999) Apparent solubilities of schwertmannite and ferrihydrite in natural stream water polluted by mine drainage. *Geochim. Cosmochim. Acta* **63**, 3407-3416.

ACKNOWLEDGEMENTS

First, I want to say my sincere thanks to **Prof. Dr. S. Peiffer**, who transferred me this research project and enriched it by numerous ideas.

I acknowledge **Prof. Dr. R. Herrmann** for the chance to perform this research at his institute.

A special thanks is due to **Andreas Brand**, for the good cooperation, fruitful discussions and for the valuable data, which I obtained of his diploma thesis. Many thanks are also to Andrea **Tritschler**, whose diploma thesis was the basis for a big part of this work.

A very big thank you to **Dr. K. Kuesel**, for the idea of a combined geochemical-microbiological project and the good cooperation.

I gratefully acknowledge **Dr. K. Maly** (museum Vysconcyny, Jihlava, Cz) and **B. Lochner** (Saalfelder Feengrotten, Thuringia), who guided me through the ore mines "Prybyslav" and the "Saalfelder Feengrotten", respectively and submitted the sampling at these unique places.

To **Daniela Arneth** and the laboratory personnel of the Limnological Research Station I am greatly indebted for much help at numerous analytic work. Many thanks for analytic works also to **Christopher Morys, Ulli Drescher** and **Jochen Schmitt**.

With best thanks also to **Prof. Dr. H. Stanjek**, for the measurement and determination of the unit cell parameters of one of my samples by X-ray diffraction.

I acknowledge **Clarissa Drummer**, **Dr. H. Keppler** (BGI) and **Dr. F. Heidenau** (IMA) for the support in measurements of the REM, FTIR and BET. Many thanks also to **Dr. G. Ilgen** (BITOEK), for the method development of the arsenite analysis (I regret that I could use it only to small extent) and to the laboratory pesonnel of the BITOEK (**Anita Gössner, Yvonne Hoffmann** and **Bettina Popp**).

My sincere gratitude also to **Prof. Dr. U. Schwertmann, Dr. J. Goettlicher** and **Prof. Dr. Pentinghaus,** for scientific support to my work.

Many thanks for further assistance, fruitful discussions and good spirits to my colleagues **Christian Blodau, Thomas Eckert, Luisa Hopp, André Krug, Silke Marczinek, Charlotte Roehm** and **Winfrid Schulz Gade**.

My sincere thanks is also to **Silke van Schwarzenberg**, who gave me much linguistic support.

I acknowledge the **Deutsche Forschungsgemeinschaft** (DFG) for financial support over two years in the priority program 546 "Geochemical processes with long-term effects in anthropogenically-affected seepage- and groundwater".

”To understand how anything very complex works, or even to know that there is something complex at work, man needs to see little tiny bits of it at a time.”

ADAMS, D., CARWARDINE, M. (1990): Last Chances to See.

APPENDIX

A) XRD-PATTERN FE(III)-HYDROXIDES CONTAINING SULFATE AND/ OR PHOSPHATE (II.2.)

(The compositions of the synthesis-solutions are shown in Table II.2-4.)

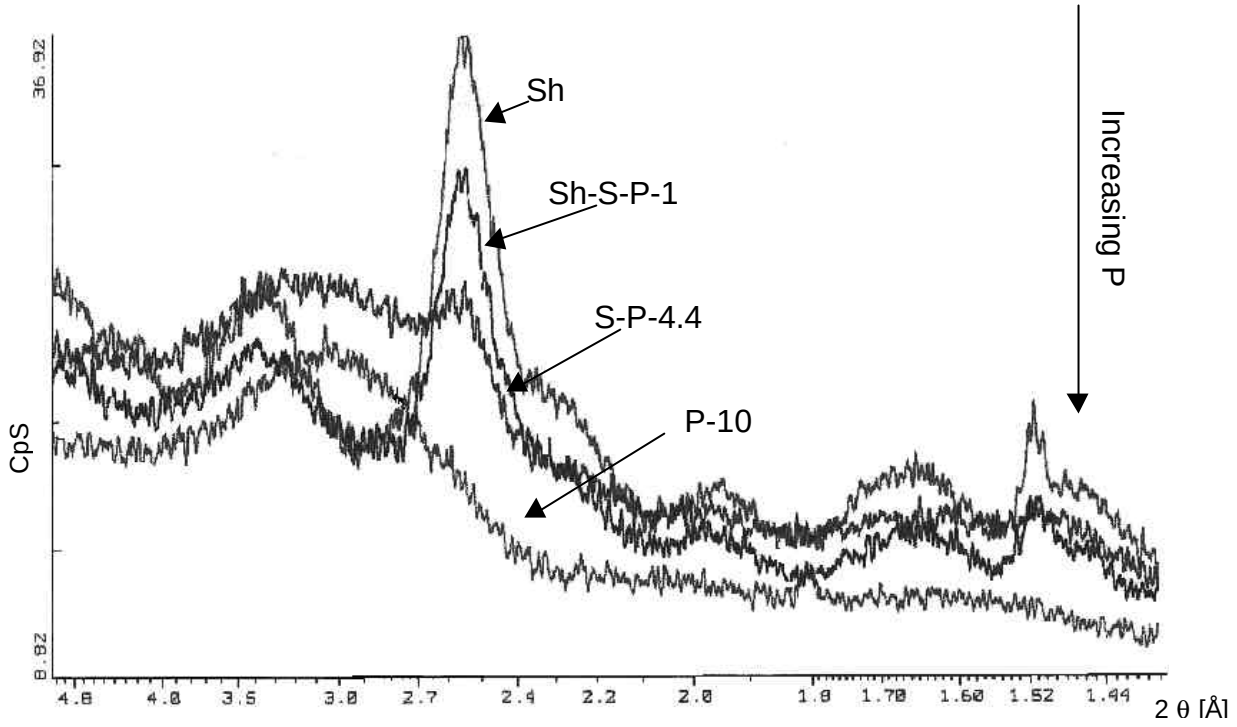

B) AS AND CR IN PRECIPITATES AND IN WATER SAMPLES OF TWO FORMER MINES (II.2.)

Measured data (graphite-tube-AAS) of As(tot) and Cr(tot) in precipitates (extracted with NH_4-oxalate, pH 3) and drainage water of the mines „Saalfelder Feengrotten“ and „Prybyslav“.

		precipitates		**drainage water**	
		As (ppm)	Cr (ppm)	As (ppb)	Cr (ppb)
Saalfelder Feengrotten	1	727	296	5	8
	2	124	34	9	< d.l.
	3	1594	126	35	5
	4	152	10	15	19
	5	101	52	12	7
	6	54	76	< d.l.	11
	7	261	12	< d.l.	6
	8	119	38	7	10
Prybyslav	1	3240	218	22	34
	2	3860	138	< d.l.	78
	3	4620	104	53	45
	4	6740	812	235	112
	5	2850	100	86	< d.l.
	6	560	145	38	38
	7	1830	102	< d.l.	< d.l.
	8	4220	296	58	174
	9	5960	156	36	6
	10	2640	112	25	10

C) FTIR-SPECTRA OF THE SCHWERTMANNITE-STABILITY EXPERIMENTS (II.2 AND III.)

The IR spectra of schwertmannite (samples Sh-S-P-1, Sh-S-As-1, Sh-S-Cr-1 and Sh-Cr-10) were recorded after suspending the samples over one year constantly at pH 4. They all show characteristic schwertmannite-bands (e.g. the FeO bands at 704 and 483 cm^{-1}). No bands indicating the formation of goethite were detected (see chapter II.2.3. and III.).

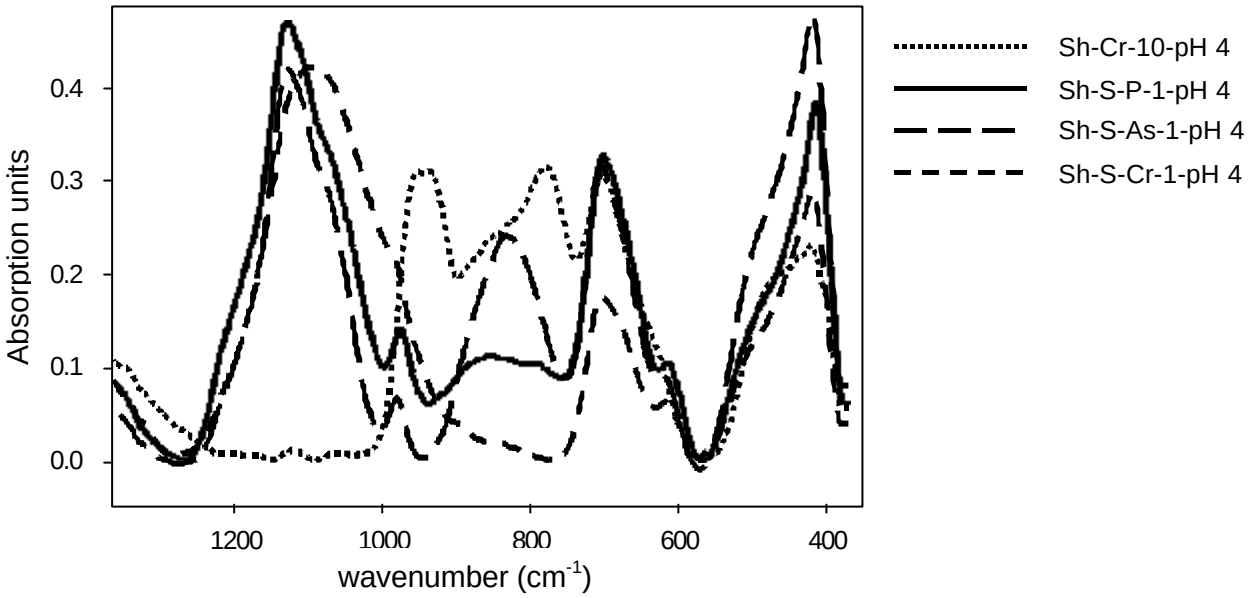

IR spectra of schwertmannite samples, which were suspended about one year at constant pH of 2, 3, 4, 5 and 7, respectively. The bands marked with arrows indicate the formation of goethite, which was observed in nearly all samples. The intensity of this band decreases with decreasing pH.

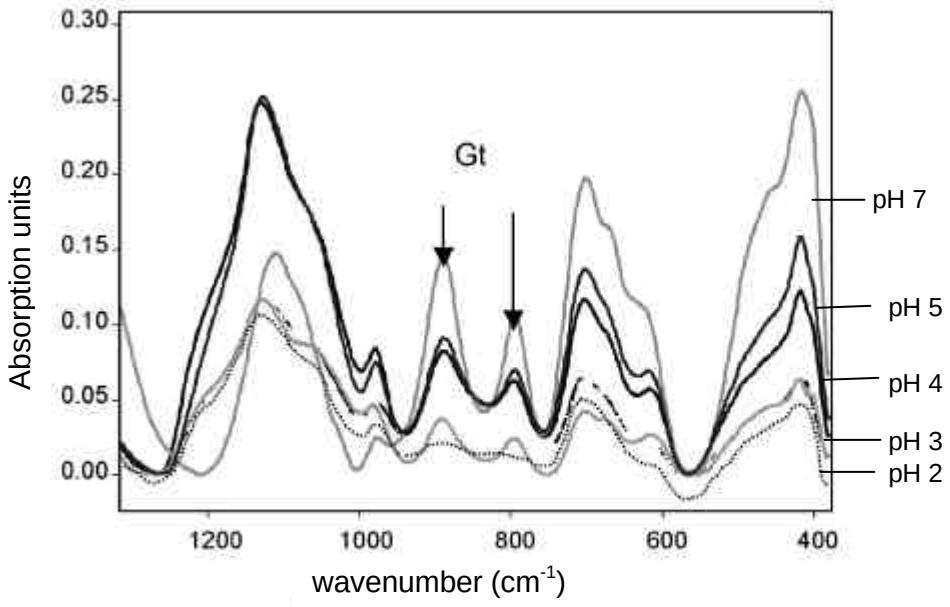

(explanation to the experiments is given in chapter III.3.5. and II.2.3.)

D) Scanning electron micrographs of synthetic Fe(III)-precipitates (II.2)

Influence of the schwertmannite composition on the particle-morphology:
(The chemical compositions of the synthetic samples are presented inTab. II.2-4.)

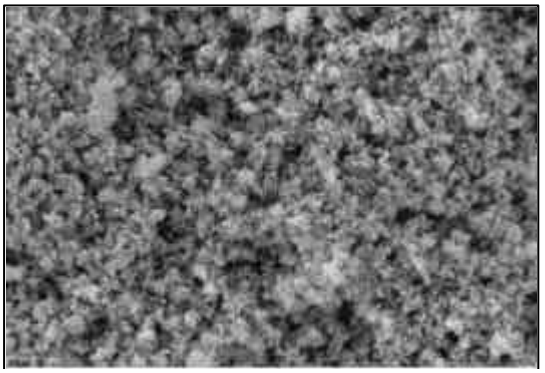

— 100 nm Sh-As-Cr

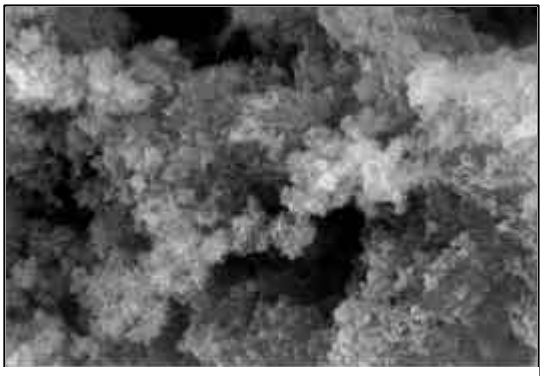

— 200 nm Sh-S-As-1

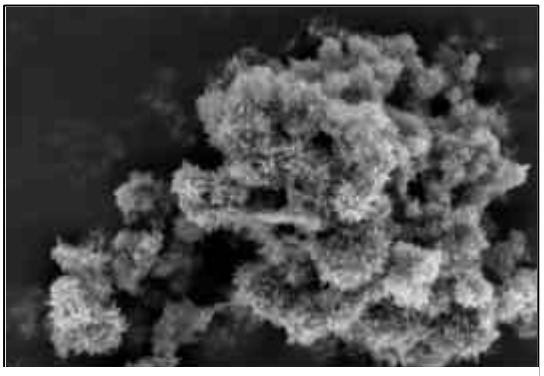

— 100 nm Sh-S-Cr-5

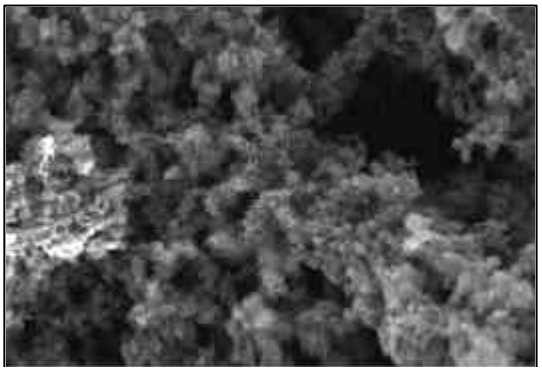

— 300 nm S-As-5

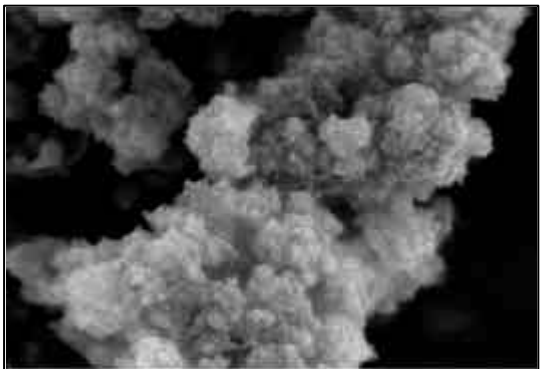

— 100 nm Sh-Cr-10

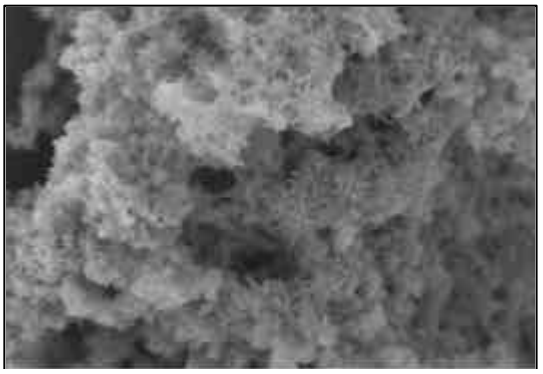

— 100 nm Sh

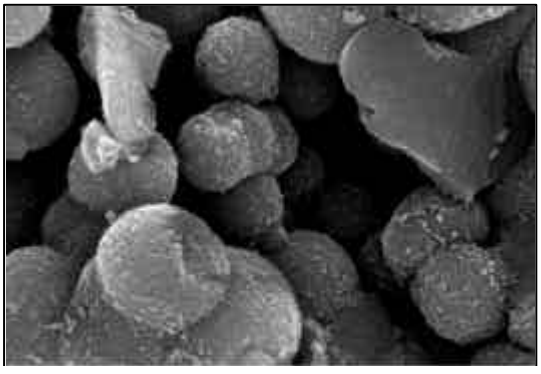

— 300 nm Sh-H_2O_2-As

— 100 nm Sh-S-Cr-1

E) ACID-BASE-TITRATION DATA (II.2 AND II.6.2)

Batch-experiment: Measured pH in suspensions of schwertmannite and goethite after 24 and 48 h, titrated with HCL or NaOH in 10^{-3} M and 10^{-4} M arsenate or chromate solutions and - as reference - without arsenate or chromate addition.

Gt(1), Gt(4), Sh(1), Sh(4): suspensions containing 1 or 4 g/L goethite or schwertmannite, respectively

Goethite

pH after 24 h

Concentration of added acid (HCl) or base (NaOH) in mM	Gt (1) 10^{-3} M CrO_4	Gt (1) 10^{-4} M CrO_4	Gt (4) 10^{-3} M CrO_4	Gt (4) 10^{-4} M CrO_4	Gt (1) 10^{-3} M AsO_4	Gt (1) 10^{-4} M AsO_4	Gt (4) 10^{-3} M AsO_4	Gt (4) 10^{-4} M AsO_4	Gt(1)	Gt(4)
HCl: 0.7	2.60	2.57	5.45	3.96	2.48	2.50	5.59	4.00	2.44	4.49
HCl: 0.5	2.92	2.76	6.37	6.04	2.85	2.73	6.57	6.19	2.67	6.45
HCl: 0.3	6.07	4.64	7.71	7.80	6.73	5.69	8.63	8.08	4.98	8.20
HCl: 0.2	6.76	6.52	8.47	8.51	7.20	6.73	9.02	8.52	6.45	8.66
HCl: 0.7	7.45	7.07	8.95	8.51	7.31	6.89	9.00	8.77	6.25	8.70
0	8.96	8.90	9.40	9.39	9.26	9.10	9.47	9.33	9.19	9.42
NaOH: 0.1	9.13	9.23	9.43	9.43	9.36	9.46	9.53	9.38	9.35	9.45
NaOH: 0.3	9.63	9.49	9.49	9.53	9.70	9.71	9.63	9.48	9.58	9.57
NaOH: 0.3	9.81	9.75	9.59	9.60	9.71	9.92	9.68	9.62	9.82	9.64
NaOH: 0.7	10.01	9.93	9.70	9.70	10.10	10.06	9.73	9.65	10.03	9.73

pH after 48 h

Concentration of added acid (HCl) or base (NaOH) in mM	Gt (1) 10^{-3} M CrO_4	Gt (1) 10^{-4} M CrO_4	Gt (4) 10^{-3} M CrO_4	Gt (4) 10^{-4} M CrO_4	Gt (1) 10^{-3} M AsO_4	Gt (1) 10^{-4} M AsO_4	Gt (4) 10^{-3} M AsO_4	Gt (4) 10^{-4} M AsO_4	Gt(1)	Gt(4)
HCl: 0.7	2.50	2.43	5.73	4.17	2.55	2.47	6.04	4.10	2.50	4.79
HCl: 0.5	2.82	2.64	6.70	6.60	2.88	2.70	8.30	6.59	2.68	7.03
HCl: 0.3	6.26	4.82	7.90	8.11	7.28	6.08	8.88	8.31	5.23	8.42
HCl: 0.2	6.99	6.94	8.58	8.68	7.50	7.09	9.21	8.74	6.88	8.85
HCl: 0.7	7.59	7.32	9.01	8.69	7.56	7.28	9.19	8.96	6.67	8.87
0	8.81	8.71	9.49	9.51	9.33	9.06	9.64	9.52	9.17	9.57
NaOH: 0.1	9.00	9.16	9.53	9.55	9.47	9.55	9.73	9.57	9.37	9.60
NaOH: 0.3	9.56	9.45	9.61	9.67	9.80	9.82	9.82	9.62	9.59	9.69
NaOH: 0.3	9.69	9.68	9.69	9.73	9.97	10.04	9.86	9.82	9.82	9.75
NaOH: 0.7	9.80	9.83	9.77	9.83	10.13	10.17	9.90	9.87	10.02	9.84

Schwertmannite

pH after 24 h

Concentration of added acid (HCl) or base (NaOH) in mM	Sh (1) 10^{-3} M CrO_4	Sh (1) 10^{-4} M CrO_4	Sh (4) 10^{-3} M CrO_4	Sh (4) 10^{-4} M CrO_4	Sh (1) 10^{-3} M AsO_4	Sh (1) 10^{-4} M AsO_4	Sh (4) 10^{-3} M AsO_4	Sh (4) 10^{-4} M AsO_4	Sh(1)	Sh(4)
HCl: 0.7	2.36	2.32	2.45	2.41	2.32	2.30	2.42	2.37	2.30	2.42
HCl: 0.5	2.51	2.44	2.58	2.51	2.47	2.46	2.54	2.53	2.44	2.52
HCl: 0.3	2.76	2.65	2.80	2.80	2.75	2.64	2.79	2.79	2.64	2.68
HCl: 0.2	2.99	2.81	2.99	3.05	2.98	2.81	2.99	2.98	2.79	2.82
HCl: 0.7	3.47	3.08	3.31	3.31	3.49	3.08	3.32	2.78	3.05	3.03
0	5.54	3.84	3.93	3.92	5.59	3.84	3.90	3.02	3.73	3.46
NaOH: 0.1	5.90	4.01	4.01	4.07	5.86	4.02	3.99	3.03	3.88	3.52
NaOH: 0.3	6.20	4.44	4.17	4.35	6.43	4.44	4.15	3.11	4.26	3.65
NaOH: 0.3	6.53	4.93	4.14	3.69	7.01	4.91	4.18	3.69	4.71	3.79
NaOH: 0.7	6.87	5.41	4.36	3.92	7.51	5.42	4.55	3.94	5.25	3.87

pH after 48 h

Concentration of added acid (HCl) or base (NaOH) in mM	Sh (1) 10^{-3} M CrO_4	Sh (1) 10^{-4} M CrO_4	Sh (4) 10^{-3} M CrO_4	Sh (4) 10^{-4} M CrO_4	Sh (1) 10^{-3} M AsO_4	Sh (1) 10^{-4} M AsO_4	Sh (4) 10^{-3} M AsO_4	Sh (4) 10^{-4} M AsO_4	Sh(1)	Sh(4)
HCl: 0.7	2.37	2.32	2.44	2.38	2.27	2.29	2.42	2.35	2.31	2.35
HCl: 0.5	2.52	2.44	2.55	2.49	2.43	2.42	2.55	2.52	2.44	2.46
HCl: 0.3	2.76	2.64	2.78	2.78	2.81	2.63	2.79	2.78	2.63	2.64
HCl: 0.2	2.99	2.80	2.97	3.04	2.96	2.80	2.99	2.97	2.78	2.79
HCl: 0.7	3.47	3.06	3.30	3.29	3.48	3.06	3.31	2.74	3.03	3.01
0	5.46	3.83	3.88	3.87	5.48	3.81	3.88	2.98	3.71	3.43
NaOH: 0.1	5.79	4.00	3.97	4.00	5.78	3.99	3.97	2.99	3.84	3.49
NaOH: 0.3	6.12	4.41	4.13	4.28	6.32	4.40	4.11	3.07	4.23	3.62
NaOH: 0.3	6.42	4.89	4.11	3.63	6.86	4.85	4.14	3.65	4.69	3.75
NaOH: 0.7	6.74	5.34	4.32	3.87	7.23	5.32	4.49	3.89	5.17	3.89

Measured oxyanion concentration in suspensions of schwertmannite and goethite (each 1 or 4 $g \cdot L^{-1}$) after 24 h in solutions of 10^{-3} M or 10^{-4} M or $5 \cdot 10^{-3}$ M arsenate or chromate.

Schwertmannite

	pH	Sulfate [µM]	Chromate [µM]		pH	Sulfate [µM]	Arsenate [µM]
Sh (1) 10^{-3} M CrO_4	2.37	276.2	177.2	**Sh (1) 10^{-3} M AsO_4**	2.32	304.7	56.4
	2.52	269.6	171		2.47	336.4	61.1
	2.76	271.6	175.5		2.75	343.6	48.1
	2.99	301.6	177.9		2.98	349	45.3
	3.47	306.8	164.2		3.49	409.2	50.3
	5.46	737.5	131		5.59	630.2	38.8
	5.79	738.8	136.4		5.86	654.6	34.1
	6.12	803.9	135.2		6.43	719.6	37.4
	6.42	847.6	136.1		7.01	727	43.8
	6.74	853.8	148.9		7.51	775	65.7
Sh (1) 10^{-4} M CrO_4	2.32	105.4	12.8	**Sh (1) 10^{-4} M AsO_4**	2.30	76.4	0.43
	2.44	93.3	11		2.46	94.07	0.55
	2.64	79.4	8.1		2.64	132.4	0.29
	2.80	69.7	13.1		2.81	180.6	0.45
	3.06	87.8	2.1		3.08	259.5	0.16
	3.83	131.8	1.96		3.84	393.2	0.2
	4.00	146.7	1.47		4.02	371.7	0.14
	4.41	181	1.42		4.44	448.6	0.42
	4.89	227	1.16		4.91	576.4	0.63
Sh (4) 10^{-3} M CrO_4	5.34	311	1	**Sh (4) 10^{-3} M AsO_4**	5.42	594.4	0.95
	2.44	386.3	37.8		2.42	564.0	1.86
	2.55	394.1	37.7		2.54	627.4	0.73
	2.78	432.7	37.75		2.79	686.7	0.66
	2.97	492.4	37.5		2.99	878.5	0.62
	3.3	596	36.8		3.32	1015	0.66
	3.88	929.1	32.4		3.90	1276	0.44
	3.97	952.6	32.9		3.99	1323	0.55
	4.13	1025	29.9		4.15	1394	0.57
	4.11	1022	31.1		4.18	1398	0.34
	4.32	1082	28.9		4.55	1454	0.98
Sh (4) 10^{-4} M CrO_4	2.38	148.8	3.1	**Sh (4) 10^{-4} M AsO_4**	2.37	232.8	0.61
	2.49	116.8	2.5		2.53	281.7	0.96
	2.78	128.9	4.6		2.79	402.5	1.00
	3.04	164.7	4.9		2.98	498.0	0.77
	3.29	344.3	4.1		2.78	670.5	0.090
	3.63	330.1	2.7		3.02	662.3	1.06
	3.87	386.6	2.6		3.03	709.3	0.309
	3.87	507.9	2.9		3.11	836.4	0.122
	4.00	534.5	7.7		3.69	972.5	0.108
	4.28	697.9	5.6		3.94	1035	0.17

	pH	Sulfate [µM]		pH	Sulfate [µM]
Sh (1)	2.33	597.0	**Sh (4)**	2.42	1065
	2.47	665.3		2.52	1234
	2.66	631.3		2.68	1121
	2.85	579.3		2.82	1212
	3	615.2		3.03	1042
	3.13	391.4		3.46	1100
	3.2	506.4		3.52	987
	3.3	538.8		3.65	1220
	3.34	506.7		3.79	1120
	3.41	498.5		3.87	1243
	3.46	471.5			
	3.48	588.4			
	3.62	455.4			
	3.68	534.8			
	4.32	484.3			
	4.32	367.4			
	5.7	713.1			
	9.79	1083			
	10.95	1141			
	11.19	1156			

	pH	Sulfate [µM]	Arsenate [µM]
Sh(1) $5 \cdot 10^{-3}$ AsO_4	6.79	902.5	1231
	6.51	737	2102
	5.3	685	1998
	4.01	599	216
	4.01	836	626.4
	4.23	841.9	691.2
	4.04	801	172.8
	3.47	753	568.8
	3.17	759.9	482.4
	2.77	709.5	640.8

Goethite

	pH	Chromate [µM]		pH	Arsenate [µM]
Gt (1) 10^{-3} M CrO_4	2.50	210.9	**Gt (1) 10^{-3} M AsO_4**	2.55	388.7
	2.82	216.1		2.88	384.2
	6.26	271.2		7.28	709.0
	6.99	284.5		7.50	723.0
	7.59	296.8		7.56	727.0
	8.81	300.2		9.33	799.2
	9.00	298.1		9.47	806.4
	9.56	303.7		9.80	824.4
	9.69	303.7		9.97	799.2
	9.80	322.7		10.1	824.4
Gt (1) 10^{-4} M CrO_4	2.43	0.91	**Gt (1) 10^{-4} M AsO_4**	2.32	0.6
	2.64	0.78		2.47	0.4
	4.82	1.83		2.70	0.8
	6.94	27.59		6.08	1.3
	7.32	29.82		7.09	5.4
	8.71	31.42		7.28	33.5
	9.16	38.80		9.06	45.4
	9.45	39.57		9.55	54.4
	9.68	36.20		9.82	49.0
Gt (4) 10^{-3} M CrO_4	9.83	35.88		10.04	89.7
	5.73	69.23	**Gt (4) 10^{-3} M AsO_4**	6.04	43.2
	6.70	71.63		8.30	154.8
	7.90	72.23		8.88	583.2
	8.58	74.53		9.21	640.8
	9.01	71.78		9.19	658.8
	9.49	73.30		9.64	738.0
	9.53	74.22		9.73	774.0
	9.61	73.45		9.82	752.4
	9.69	74.38		9.86	770.4
	9.77	74.22		9.90	835.2
Sh (4) 10^{-4} M CrO_4	4.17	0.20	**Gt (4) 10^{-4} M AsO_4**	4.10	0.1
	6.60	7.07		6.59	0.1
	8.11	7.42		8.31	1.1
	8.68	7.62		8.74	2.5
	8.69	7.50		8.96	3.3
	9.51	14.81		9.52	1.3
	9.55	15.22		9.57	1.8
	9.67	18.17		9.62	1.7
	9.73	18.10		9.82	3.7
	9.83	18.40		9.87	9.5

Titration curves of goethite in presence of arsenate or chromate (chapter II.6.2)

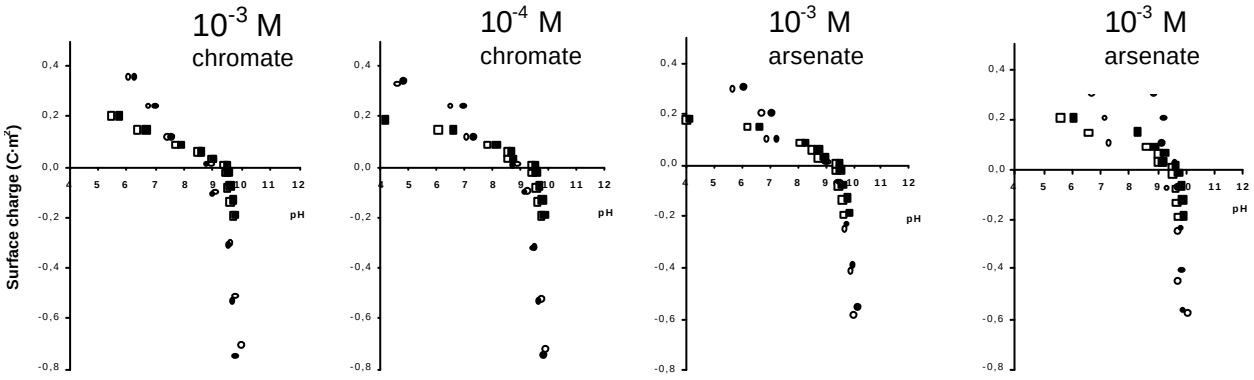

❍ 1 g·L^{-1} goethite, 24 h of reaction
● 1 g·L^{-1} goethite, 48 h of reaction
□ 4 g·L^{-1} goethite, 24 h of reaction
■ 4 g·L^{-1} goethite, 48 h of reaction

F) SURFACE-WATER ANALYSIS OF THE MINING LAKES (III.) (BRAND, 2001)

Mining lake	depth	T	O_2	pH	pe	Fe^{2+}	Fe^{3+}	Al^{3+}	Na^{+}	NH_4^{+}	K^{+}	Ca^{2+}	Mg^{2+}	F^{-}	Cl^{-}	NO_3^{-}	SO_4^{2-}
	[m]	[°C]	[mg/l]			[µmol/l]	[µmol/l]	[µmol/l]	[µmol/l]	[µmol/l]	[µmol/l]	[µmol/l]	[µmol/l]	[µmol/l]	[µmol/l]	[µmol/l]	[µmol/l]
Spreetal NO	1	22	7.97	3.6	10.86	12.9	0.1	176.9	1003.0	n.d.	379.4	7674	2561	n.d.	798.1	n.d.	10463
	20	16	8.22	4.8	7.18	3.3	n.d.	45.7	769.3	178.4	369.9	12673	2487	n.d.	770.1	n.d.	12133
	31	8	7.56	4.1	9.12	3.1	1.4	87.5	891.9	168.6	365.7	12518	2592	n.d.	778.0	n.d.	11356
Laubusch	0	17	8.64	6.5	5.43	n.d.	n.d.	n.d.	3460.0	n.d.	222.7	2657	530.8	42.2	720.4	59.4	3457
	1.5	17	8.75	6.7	5.48	n.d.	n.d.	n.d.	2749.9	n.d.	219.8	2658	526.6	29.1	719.1	59.2	3001
Koschen	1	19	8.53	3.1	12.46	10.9	219.1	59.5	1524.6	129.3	296.6	4661	1158	n.d.	1170	n.d.	7584
	10.5	17	7.74	3.1	12.51	9.8	254.3	63.6	1525.6	125.2	285.5	4497	1161	n.d.	1152	n.d.	8957
	19	7	7.52	3.0	12.62	9.0	304.9	57.7	1502.8	139.9	292.7	4696	1171	n.d.	1201	n.d.	9069
Kortitzmühle	0	20	8.63	4.7	7.77	n.d.	n.d.	n.d.	960.9	206.2	293.6	13364	2177	n.d.	856.2	44.8	12443
	2.9	19	7.94	4.5	8.19	n.d.	3.8	n.d.	962.6	207.8	293.2	13648	2213	n.d.	869.3	45.8	14657
Bluno	0	19	8.57	2.9	13.24	16.2	835.2	236.5	791.2	108.8	322.4	5015	1784	n.d.	781.9	n.d.	13733
	2	19	8.64	2.8	13.28	13.4	851.9	272.3	794.5	109.4	327.3	5679	1786	n.d.	779.1	n.d.	18033
RL 111	0	19	8.5	2.7	13.28	55.2	2574	1561	266.2	198.1	154.1	5296	1250	33.7	251.4	n.d.	14944
	5	13	9.39	2.6	13.51	23.7	2686	1538	242.8	182.9	143.8	5163	1061	32.4	255.5	n.d.	14176
Skado	0	18	9.02	2.8	13.38	16.9	1541.1	302.1	866.5	224.6	284.9	7006	2079	n.d..	788.7	n.d.	18749
	8	17	6.28	2.8	13.58	12.1	1609	302.1	853.0	241.4	275.4	6241	2103	n.d.	809.4	n.d.	18533
Sedlitz	0	18	8.89	3.0	13.24	9.6	421.4	343.9	2293.0	218.2	336.1	7806	1841	n.d.	899.4	n.d.	18593
	7.5	18	8.62	3.0	13.19	10.5	415.8	355.8	1216.4	219.1	332.5	8071	1833	n.d.	911.5	n.d.	14362
Borna Ost	0	18	8.68	2.9	13.65	21.0	1189.4	791.1	423.4	n.d.	112.5	8906	1436	31.6	474.9	n.d.	19406
	10	12	3.69	2.8	13.76	18.2	1221.2	749.3	400.8	n.d.	116.2	8947	1395	31.9	468.5	n.d.	19926
RL 13	0	15	9.42	2.9	12.76	28.9	237.5	272.3	259.6	47.5	171.5	2532	234.1	n.d.	273.4	99.6	7535
	6.5	14	9.27	2.9	12.69	27.5	379.2	403.5	353.2	67.8	114.6	3093	351.3	n.d.	415.2	n.d.	8189
RL F	0	15	n.m.	2.8	12.92	24.4	440.3	451.2	345.3	116.5	198.3	13027	1885	n.d.	872.5	n.d.	16778
Niemegck	0	16	9.08	6.7	4.47	n.d.	n.d.	n.d.	1303.5	n.d.	151.3	2462	551.5	n.d.	1150	243.2	3438
	13	12	8.43	4.7	4.07	n.d.	n.d.	n.d.	1426.7	n.d.	175.1	2734	633.0	n.d..	1135	274.2	2080
RL 107	0	15	n.m.	2.3	13.79	38.7	11162	2936.1	217.8	448.3	326.7	9451	634.0	n.d.	163.3	n.d.	65653
RL 117	0	12	9.56	3.0	13.38	4.2	309.7	69.6	390.4	120.5	139.6	2468	574.8	n.d.	398.2	n.d.	9372
	12	12	9.32	3.0	13.35	3.4	304.8	63.6	386.7	122.7	172.4	2383	563.4	n.d.	398.2	n.d.	7907
Murnersee	0	21	8.02	3.3	13.35	28.1	25.5	222.2	241.3	n.d.	108.9	1922	389.2	n.d..	307.7	n.d.	3223
	35	5	9.65	3.1	n.m.	n.d.	84.0	222.2	248.6	n.d.	109.5	1865	380.7	n.d.	295.6	n.d.	3246
Ausee	0	24	7.97	3.0	n.m.	33.2	183.4	370.4	397.1	39.7	137.9	1424	350.1	n.d.	337.7	n.d.	4625
	28	5	7.47	2.9	n.m.	36.0	258.4	407.4	494.7	42.5	133.3	1415	349.0	n.d.	358.0	n.d.	4585
Brückelsee	0	20	8.79	3.1	n.m.	24.0	53.9	296.3	196.5	n.d.	114.5	3998	358.4	n.d.	256.0	n.d.	3393
Lindensee	0	23	7.78	2.8	n.m.	78.0	270.8	870.4	158.4	42.5	117.1	5862	338.2	31.2	228.2	n.d.	6673
	12	9	8.8	2.7	n.m.	31.0	365.8	870.4	197.6	60.9	146.6	6511	374.6	n.d.	211.1	n.d.	6078

n.m. not measured
n.d. not determinable (signal overlap in the ionic-chromatographic measurement due to higher concentrated ions)

G) PHREEQC: CALCULATED SPECIES IN SURFACE WATERS OF THE ML (III.), BRAND (2001)

Mining lake	Depth [m]	log $a(Fe^{2+})$	log $a(Fe^{3+})$	log $a(K^{+})$	log $a(SO_4^{2-})$	log $a(Fe(OH)^{2+})$	log $a(Fe(OH)_2)^{+}$	log $a(Fe(OH)_3$	log $a(Fe(SO_4)^{+})$	log $a(Fe(SO_4)_2^{-}$
Spreetal NO	31	-5.89	-8.01	-3.52	-2.42	-6.61	-6.34	-9.52	-6.56	-7.67
Koschen	1	-5.31	-5.37	-3.60	-2.50	-4.66	-5.19	-9.15	-3.89	-5.06
	10.5	-5.37	-5.34	-3.62	-2.42	-4.69	-5.26	-9.25	-3.80	-4.90
	19	-5.39	-5.14	-3.61	-2.42	-4.85	-5.68	-9.96	-3.69	-4.80
Kortitzmühle	2.9	-10	-8.71	-3.63	-2.32	-6.53	-5.59	-8.07	-7.05	-8.05
Bluno	0	-5.21	-4.95	-3.58	-2.29	-4.45	-5.18	-9.34	-3.26	-4.23
	2	-5.34	-5.05	-3.58	-2.19	-4.56	-5.31	-9.49	-3.26	-4.11
RL 111	0	-4.66	-4.38	-3.90	-2.37	-4.03	-4.91	-9.22	-2.76	-3.80
	5	-5.01	-4.26	-3.92	-2.39	-4.18	-5.27	-9.80	-2.74	-3.81
Skado	0	-5.24	-4.76	-3.64	-2.21	-4.36	-5.20	-9.46	-3.00	-3.88
	8	-5.38	-4.73	-3.66	-2.20	-4.32	-5.12	-9.35	-2.98	-3.86
Sedlitz	0	-5.50	-5.37	-3.57	-2.18	-4.73	-5.31	-9.32	-3.58	-4.44
	7.5	-5.41	-5.25	-3.57	-2.30	-4.65	-5.27	-9.32	-3.58	-4.56
Borna Ost	0	-5.15	-4.88	-4.05	-2.20	-4.39	-5.12	-9.28	-3.12	-3.99
	10	-5.20	-4.82	-4.03	-2.19	-4.55	-5.46	-9.80	-3.10	-3.97
RL 13	0	-4.87	-5.29	-3.83	-2.45	-4.81	-5.53	-9.69	-3.80	-4.93
	6.5	-4.90	-5.09	-4.01	-2.44	-4.65	-5.40	-9.59	-3.60	-4.72
RL F	0	-5.05	-5.19	-3.80	-2.29	-4.84	-5.70	-9.98	-3.54	-4.52
RL 107	0	-5.07	-4.28	-3.63	-1.85	-4.42	-5.75	-10.5	-2.19	-2.72
RL 117	0	-5.73	-5.24	-3.93	-2.35	-4.79	-5.50	-9.66	-3.68	-4.72
	12	-5.80	-5.19	-3.83	-2.42	-4.71	-5.41	-9.54	-3.69	-4.79
Murnersee	0	-4.80	-6.22	-4.01	-2.77	-5.23	-5.50	-9.18	-4.99	-6.43
	35	-10	-5.37	-4.01	-2.76	-4.99	-5.70	-9.88	-4.30	-5.76
Ausee	0	-4.76	-5.37	-3.92	-2.64	-4.59	-5.09	-9.01	-3.98	-5.28
	28	-4.70	-4.94	-3.93	-2.64	-4.84	-5.82	-10.3	-3.75	-5.09
Brückelsee	0	-4.87	-5.78	-4.00	-2.83	-4.98	-5.43	-9.30	-4.61	-6.10
Lindensee	0	-4.43	-5.17	-4.00	-2.63	-4.61	-5.32	-9.45	-3.78	-5.07
	12	-4.80	-4.83	-3.90	-2.68	-4.71	-5.72	-10.2	-3.63	-4.99

H) ULTRAFILTRATION

Total iron and sulfate concentration ($mmol \cdot L^{-1}$) in the filtrates obtained by the mass balance approach , Brand (2001).

	< 0.22 µm		**< 100 kDa**		**< 10 kDa**		**< 1 kDa**	
	$Fe_{(tot)}$	SO_4^{2-}	$Fe_{(tot)}$	SO_4^{2-}	$Fe_{(tot)}$	SO_4^{2-}	$Fe_{(tot)}$	SO_4^{2-}
Borna Ost	1.188	18.76	1.211	n.m.	1.179	n.m.	1.004	18.309
ML 117	0.301	6.48	0.298	n.m.	0.299	n.m.	0.233	8.23
ML 77	1.915	14.31	1.918	n.m.	1.875	n.m.	1.298	9.973

n.m. not measured

I) SCHWERTMANNITE-STABILITY: RELEASE OF SULFATE AND IRON (III.)

Activity of released sulfate and iron of schwertmannite, suspended at constant pH (2, 3, 4, 5 and 7; III) over 362 days .

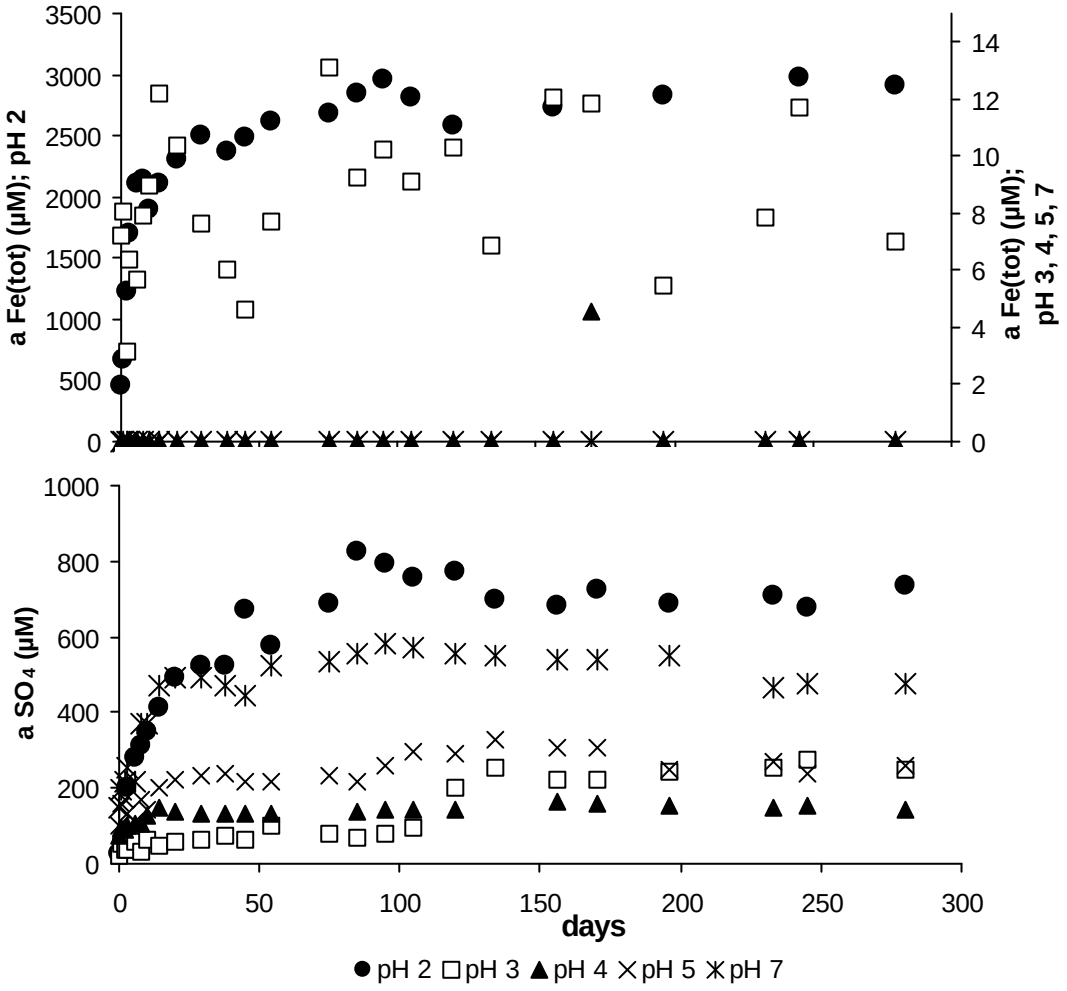

Hiermit erkläre ich, dass ich die Arbeit selbstständig verfasst und keine anderen als die von mir angegebenen Quellen und Hilfsmittel verwendet habe.

Ferner erkläre ich, dass ich anderweitig mit oder ohne Erfolg nicht versucht habe, diese Dissertation einzureichen. Ich habe keine gleichartige Doktorprüfung an einer anderen Hochschule endgültig nicht bestanden.

Bayreuth,